UNIVERSITY OF MINNESOTA
ST. ANTHONY FALLS HYDRAULIC LABORATORY

Project Report No. 264

MIXING OF TEMPERATURE-STRATIFIED LAKE WATER BY A HORIZONTAL BUOYANT JET

by

Ruochuan Gu and

Heinz G. Stefan

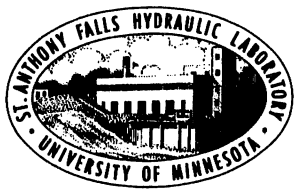

Prepared for

LEGISLATIVE COMMISSION ON MINNESOTA RESOURCES

St. Paul, Minnesota

August 1987

Minneapolis, Minnesota

University of Minnesota
St. Anthony Falls Hydraulic Laboratory
Mississippi River at 3rd Ave. S.E.
Minneapolis, Minnesota 55414

Project Report No. 264

MIXING OF TEMPERATURE-STRATIFIED LAKE WATER BY A HORIZONTAL BUOYANT JET

by

Ruochuan Gu

and

Heinz G. Stefan

Prepared for

LEGISLATIVE COMMISSION ON MINNESOTA RESOURCES
St. Paul, Minnesota

August 1987

CONTENTS

ABSTRACT

A turbulent buoyant jet in a stratified ambient fluid is investigated. The theoretical integral analysis approach has been used. By applying similarity hypothesis for velocity and temperature profiles and deriving an entrainment function, a general model is developed to predict jet trajectories, centerline temperature or density and velocity decay, and the dilution on the axis of a turbulent buoyant jet discharged at arbitrary angles to stratified or uniform ambients. The effects of pressure to which density difference and curvature of the jet contribute are evaluated. Predictions obtained with the model are compared with experimental data.

One of the practical problems to apply the jet model is an examination of the mixing of temperature stratified lakes and reservoirs by means of buoyant jets which are created by a pumping system for thermal destratification. The physical aspects of the mixing process are investigated. A one-dimensional simulation model is devised to predict the process of mixing which is reflected by changes in the temperature-depth profiles. The simulation results are compared with existing field data.

Experimental investigation of the mixing of stratified water by buoyant jets is carried out in the laboratory. The results of laboratory experiments are presented and compared with those predicted by the simulation model to verify the validity of the model.

The results of a series of numerical experiments and laboraroty experiments are summarized and condensed to provide some design information for the selection of mixing systems for lake and reservoir destratification.

List of Symbols

A	area
b	measure of half width of the jet
B	buoyancy flux
C	concentration
C_p	specific heat of water
d	depth from the surface
D	jet diameter
D_0	discharge jet diameter
E	entrainment rate
Fr	densimetric Froude number
Fr_0	discharge densimetric Froude number
g	acceleration of gravity
h	enthalpy
h_e	characteristic distance
h_m	characteristic distance
h_t	characteristic distance
l_Q	characteristic length scale
l_M	characteristic length scale
l_b'	characteristic length scale
L	distance between the jet and withdrawal
M	momentum flux
N	buoyancy frequency
p	pressure
p_d	dynamic pressure

p_h	hydrostatic pressure
q_e	transport flow rate per unit depth
Q	discharge, volume flux
Q_j	jet discharge at the origin
r	radial coordinate, distance from jet centerline
Ri	Richardson number
Ri_0	discharge Richardson number
Ri_1	local Richardson number
s	streamwise coordinate, distance along the jet axis
St	stratification number
S_M	dilution = C_0/C_m
t	time
t^*	dimensionless time = $t/(V/Q)$
T	temperature
ΔT	temperature difference = $T - T_a$
u	component of velocity parallel to jet axis
u_m	centerline velocity of the jet
v	effective transport velocity
V	volume
u_e	entrainment velocity
W_0	discharge jet width
x	horizontal coordinate
y	coordinate normal to the jet axis
z	vertical coordinate
z^*	dimensionless vertical coordinate = z/L
z_t	top of the jet = $z_m + b$

z_m elevation of jet centerline where $\Delta u_m = 0$

z_n elevation of jet centerline where $\Delta T_m = 0$

ρ density

$\Delta\rho$ density difference = $\rho - \rho_m$

Θ angle between jet centerline and horizontal

Θ_0 discharge angle, Θ at s = 0

ϕ angle coordinate

μ dynamic viscosity

β thermal coefficient of volumetric expansion

η similarity variable = r/b

σ standard deviation

λ dispersion ratio

α entrainment coefficient

Subscripts

$( )_a$ ambient value

$( )_j$ jet

$( )_m$ at the jet centerline, y = 0

$( )_0$ at the jet origion, s = 0

$( )_p$ plume

$( )_r$ round

$( )_s$ slot

List of Tables and Figures

Tables

Figures

CHAPTER 1 Introduction

The most common method for the disposal of waste water and waste heat from power plants is by discharge into a large ambient body of water. Mixing the water from various levels within a temperature-stratified lake or reservoir is one method to improve their water quality by eliminating the temperature stratification (called "destratification") to which the quality of water in lakes and reservoirs is often interrelated. Both these problems are similar as far as mixing with the ambient fluid is concerned. However, the emphasis in the former is on the discharge characteristics while in the latter it is on the ambient characteristics. The present study deals with the gross behavior of such a discharge into a quiescent stratified water body and the process of mixing induced by the discharge in the receiving ambient fluid.

1-1 Concepts and Definition

A definition of a jet and a plume was given by Fischer et al (1979): a jet is the discharge of fluid from an orifice or slot into a large body of the same or similiar fluid and a plume is a flow which looks like a jet, but is caused by a potential energy source that provides the fluid with positive or negative buoyancy relative to its surroundings. Some investigators, e.g. Fox (1970), Ditmars (1970) and List (1982), referred to the buoyant jet as a forced plume. The term "buoyant jet" is adopted in this paper instead of "forced plume".

Jets may be classified according to three classes of parameters:

jet parameters, ambient parameters and combined factors of jets and ambients, as shown in Fig. 1-1. We have round (circular) and slot (planar), 3-d and 2-d and vertical, inclined and horizontal jets according to their shapes, dimensions and orientations respectively. Jets can be either laminar or turbulent. Fischer et al (1979) have shown that in most cases, provided a Reynolds number exceeds 2000 the jet flow will be turbulent. Symons et al (1972) have shown that the critical Reynolds number is about 4000 for buoyant jets. The environmental parameters include currents and density or temperature stratification. The combined jet and ambient factors are submergence and buoyancy. The surface jets are not of interest in this study. Buoyant jets can be positive if they are lighter than surrounding fluid and negative if heavier. The buoyancy is independent of jet orientation, however Pantokratoras (1986) used "negative buoyancy" in his paper dealing with a jet of fluid with density lower than ambient discharged downward into an ambient region of the same fluid. This may lead to a confussion between "positive" and "negative" buoyancy. This paper is restricted to the study of one sub-class of jets, namely turbulent buoyant jets issuing into quiescent stratified ambient fluids, which have found particular attention because of their relative simplicity as compared to more general situations with cross-flow, surface discharge, and interaction with boundaries and their wide application to the artificial mixing of lakes and reservoirs. In a lake or reservoir as considered herein the ambient will be quiescent.

The discharge of buoyant jets into a natural water body for

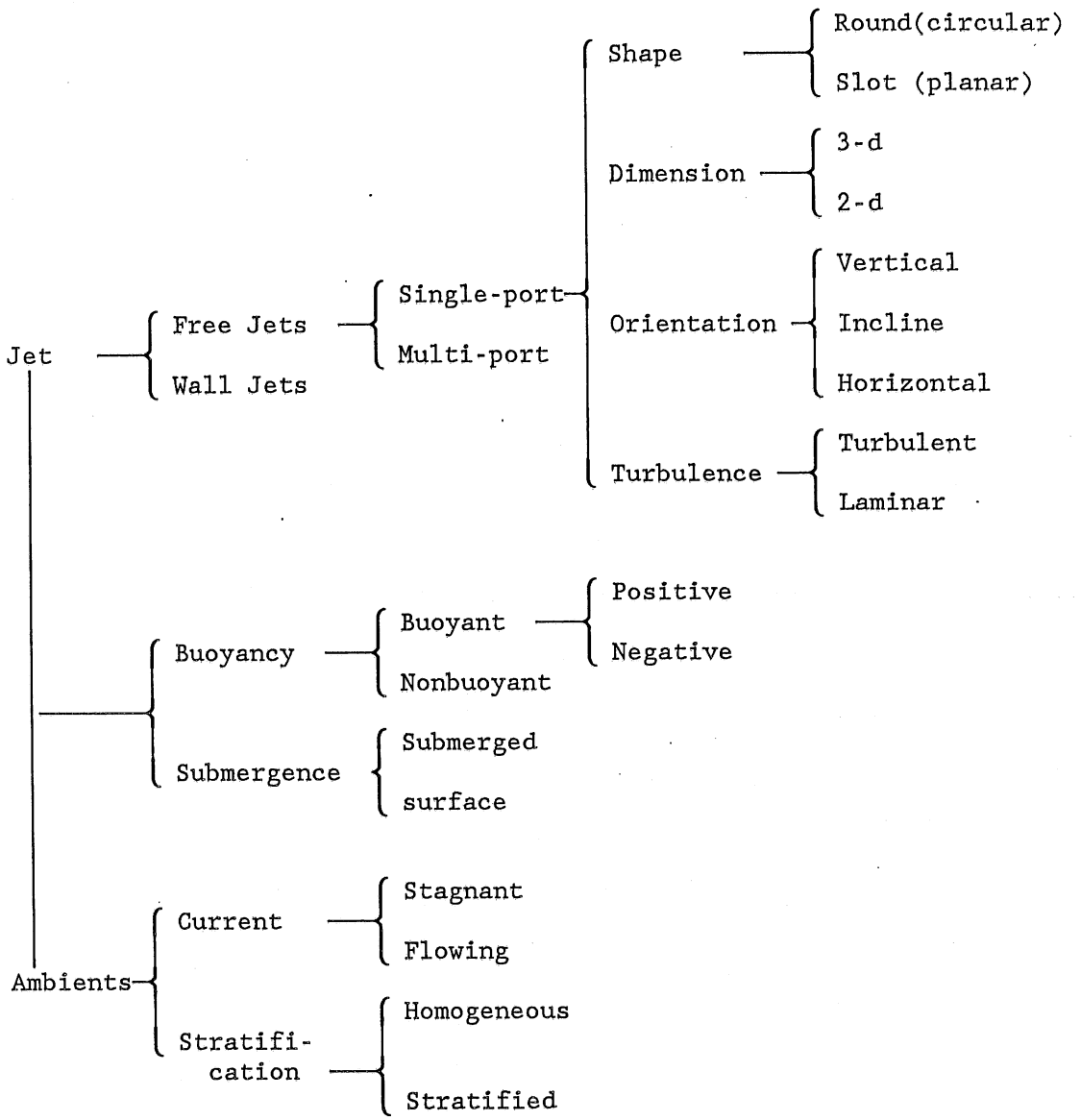

Fig. 1-1 Jet Classification According to Jet Parameters, Ambient Parameters and Combined Factors

destratification will always induce mixing of the discharged and ambient water and changing of temperature of the receiving environmental water. In the immediate vicinity of the discharge, the discharge mixes to some extent with the ambient water and the discharge flow characteristics are the major determinants of the temperature distributions. The turbulent mixing and entrainment induces velocities in the ambient water surrounding the discharge. This region, characterized by mixing processes induced by the discharge, is designated as the near field. The temperature of the discharge is changed primarily by dilution within the nearfield. Outside of the nearfield, and covering a much larger aera, is the far-field where the temperature distributions are determined by natural heat transfer processes, diffusion and convection, and external effects which are beyond the scope of this study.

1-2 Review of Previous Investigations

Analysis of turbulent buoyant jets has its origins in the papers by Morton, Taylor and Turner (1956). The theoretical integral analysis approach of Morton et al has been essentially followed by a number of others, in which the partial differential equations are reduced to ordinary ones. The mechanics of buoyant jets and plumes in uniform or stratified environments have been formulated theoretically and verified experimentally by several investigators. The buoyant jets in a uniform ambient have been studied by Anwar (1969), Abraham (1963), Fischer et al (1979), Liseth (1976), List and Imberger (1973), Rouse et al (1952), Yannopoulos (1986) and Fan and Brooks (1966). The buoyant jets in a linearly stratified environment have been studied by

Abraham (1972), Brooks (1980), Fox (1970), Fischer et al (1979), Koh and Brooks (1975), Hart (1961), Sotil (1971), Hirst (1971), Wright (1979) and Lee (1986). The scopes of these investigations differ in the terms of jet geometry (shapes or dimensions and orientations or discharge angles).

In addition to the integral approach, with advances in computer technology and numerical methods for solving differential equations, the so-called field methods became increasingly popular. With the origional partial differential equations (constitutive equations), Hossain and Rodi (1982) developed an algebraic stress/flux model which is a buoyancy extension of the widely tested and used k-ε model and applied this model to vertical turbulent buoyant jets. A buoyancy-extended k-ε model of turbulence has also been developed from the original Reynolds equations by Sini and Dekeyser (1986) for calculating the dynamical and thermal fields in plane jets vertically discharged into a stably stratified environment.

Various destratification devices are used in lakes and reservoirs. However, the mechanical pumping systems for mixing are thought of providing more efficient mixing and being better suited for mixing large impoundments (Ditmars, 1970). Dortch and Holland (1980) discussed on methods of total lake destratification. Grim (1952) pumped the warm water from the top to the bottom and Hooper et al (1952) pumped cold from bottom to the top of the lake. The latter pumping system generates negative buoyant jets which move downward as well as horizontally and the former is operated in the reverse manner. A series of reservoir mixing experiments with pumping systems has been

performed by Irwin and Symons (1966). Ditmars (1970) studied both theoretically and experimentally the mixing of density-stratified impoundments with buoyant jets. Some basic methods and assumptions are followed and extended in the second portion of this study.

1-3 Scope of Present Study

In the first part of the present study a turbulent buoyant jet in a stratified fluid is investigated by following the basic elements of the jet diffusion theory and extending the existing knowledge. The theoretical integral analysis approach has been used and a general model is devised to predict the development of turbulent buoyant jets discharged at arbitrary angles to infinite, quienscent and stratified ambients.

The second part of the study is an examination of artificial mixing of temperature-stratified lakes and reservoirs by means of mechanical pumping systems which create buoyant jets. The jets are buoyant because water is withdrawn from the stratified lake at one level and injected at another level thus creating buoyancy. It seeks to describe the physical features of thermal destratification by buoyant jets and to provide a simulation model which predicts the process of mixing.

The results of laboratory experiments on the mixing of stratified water by buoyant jets are given in the third part of the study and are compared with those predicted by the simulation technique.

In the final section all results are summarized and condensed into design information for the selection of lake or reservoir destratification systems.

CHAPTER 2 Turbulent Buoyant Jets In Stratified Environments

2-1 Flow Behavior and Analysis of a Buoyant Jet

The jets considered in this study are generated by discharging fluid from a point or slot source at an arbitrary angle into stagnant stratified ambients. The uniform surroundings are regarded as a limiting case of stratified ones. The general flow situation involving both initial momentum and buoyancy flux is sketched in Fig. 2-1. It is assumed that at the point of discharge the jet fluid is lighter than the ambient. Under these circumstances the jet fluid is immediately subjected to a buoyant force proportional to the difference in density between the jet fluid and the heavier surrounding fluid. Thus at the point of discharge it has not only kinetic energy due to its initial velocity but also potential energy due to its submergence. Both kinds of energy are dissipated in the turbulent mixing of the jet with the surrounding fluid while the jet is driven upward as a result of the positive buoyancy forces and initial momentum. Due to both the upward movement and the stable stratification of ambients, and the turbulent mixing, the difference in density between the jet and the ambient fluid decreases, until at a certain distance above the point of discharge the density difference is reduced to zero (neutral point). Above this level the jet fluid is heavier than the environmental fluid, the jet begins to be negatively buoyant. Accordingly, the jet fluid can rise above this level only if it has sufficient kinetic energy to do so when reaching a neutral

level. The rise is limited by the presence of the stable stratification in the environment. During the penetration the jet fluid gradually loses the kinetic energy, and so cannot penetrate in a vertical direction beyond a certain ceiling level or maximum rise.

In addition to the action of the buoyant force and initial momentum, fluid is entrained into the jet at the boundary between the jet and the ambient fluid. This results in spreading and dilution of the jet. The stable stratification in the ambient has a damping effect on the turbulence and therefore inhibits the mixing and the spreading of jets. In general, the buoyant turbulent jet can be characterized as a turbulent shear flow region that increases in size away from the jet discharge with a distinct boundary between the turbulent jet flow and a potential stagnant ambient fluid.

The negative buoyancy destroys the initial momentum and the momentum generated by any positive buoyancy. When the momentum is totally destroyed the jet ceases to rise and fall down upon the succeeding jet fluid and then spreads out. As a consequence, the succeeding fluid is pushed sideways. The downflow region at the spreading level (ceiling level) extends downwards to the level where the density of the descending jet fluid coincides with the density of the ambient fluid. At this level, the equilibrium level, the liquid gets stored.

In the case of very small discharge angle, e.g. $\Theta_0=0°$, and large initial momentum, i.e. high velocity, the jet flow is gradually deflected from a flow in an inclined direction in the near source region to a horizontal flow at the ceiling level. Hence, the jet

fluid, having reached the highest level, does not fall upon the succeeding fluid but on the downstream side of it, flowing continuously in the same direction. The jet fluid may fluctuate around the equilibrium level, the amplitude of the fluctuations decreasing with increasing distance from the point of discharge.

The jet consists of two regions, shown in Fig. 2-2. The first region extends to a short distance from the discharge and is called the zone of flow establishment (ZFE). In this region the shear layer is still "eating" away at the constant velocity core of the jet flow as it comes out of the nozzle. The potential core has a conical shape. The mean flow profiles in the region, which can be considered as a slug flow, undergo a transition to the fully developed profiles. Fig. 2-2 shows schematically velocity profiles in this region. The end of the ZFE is considered as the point along the jet trajectary where the jet centerline velocity starts to decay and the velocity and excess temperature (or density) profiles are considered fully developed. Generally, as scalar quantities diffuse faster than velocity, the centerline excess temperature starts to decay before the end of the ZFE. The second region, the zone of established flow (ZEF), is the region where turbulent mixing has reached the jet centerline and where the assumption of similar velocity and excess temperature profiles can be considered reasonable. In this region the jet velocity and temperature difference profiles are determined by a combination of the ambient conditions and the jet buoyancy and momentum. The effect of the buoyancy is to cause the jet centerline to move upward and also to affect the rate of entrainment of ambient

fluid into the jet. These buoyancy effects then result in the jet no longer being axisymmetric, but assumption of axisymmetry has been found to be reasonably accurate in determining important parameters such as jet trajectory and dilution. Moreover, the similarity of velocity and excess temperature profiles implies the spread of jets to be linear with distance from the orifice as shown by Rouse (1952).

A buoyant jet has jetlike characteristics depending on its initial volume and momentum fluxes, and plumelike characteristics depending on its initial buoyancy fluxes. As we have seen the effect of buoyancy is to generate an increasing momentum flux. Thus any jet with an initial buoyancy is to generate an increasing momentum flux continuously added to it. When the flux generated by the weight difference is significantly larger than the initial momentum flux then the jet becomes more plumelike. This transition from jet to plume is reasonably fixed by a characteristic length scale defined by the initial specific fluxes of momentum, buoyancy, which will be discussed further and quantified below in a later section. Moreover, the trajectory of a buoyant jet has an initial inertia-dominated pure-jet region, an intermediate transition region and a final buoyancy-dominated pure-plume region.

2-2 Characterizing Parameters

The gross behavior of a jet and its ambient is defined by several characterizing parameters. The discharge characteristics such as the velocity, U, excess temperature (or density), and diffusor diameter, D_0, are collected in a dimensionless form called densimetric Froude number. The number is the ratio of inertial forces due to the jet

discharge velocity to the buoyant forces due to the discharge temperature (or density) difference with respect to ambient. Formally, this is expressed as

$$Fr = U_0/(gD_0\Delta\rho_0/\rho_0)^{1/2} \tag{2.1}$$

where $\Delta\rho_0$ is the density difference between the initial jet and the ambient. This number has been used extensively as a correlation parameters in jet analysis. The bulk Richardson number, defined for buoyant jets as

$$Ri = (gD_0\Delta\rho_0/\rho_0)/U_0^2 \tag{2.2}$$

is also used in large measure by investigators. The Richardson number is the combination of the kinematic momentum flux, the volume flux and the buoyant flux. The two numbers are related to each other by

$$Ri = Fr^{-2} \tag{2.3}$$

The sign of Ri determines whether a jet is curved upwards or downwards. The curvature of the axis of the jet depends on the magnitude of Ri and θ_0. The curvature is small for small value of $|Ri|$.

The ambient stratification is represented by the buoyancy frequency

$$N = (\varepsilon g)^{1/2} \tag{2.4}$$

where $\varepsilon = -(1/\rho_0)(d\rho_a/dz)$

Simply the ambient density or temperature gradient $d\rho_a/dz$ or dT_a/dz can be used to describe the stratification. Hirst (1971) and Shirazi (1972) suggested a stratification number

$$St = (\Delta\rho_0/D_0)/(\Delta\rho_a/\Delta z) \tag{2.5a}$$

where $\Delta\rho_a/\Delta z$ is the local ambient density gradient in the vertical

direction. If the coefficient of volumetric expansion is assumed constant, this parameter can be written as

$$St = (\Delta T_0/D_0)/(\Delta T_a/\Delta z) \qquad (2.5b)$$

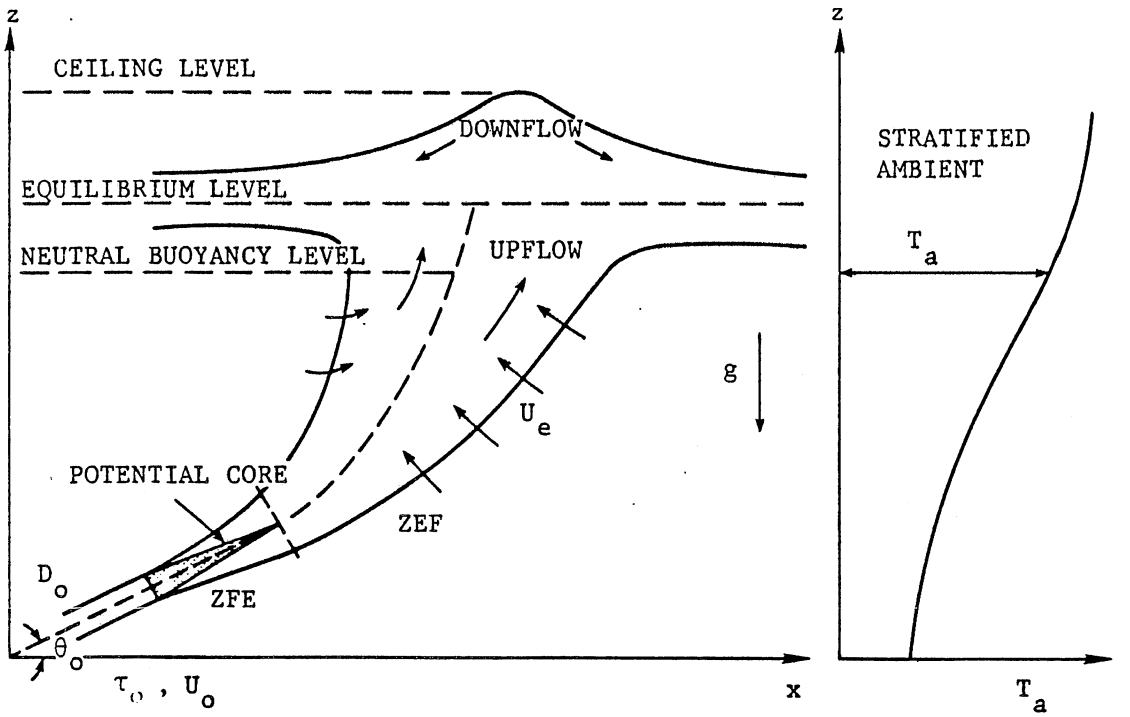

Fig. 2-1. Schematic diagram of a buoyant jet in a stratified ambient.

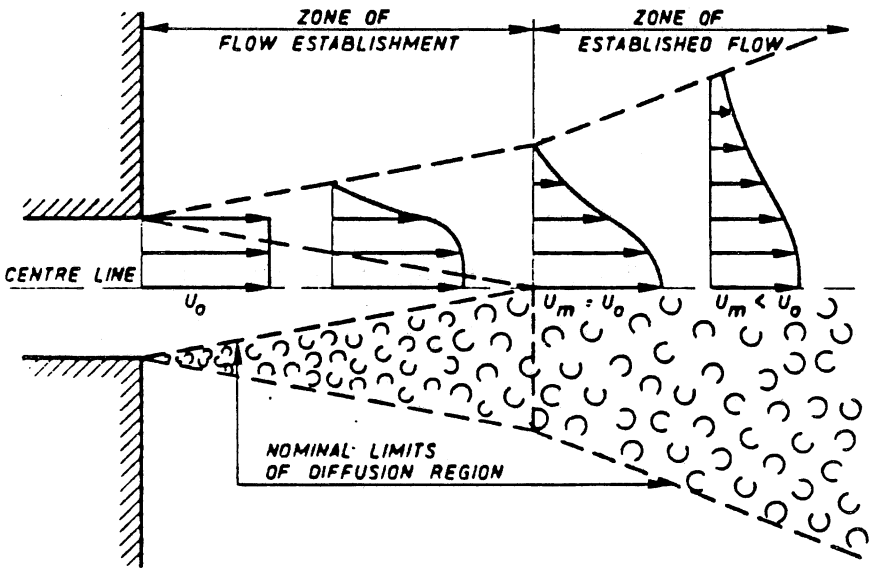

Fig. 2-2. Schematic diagram of flow establishment [After Albertson et al., 1950].

2-3 Theoretical Investigation and Analytical Model

As described in the foregoing section, the motion behavior of turbulent buoyant jets in stratified ambients is quite complex. The exact equations describing general turbulent buoyant flows are the Navier-Stokes and temperature or concentration equations. These equations describe all the details of the turbulent jet motion. As found by number of previous investigators, Abraham (1965), Hirst (1971) and Brooks (1975), the conservation equations of mass, momentum, and energy are still rather complicated, even after various simplifying assumptions. For practical problems integral methods were developed in which the partial differential equations are integrated over the jet cross-section area and a set of coupled ordinary differentual equations is obtained by introducing empirical similarity profiles for velocity, temperature difference in the lateral direction and an entrainment principle. The resulting ordinary differential equations describe the axial variation of the velocity, excess temperature or concentration scales, and the characteristic shear-layer width. The solution to the resulting equations yields results for the centerline trajectory of the jet and gives useful results about jet centerline dilution and jet width. The main purpose of the integral approach is to describe the gross behaviour of the jet for practical problems and to avoid the specification of turbulent transport terms in the conservation equations.

2-3-1 Formulation of Basic Equations

The conservation of mass, momentum, and mechanical and internal

energy are applied, along the assumption of incompressibility, to yield the governing equations for motion and state. In tensor notation they are

continuity

$$\frac{d\rho}{dt} + \rho \frac{\partial V_i}{\partial X_i} = 0 \tag{2.6}$$

momentum

$$\rho \frac{dV_j}{dt} = -\nabla p + \rho g_j + \mu \nabla^2 V_j \tag{2.7}$$

mechanical energy

$$\rho V_j \cdot \frac{dV_j}{dt} = -V_j \cdot \nabla p + \rho V_j \cdot \nabla g_j + \mu V_j \cdot \nabla^2 V_j \tag{2.8}$$

internal energy

$$\rho \frac{dh}{dt} = 0 \tag{2.9}$$

or incompressibility

$$\frac{d\rho}{dt} = 0 \tag{2.10}$$

Gibb's equation

$$h = C_p T \tag{2.11}$$

state

$$\rho = \rho(T) \tag{2.12}$$

where ρ is the density within the jet, V_j and V_i is the velocity field, g_j is the body force vector, p is the pressure field, μ is the dynamic viscosity, and h is the enthalpy. Equation 2.10 is a statement of the assumed incompressibility proposed by Fox (1970) and followed by investigators who did not use the thermal energy equation. Note that equation 2.10 neglects the effects of molecular diffusivity.

Proceeding from these equations, the following assumption are

required:

1). The motion is two-dimensional (or axisymmetric) and steady in the mean, i.e. $\partial / \partial t = 0$, $\partial / \partial X_3 = 0$.

2). The flow field is long and narrow, so that ordinary boundary-layer approximation of fluid dynamics can be evoked, i.e. the mean flow velocity transverse to the main flow are very small compared with the main flow velocity, and changes of quantities in the direction of the main flow are correspondingly slow with respect to those in transverse direction.

3). The flow in jets is effectively turbulent. The laminar shear stress represented by $\mu \nabla^2 V_j$ is neglected.

4). The Reynolds approach to turbulence, namely that the velocity and density fields are composed of mean and fluctuating components, is adopted. The equations are then averaged by accepted procedure.

5). Molecular transport terms are neglected.

6). The Boussinesq approximation is applied. The difference between the time-averaged local fluid density ρ and the ambient density ρ_a is small compared to the reference density ρ_0, the density of environmental fluid at the discharge. Thus the utilization of ρ_0 instead of the local density ρ produces a slight error in the description of the inertial force. However, the difference $|\rho - \rho_a|$ may be important in the description of the gravitational body force. The density difference can be neglected except where multiplied by g as in the Richardson number. This is equivalent to ignoring $(\rho - \rho_a)/\rho_0$ in the inertia terms in the equations of motion; in other words, the fluid is treated as having uniform mass but variable

weight. The local density ρ is, therefore, retained in the body force term.

Previous investigators assumed a hydrostatic pressure variation and neglected the pressure due to the change of density and the jet curvature in their integral analysis, but in the field methods (k-ε model). This assumption makes the pressure gradient term result solely from the hydrostatic pressure gradient outside the flow region. The present study takes account of both hydrostatic pressure p_h and pressure due to the density difference and the jet curvature p_d in the integral model ($p = p_d + p_h$).

With the assumptions mentioned above and the simplification of the Reynolds equations, and the consideration of relations

$$\partial p_h/\partial z = -\rho_a g \tag{2.13}$$

$$\partial z/\partial s = \sin\theta \tag{2.14}$$

and

$$\partial z/\partial y = \cos\theta \tag{2.15}$$

the resulting system of governing equations can be written in either an axisymmetric or a two-dimensional natural coordinate system as

continuity

$$\frac{\partial(uy^\beta)}{\partial s} + \frac{\partial(vy^\beta)}{\partial y} = 0 \tag{2.16}$$

s-momentum

$$u\frac{\partial u}{\partial s} + v\frac{\partial u}{\partial y} = -\frac{1}{y^\beta}\frac{\partial(y^\beta\overline{u'v'})}{\partial y} - \frac{\partial\overline{u'^2}}{\partial s} - \frac{\Delta\rho}{\rho_0}g\sin\theta - \frac{1}{\rho_0}\frac{\partial p_d}{\partial s} \tag{2.17}$$

y-momentum

$$u\frac{\partial v}{\partial s} + v\frac{\partial v}{\partial y} = -\frac{1}{y^\beta}\frac{\partial(y^\beta\overline{v'^2})}{\partial y} - \frac{\Delta\rho}{\rho_0}g\cos\theta(\sin\phi)^\beta$$

$$- \frac{1}{\rho_0}\frac{\partial p_d}{\partial y} - u^2 \frac{\partial \Theta}{\partial s} (\sin\phi)^\beta \qquad (2.18)$$

mech. energy

$$u \frac{\partial (u^2/2)}{\partial s} + v \frac{\partial (u^2/2)}{\partial y} = - \frac{u}{y^\beta} \frac{\partial (y^\beta \overline{u'v'})}{\partial y} - u \frac{\partial \overline{u'^2}}{\partial s} - \frac{u}{\rho_0}\frac{\partial p_d}{\partial s}$$

$$- u \frac{\Delta\rho}{\rho_0} g\sin\Theta \qquad (2.19)$$

internal energy

$$u \frac{\partial T}{\partial s} + v \frac{\partial T}{\partial y} = - \frac{1}{y^\beta} \frac{\partial (y^\beta \overline{v'T'})}{\partial y} \qquad (2.20)$$

or incompressibility

$$u \frac{\partial \rho}{\partial s} + v \frac{\partial \rho}{\partial y} = - \frac{1}{y^\beta} \frac{\partial (y^\beta \overline{v'\rho'})}{\partial y} \qquad (2.21)$$

state

$$\rho = \rho(T) \qquad (2.22)$$

where $\Delta\rho = \rho - \rho_a$, $\Delta\rho$ is the difference between the jet density and the ambient density, u is the velocity in the main flow direction, v is the velocity in the transverse direction, $\beta = 0$ for a two-dimensional jet discharged from a slot source, and $\beta = 1$, $y = r$ for a three-dimensional jet discharged from a round source. The coordinate system is shown in Fig. 2-3, which follows the jet trajectory. The jet centerline is taken as the s-coordinate and measures the distance from the discharge or jet origion (Fig. 2-3a). For the case of the circular jet the cylindrical polar coordinates (s,r,ϕ) are used, as shown in Fig. 2-3c.

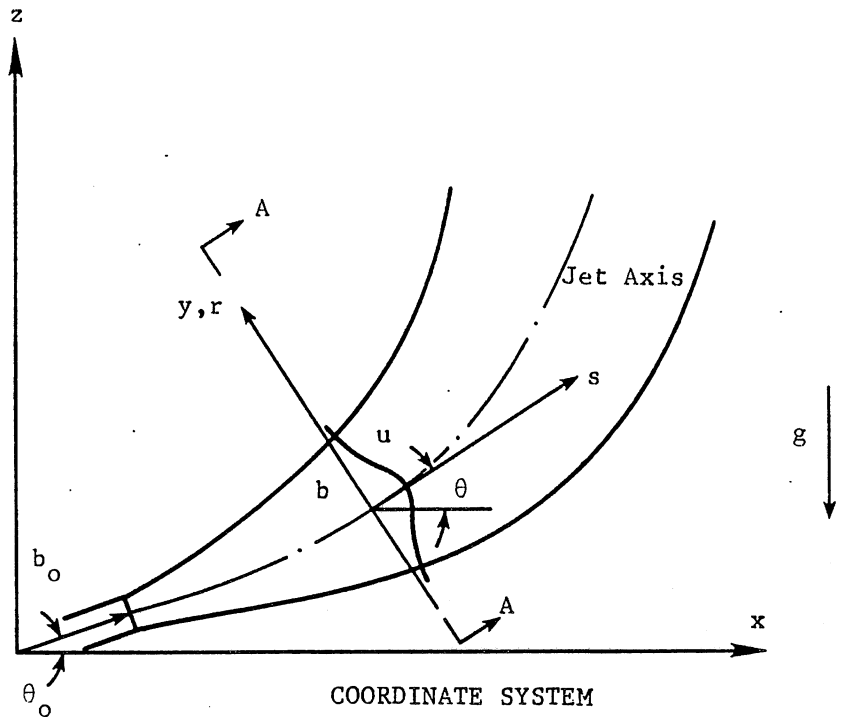

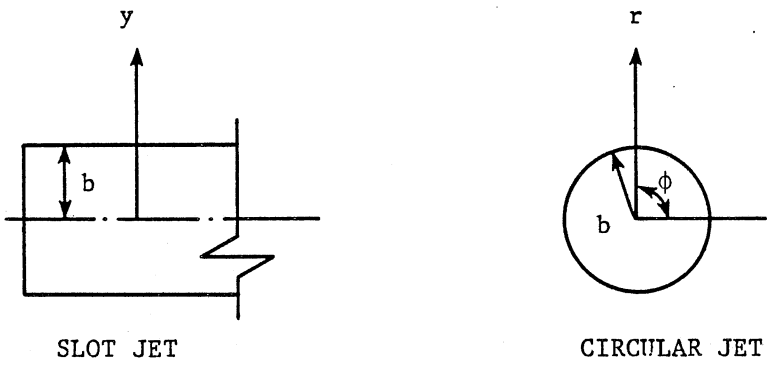

Fig. 2-3. Coordinate system used for buoyant jet analysis.

2-3-2 Analysis of the Governing Equations

a). The equation of state

If jet fluids do not contain some species of dissolved or suspended material the density is only related to the fluid temperature through the equation of state $\rho = \rho(T)$. However, when fluids are discharged with some species a concentration equation for tracer concentration

$$u\frac{\partial C}{\partial s} + v\frac{\partial C}{\partial y} = -\frac{1}{y^{\beta}}\frac{\partial(y^{\beta}\overline{v'C'})}{\partial y} \qquad (2.23)$$

is added to the governing equations and consequently the equation of state becomes $\rho = \rho(T,C)$ where C is the tracer concentration and equal to unity for pure fluids (no tracer). A linear equation of state is assumed by some investigators such as Shirazi and Davis (1972), Sini and Pekeyser (1986), and Sotil (1971). This assumption is represented by Oberbeek-Boussinesq equation $\rho = \rho_1(1 - \beta(T-T_1))$ where β is the thermal coefficient of volumetric expansion of the fluid, assumed constant sometimes for cases with limited temperature ranges. In this study, a non-linear function of state for pure water is adopted. It reads

$$\rho = 1000(0.999876 + 6.166*10^{-5}T - 8.14577*10^{-6}T^2 + 4.7612*10^{-8}T^3) \qquad (2.24)$$

This empirical relation is valid for the temperature range from 0°C to 30°C which is often encountered in temperature stratified lakes and reservoirs.

b). The Conservation Equation of Thermal Energy and Buoyancy

Either equation 2.20 or 2.21 can be taken as one of the governing equations. With the assumption of a linear temperature-density relationship (with a constant β) equations 2.20 and 2.21 are equivalent. However the thermal coefficient for volumetric expansion for water β is a strong function of temperature in the range 5°C-40°C, as indicated in Fig. 2-4, Tatom (1985) has studied errors from using the conservation of buoyancy approach derived from both equation 2.21 and an approximation form of the conservation of thermal energy equation 2.20 with a constant β. He concluded that any jets predicted by models based on the conservation of buoyancy principle will tend to overestimate the effect of buoyancy. Some indication of the magnitude of these errors is obtained for specific cases ($\theta_0 = 30°$, uniform ambients and low temperature range 5°C-22°C) by comparing the simulation results of using density and temperature respectively as a substance (dilution factor 20% larger, velocity 40% higher, width 12% smaller and horizontal penetration 21% shorter).

Moreover the Boussinesq approximation for inertial terms of the basic equations may reduce the validity of equation 2.21. It is therefore proposed that the use of the conservation of buoyancy principle should be avoided wherever possible, especially for cases involving low water temperatures and large Richardson number, and energy equation 2.20 should be employed instead of equation 2.21.

c). **The y-Momentum Equation**

With the assumption of hydrostatic pressure variations, equation 2.18 could be cancelled from the governing equations and replaced by $p = p_h$. This leads to the previous analytical models

commonly used by many investigators (Hirst 1971, Fox 1970, Abraham 1972, Fan and Brooks 1966, Anwar 1969). Anwar (1969) gave an explaination for this approximation that the pressure force $(\Delta\rho/\rho_0$ $g\cos\Theta(\sin\Phi)^\beta)$ due to the change of density with the jet acting over the cross-sectional area does not enter into the momentum equation because this force is almost equal, but in the opposite direction to the eddy stress $(-1/y^\beta\ \partial(y^\beta\overline{v'^2})/\partial y\ )$ occuring at the edge of the jet. Meanwhile, the force due to the curvature of the jet, i.e. $-u^2\ \partial\Theta/\partial s$ $(\sin\Phi)^\beta$, was ignored. In the present study approximate " order of magnitude analysis " is applied to equation 2.18 to examine the significances of the pressure force (due to the change of density) term and centrifugal force term under various conditions.

Using the boundary layer type of assumptions (V<<U and Y<<S), the density difference term in equation 2.18 is of the order of $Ri_1\cos\Theta(\sin\phi)^\beta$ and the curvature term is of $d\Theta/ds\ (\sin\phi)^\beta Y$, while the order of the term of pressure is unity, where Ri_1 is the local Richardson number of the jet, which is expressed as

$$Ri_1 = (\Delta\rho/\rho_0)\ g\ Y/U^2 \qquad (2.25)$$

where Y is the length scale for y and ∂y and U is the velocity scale for u and ∂u. It is obvious that the orders can rise to unity for cases of high Richardson number and large curvature of the jet and the hydrostatic pressure assumption is acceptable only for the case of lower local Richardson number and small jet curvature. The equation 2.18, therefore, is retained as one of the governing equations. The effects of taking account of the pressure p_d are discussed with the examination of each term of fluxes in the conservation equations in

section 2-3-3 and the calculated results in section 2-4.

2-3-3 The Integral Model

The y-momentum equation 2.18 is integrated with respect to y from y to ∞ to obtain the expression for the pressure p_d. With the substitution of p_d into the axis-momentum equatiion 2.17 and the mechanical energy equation 2.19, the partial differential equations 2.16-2.20 are integrated over the jet cross-section area with respect to y from 0 to ∞ by employing the Leibniz rule. Then a set of coupled ordinary differential equations are obtained. The integral approach has been to apply similarity hypothesis for velocity and temperature profiles and the concept of entrainment coefficient.

a). Round Jets

First of all, integrating the radial momentum equation with respect to ϕ from 0 to π leads to a 2-dimensional r-momentum equation for round jets with the assumption that variables involved in the equation are independent of ϕ. Then the integral of the mentioned 2-d equation from r to ∞ gives the expression for p_d, on which the boundary conditions $\overline{v'^2} = 0$ and $p_d = 0$ at $r = \infty$ hold

$$p_d = -\rho_0\overline{v'^2} + 2\rho_0\int_r^\infty(\Delta\rho/\rho_0\ g\cos\theta + u^2 d\theta/ds)dr/\pi \qquad (2.26)$$

Using this equation to eliminate p_d in equation 2.17 and 2.19, concerning

$$\partial p_h/\partial z = -\rho_a g \qquad (2.27)$$

$$\partial p_h/\partial r = -\rho_a g\cos\theta \qquad (2.28)$$

$$\partial p_h/\partial s = -\rho_a g\sin\theta \qquad (2.29)$$

assuming

$$\partial\overline{u'^2}/\partial s \approx \partial\overline{v'^2}/\partial s \qquad (2.30)$$

and letting

$$p_{bc} = \frac{2}{\pi}\int_r^\infty \left(\frac{\Delta\rho}{\rho_0} g\cos\Theta + u^2\frac{d\Theta}{ds}\right)dr \qquad (2.31)$$

the integral conservation equations of the volume, the momentum, the internal energy and the mechanical energy can be written in the following forms:

$$\frac{d}{ds}\int_0^\infty rudr = \lim_{r\to\infty}(rv) = E \qquad \text{(by definition)} \qquad (2.32)$$

$$\frac{d}{ds}\int_0^\infty (ru^2 + rp_{bc})dr = -\int_0^\infty r\frac{\Delta\rho}{\rho_0} g\sin\Theta dr \qquad (2.33)$$

$$\frac{d}{ds}\int_0^\infty \left(r\frac{u^3}{2} + rup_{bc}\right)dr = -\int_0^\infty ru\frac{\Delta\rho}{\rho_0} g\sin\Theta dr - \int_0^\infty u\frac{\partial(\overline{ru'v'})}{\partial r}dr \qquad (2.34)$$

$$\frac{d}{ds}\int_0^\infty ru\Delta Tdr = -\int_0^\infty rudr\frac{dT_a}{ds} \qquad (2.35)$$

where $\Delta T = T - T_a$

where T_a is the ambient temperature, equation 2.32 is the definition of the entrainment function which is discussed later in the section 2-3-4. The solution of the above equations requires the specification of the velocity and the temperature difference profiles. The most common profile used by investigators is Gaussian which is suggested from experiment (Rouse 1952, Rodi et al, 1982 and 1986). The use of the Gaussian profile requires the assumption of axisymmetry , which is generally valid for simple jets in uniform environments with small centerline curvatures. The velocity profile is defined as

$$u = u_m\exp(-\eta^2)$$

whre u_m is the centerline velocity, and η is the similarity variable defined by

$$\eta = r/b$$

where b is an arbitrarily defined characteristic width of the jet velocity profile, Here for Gaussian form the nominal half width of the jet is $b = \sqrt{2}\sigma$, where σ is the standard deviation, i.e. the measure of dispersion, defined as $\sigma^2 = \int_0^\infty (r-r_c)^2 u dr / \int_0^\infty u dr$ ($r_c = 0$).

Experiments further suggest a Gaussian distribution for the temperature difference. The profile has been observed to reach a fully developed stage much earlier than the velocity profile. This results in a decay of the centerline temperature difference from the jet discharge before the end of the velocity potential core of ZFE. The difference in the relative rates of development of the two profiles is characterized by a coefficient λ which is related to the turbulent Schimidt or Prandtl number by $Sc = 1/\lambda^2$ and defined as the ratio of the width of the temperature difference profile to the width of the velocity profile. The coefficient λ can therefore be thought of as a measure of the jet's ability to disperse temperature relative to momentum, a dispersion ratio. With this definition of λ, the temperature difference profile is written as

$$\Delta T = \Delta T_m \exp(-\eta^2/\lambda^2)$$

Substitution of the velocity and temperature difference profiles into equation 2.32-2.35 results in a set of coupled ordinary differential equations as follows:

$$\frac{d(u_m b^2/2)}{ds} = E_r \qquad (2.36)$$

$$-\left(\frac{d}{ds}\left(\frac{u_m^2 b^2}{4} + P_{bc}\right)\right) = -\frac{1}{2}\frac{\Delta\rho_m}{\rho_0} g b^2 \lambda^2 \sin\Theta \tag{2.37}$$

$$-\left(\frac{d}{ds}\left(\frac{u_m^3 b^2}{6} + u_m P^*_{bc}\right)\right) = -\frac{\Delta\rho_m}{\rho_0} g u_m b^2 \frac{\lambda^2}{1+\lambda^2} \sin\Theta - 2 I_r u_m^3 b \tag{2.38}$$

$$-\left(\frac{d}{ds}\left(\Delta T u_m b^2 \frac{\lambda^2}{2(1+\lambda^2)}\right)\right) = -\frac{u_m b^2}{2}\frac{dT_a}{ds} \tag{2.39}$$

where $P_{bc} = 2/\pi(I_{6r} b^3 \lambda^3 \cos\Theta g \Delta\rho_m/\rho_0 + I_{5r} u_m b^3 d\Theta/ds)$

$P^*_{bc} = 2/\pi(T_{6r} b^3 \lambda^3 \cos\Theta g \Delta\rho_m/\rho_0 + T_{5r} u_m b^3 d\Theta/ds)$

$$I_r = \frac{1}{u_m^3 b}\int_0^\infty u \frac{\partial(r\overline{u'v'})}{\partial r} dr$$

In which $I_{5r} = \int_0^\infty \psi \int_\psi^\infty \exp(-2\eta^2) d\eta d\psi$

$$T_{5r} = \int_0^\infty \psi \exp(-\psi^2) \int_\psi^\infty \exp(-2\eta^2) d\eta d\psi$$

$$I_{6r} = \int_0^\infty \tau \int_\tau^\infty \exp(-\xi^2) d\xi d\tau$$

$$T_{6r} = \int_0^\infty \tau \exp(-\tau^2) \int_\tau^\infty \exp(-\xi^2) d\xi d\tau$$

By a numerical integration technique, the constants are obtained as $I_{5r} = 0.29$, $I_{6r} = 0.41$, $T_{5r} = 0.193$ $(=2I_{5r}/3)$ and $T_{6r} = 0.273$ $(= 2I_{6r}/3)$. The shear stress integral in equation 2.38 is assumed to be similar so that it scales as

$$\int_0^\infty u \frac{\partial(r(\overline{u'v'}))}{\partial r} dr = I_r u_m^3 b \tag{2.40}$$

b) Slot Jets

The similarities between axisymmetric and plane jets are indeed significant; however, the equations describing each are dissimilar enough to establish certain quantitative differences in the motion. The experimental data of Kotsovinos (1977) show that velocity and temperature difference distributions of slot jets also can be adequately represented by Gaussian distributions.

Applying the same integral approach as used for round jets to the governing equations for slot jets yields the following integral equations

$$\frac{d(\sqrt{\pi}u_m b/2)}{ds} = E_s \tag{2.41}$$

$$\frac{d}{ds}\left(\frac{\sqrt{\pi}u_m^2 b}{2\sqrt{2}} + P_{bcs}\right) = -\frac{\sqrt{\pi}}{2}\frac{\Delta\rho_m}{\rho_0} gb\lambda\sin\theta \tag{2.42}$$

$$\frac{d}{ds}\left(\frac{\sqrt{\pi}u_m^3 b}{2\sqrt{3}} + u_m P^*_{bcs}\right) = -\frac{\sqrt{(\pi\lambda^2)}}{\sqrt{(1+\lambda^2)}} gu_m b \frac{\Delta\rho_m}{\rho_0}\sin\theta - 2I_s u_m^3 \tag{2.43}$$

$$\frac{d}{ds}\left(\Delta T_m u_m b \frac{\sqrt{\pi}\lambda^2}{2\sqrt{(1+\lambda^2)}}\right) = -\frac{\sqrt{\pi}u_m b}{2}\frac{dT_a}{ds} \tag{2.44}$$

where $P_{bcs} = I_{6s}\Delta\rho/\rho_0\ g\lambda^2 b^2\cos\theta + I_{5s}u_m^2 b^2\ d\theta/ds$

$P^*_{bcs} = T_{6s}\Delta\rho/\rho_0\ g\lambda^2 b^2\cos\theta + T_{5s}u_m^2 b^2\ d\theta/ds$

$$I_s = \frac{1}{u_m^3}\int_0^\infty u\frac{\partial(\overline{u'v'})}{\partial y}\,dy$$

in which $I_{5s} = 0.50$, $I_{6s} = 0.707$, $T_{5s} = 0.577$ $(= \sqrt{(2/3)}\ I_{5s})$ and $T_{6s} = 0.408$ $(= \sqrt{(2/3)}\ I_{6s})$ from the numerical integral of $\int_0^\infty\int_\eta^\infty \exp(-2\eta^2)d\eta d\eta$, $\int_0^\infty\int_\xi^\infty \exp(-\xi^2)d\xi d\xi$, $\int_0^\infty \exp(-\eta^2)\int_\eta^\infty \exp(-2\eta^2)d\eta d\eta$

and $\int_0^{\infty}\exp(-\eta^2)\int_{\xi}^{\infty}\exp(-\eta^2)d\xi d\eta$.

c). The Examination of Flux Terms

The present model takes account of the pressure (p_{bc}) due to the change of density and the curvature of jets. The contribution of the flux terms due to the density difference and the curvature through the pressure on the left-hand side of the conservation equations 2.37-2.38 for round jets and 2.42-2.43 for slot jets is examined. One can then see the significance of these terms and thus, the simplication of the integral model can be made for practical application.

Let F_i represent the inertia term of fluxes in the left-hand side of the equations, F_b the pressure term (due to density difference) of fluxes and F_o the centrifugal force term. Then the ratios of fluxes are as follows:

$F_b/F_i = 0.522\lambda^3 Ri_1\cos\Theta$ and

$F_c/F_i = 0.74 d\Theta/ds\ b$ for round jets

and $F_b/F_i = 0.564\lambda^2 Ri_1\cos\Theta$ and

$F_c/F_i = 0.80 d\Theta/ds\ b$ for slot jets, where b is the measure of jet width, and Ri_1 is the local Richardson number, $Ri_1 = (\Delta\rho_m/\rho_0)\ (g2b/u_m^2)$, which is in the range 0–1.0, λ is in the range 0.8–1.3, details for λ will be given in section 2-3-4.

It is obvious that the ratios could reach about unity for both round and slot jets. The density difference and curvature terms could be of about the same order. The effects of density difference and curvature on the jet motion separately through the pressure and then the contribution of these terms to the fluxes on the left-hand side of

the conservation equations can be considered of importance compared to the dominant inertia term.

However, it is found that the pressure force due to the density difference and the centrifugal force are of the same order, but always of the opposite sign and change their signs due to $\Delta\rho_m$ and $d\theta/ds$ changing signs along the trajectory of the jet in stratified ambients. The centerline trajectory of the jet can be divided into three regions, as shown in Fig. 2-5, positive buoyancy, neutral buoyancy and negative buoyancy. There is no negative buoyancy region for jets in uniform environments (ρ_a = constant). Based on the above mentioned characteristics of the forces and the jet trajectory in stratified ambients, it can be seen that the effects of density difference and curvature respectively are negligible in the neutral region, significant but counteracting each other in positive and negative regions. Quantitative analysis of these effects on the jet motion through the pressure will be presented with the calculation results in section 2-4.

2-3-4 **Entrainment and Dispersion**

A flow predominantly in one direction whose magnitude (flowrate) changes in that direction must, in order to satisfy continuity, induce a secondary flow in a plane normal to the primary flow direction. In the jet, this secondary flow has been called entrainment because it brings environmental fluid into the jet. With entrainment, the concentration of a tracer carried by the jet is reduced with increasing distance from the source. A generalized entrainment function is formulated which accounts for the effects of buoyancy and

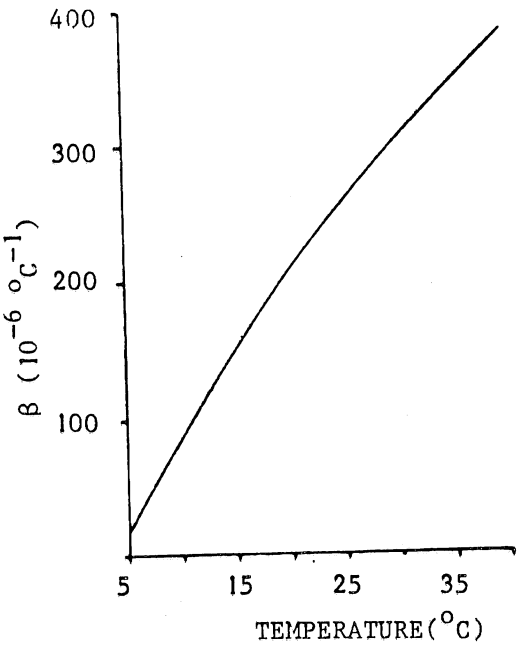

Fig. 2-4. Thermal coefficient of volumetric expansion for water as function of temperature (after Tatom).

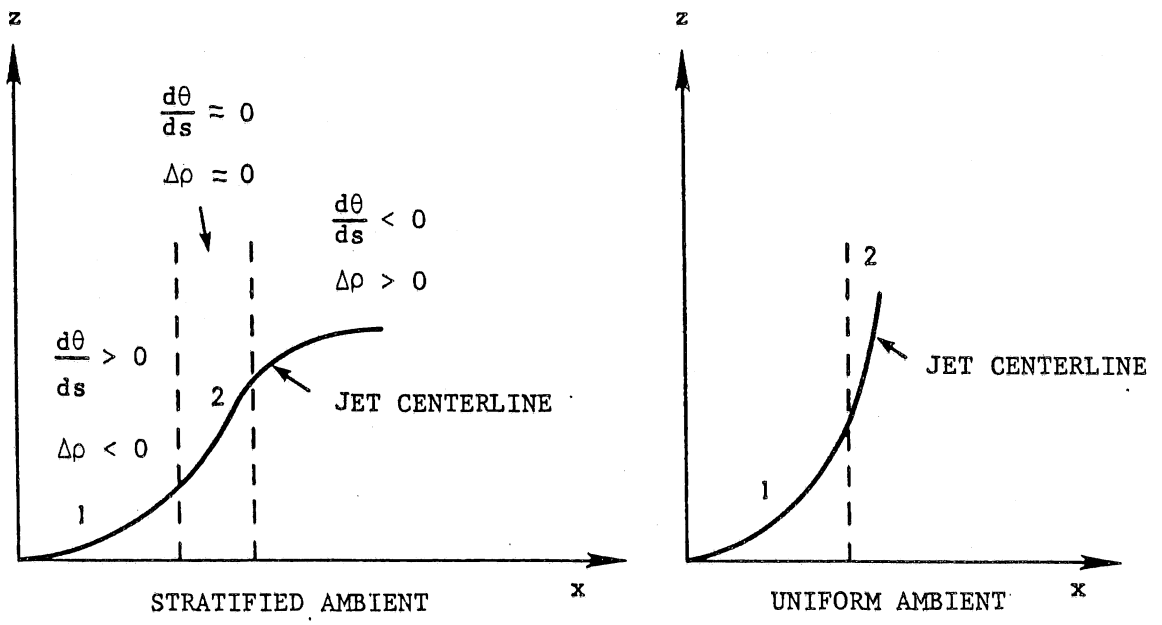

Fig. 2-5. Schematic diagram of jet centerline trajectory.

jet orientation.

The above formulation of the equation describing the jet does not explicitly include any effects of turbulence. However the entrainment function defined in equation 2.33, and the coefficient λ are an indirect way of including turbulence effects. The entrainment principle implies a general valid unique relationship to exist between the local rate of entrainment and local conditions. The general approach has been to assume that the entrainment rate , E, is proportional to the jet periphery and the jet centerline velocity. this relationship is formulated as

$$E_r = bu_{er} \text{ and } u_{er} = \alpha_r u_m \quad \text{for round jets, and}$$

$$E_s = u_{es} \text{ and } u_{es} = \alpha_s u_m \quad \text{for slot jets}$$

where u_{er} or u_{es} is called the entrainment velocity and α_r and α_s is the entrainment coefficient. The simplest generalization of the entrainment function (as well as the one most frequently used) is that α is assumed to be a universal constant. The typical values are α_{jr}=0.057, α_{js} = 0.063, α_{pr} = 0.083 and α_{ps} = 0.16 (Koh and Brooks 1975) where subscripts j, p, r, and s indicate jets, plumes, round and slot respectively. A number of investigators have found however that there is no unique entrainment coefficient, and they employed different assumptions for entrainment functions for turbulent jets. Fox (1970) developed an interesting and useful method for determining a (vertical) plume in a stratified or uniform ambient by using the integral conservation equations. Abraham (1965) replaced the entrainment assumption by essentially assuming a rate or spread of the jets while List and Imberger (1973), through dimensional reasoning and

from experimental data, deduced that α and λ must be functions of the local Froude number and local jet spreading angle in the case of a vertical buoyant jet in a uniform environment.

According to Fox the entrainment relationship did not require any external specificaton other than the assumption of similarity common to all plume theories, and the added assumption of a similar distributed (u'v'). The difficulty of specifying the entrainment has been avoided in Fox's analysis by use of a mean kinetic energy balance, i.e. the mechanical energy equation. A more general formulation suitable for buoyant jets discharged at arbitrary angle can be derived by using the method used by Fox, which accounts for the effects of buoyancy and jet orientation.

Combination of equation 2.36, 2.37 and 2.38 yields expression for the entrainment function for round jets

$$\alpha_r = -\lambda^2 Ri_1 \sin\theta/2 + \{Ri_1 \sin\theta(2\lambda^2-\lambda^4)/(1+\lambda^2) + 12I_r\} / \{2 + 8(I_{6r}\lambda^3 - 2I_{5r}\lambda^2)Ri_1\cos\theta/\pi\} \quad (2.45)$$

where the local Richardson number $Ri_1 = \Delta\rho_m g 2b/\rho_0 u_m^2$, 2b is equal to the diameter of the jet, D.

Solving the equation 2.41, 2.42 and 2.43 leads to the entrainment relationship for slot jets

$$\alpha_s = -\sqrt{\pi}\lambda Ri_1 \sin\theta/2\sqrt{2} + 0.5\pi\{Ri_1 \sin\theta\sqrt{(5\lambda^2-\lambda^4)}/\sqrt{2(1+\lambda^2)} + 4\sqrt{3}I_s/\sqrt{\pi}\} / \{\sqrt{\pi} + (\sqrt{2}I_{6s}\lambda_2 - 2I_{5s}\lambda^2)Ri_1\cos\theta\} \quad (2.46)$$

where $Ri_1 = \Delta\rho_m g 2b/\rho_0 u_m^2$.

With the assumption of hydrostatic pressure, i.e. excluding the effects of buoyancy and curvature through the dynamic pressure, the entrainment relations 2.45 and 2.46 could be simplified to

$$\alpha_r = (-\lambda^2 + 3\lambda^2/(2 + 2\lambda^2))\sin\theta Ri_l + 6I_r \quad (2.47)$$

$$\alpha_s = (-\sqrt{(\pi/2)}\lambda + \sqrt{(3\pi^2/(4 + 4\lambda^2))})\sin\theta Ri_l + 2\sqrt{3}I_s \quad (2.48)$$

Equation 2.47 is similar to one derived by Hirst (1971) and 2.48 is the extension of Fox's equation for vertical jets to any jet angle. The terms containing Ri_l in the entrainment relationships represent the incremental entrainment due to the buoyancy force. The terms containing I_r and I_s represent the entrainment due to internal jet turbulence. Equation 2.47 and 2.48 shows that coefficient α is not a universal constant.

In order to determine α_r and α_s one must decide upon the values of λ_r and λ_s , the dispersion ratio, and the values of $|I_r|$ and $|I_s|$, the shear stress integral.

Due to the difficulty of specifying the shear stress profile ($u'v'$), the integral I_r and I_s was determined only empirically by several investigators. For nonbuoyant jets ($Fr = \infty$, $Ri = 0$), Albertson's data suggest that $6I_r = 0.057$. Fan's study recommends that $\alpha_{js} = 0.063$ for a simple momentum jet (slot). Brooks and Koh (1975) suggested $\alpha_{js} = 0.068$. The value of I_s is therefore determined by expression $2\sqrt{3}I_s = 0.063$ if $\alpha_{js} = 0.063$ is chosen.

Fostal and Gaylord (1955), among others, have shown experimentally that the turbulent Schmidt number lies in the range $0.75 < S_c < 0.85$ for round jets, for which $1.08 < \lambda_r < 1.16$. Hirst's study shows that $\lambda_r = 1.11$ for large Fr and $\lambda_r = 1.16$ for small Fr. According to Koh and Brooks' study, empirical values of λ_r are found to be 1.16, which is common used.

Various values of λ_s (for slot jets), $0.89 < \lambda_s < 1.40$, are chosen

by a number of investigators (Wright 1980, Brooks 1980, and Sotil 1971). The common used value of λ_s which is suggested by the experiments of Rouse et al (1952) is 0.9.

One could adjust the parameters I, the shear stress integral, and λ, the dispersion ratio, in such a way that the predictions of experimental data are, in some sense, optimized, but this optimization is highly subjective and somewhat dependent on the experimental flows considered. The way for specifying the value of the dispersion ratio λ may be specifying one that agrees well with experimental results. The results of varying the value of λ over a wide range (0.8-1.4) are investigated in section 2-4.

With the specification of I_r and I_s and the choice of $\lambda_r = 1.16$ and $\lambda_s = 0.9$, equation 2.47 and 2.48 can be written as

$$\alpha_r = 0.057 - 0.485 Ri_1 \sin\theta \qquad (2.49)$$

and

$$\alpha_s = 0.063 - 0.101 Ri_1 \sin\theta \qquad (2.50)$$

2-3-5 Final Set of Differential Equations

The integral conservation equations 2.36-2.39 and 2.41-2.44 can be normalized and nondimensional solutions can be presented with quadrature for linearly stratified ambients. A method of solution for the case of a buoyant jet in an arbitrary stratification has been determined by Ditmars (1969) and Sotil (1971). Since the temperature gradient dT/dz is no longer constant with elevation and along the jet trajectory, the equations can not be normalized as in the case of linear stratification. The solution is found in dimensional parameters. By simplifying and combining the equations, the following

set of first-order ordinary differential equations for quadrature is obtained:

$$\frac{du_m}{ds} = 2\left(\alpha - \frac{db}{ds}\frac{u_m}{b}\right) \tag{2.51a}$$

$$\frac{db}{ds} = [\pi\alpha + \pi Ri_1\lambda^2\sin\theta/4 + A_r(\cos\theta d\Delta\rho_m/ds - \Delta\rho_m\sin\theta d\theta/ds) + 4\alpha I_{5r}bd\theta/ds] \,/\, [0.5\pi - 3\lambda^3 I_{6r}Ri_1\cos\theta + 2I_{5r}bd\theta/ds] \tag{2.52a}$$

$$\frac{d\Delta T_m}{ds} = -\left(\frac{1+\lambda^2}{\lambda^2}\sin\theta\frac{dT_a}{dz} + \frac{2\alpha\Delta T_m}{b}\right) \tag{2.53a}$$

where $A_r = 2\lambda^3 gb^2 I_{6r}/(u_m^2\rho_0)$, for round jets.

$$\frac{du_m}{ds} = \left(\frac{2\alpha}{\sqrt{\pi}} - \frac{db}{ds}\frac{u_m}{b}\right) \tag{2.51b}$$

$$\frac{db}{ds} = [\sqrt{2}\alpha + \sqrt{\pi}Ri_1\lambda\sin\theta/4 + A_s(\cos\theta d\Delta\rho_m/ds - \Delta\rho_m\sin\theta d\theta/ds) + 4\alpha I_{5s}bd\theta/ds/\sqrt{\pi}] \,/\, [0.5\sqrt{(\pi/2)} - \lambda^2 I_{6s}Ri_1\cos\theta] \tag{2.52b}$$

$$\frac{d\Delta T_m}{ds} = -\left(\frac{\sqrt{(1+\lambda^2)}}{\sqrt{\lambda^2}}\sin\theta\frac{dT_a}{dz} + \frac{2\alpha\Delta T_m}{\sqrt{\pi}\,b}\right) \tag{2.53b}$$

where $A_s = \lambda^2 gb^2 I_{6s}/(u_m^2\rho_0)$, for slot jets.

The T-ρ relationship (equation 2.24), the appropriate entrainment function (equation 2.45-2.46) and jet geometry equations

$$\frac{d\theta}{ds} = -2\lambda^2\Delta\rho_m g\cos\theta/(u_m^2\rho_0) \tag{2.54a}$$

$$\frac{d\theta}{ds} = -\sqrt{2}\lambda\Delta\rho_m g\cos\theta/(u_m^2\rho_0) \tag{2.54b}$$

$$dx/ds = \cos\theta \tag{2.55}$$

$$dz/ds = \sin\Theta \tag{2.56}$$

are required for the final set of differential equations. Equations 49a and 49b are obtained by writing z-momentum equations for the jet flow, applying the integral approach and combining them with the integral equations (Eqns. 2.37 and 2.42 from the s-momentum equations).

When the jet fluid contains some contaminants , equations for tracer concentration derived from the conservation equation of tracer mass (equation 2.23), have to be added.

$$Cu_m b^2 = C_0 u_0 b_0^2 \tag{2.57a}$$

for round jets and

$$Cu_m b = C_0 u_0 b_0 \tag{2.57b}$$

for slot jets.

The seven variables u_m, b, ΔT_m, Θ, x, y and C are function of s only. Then the centerline trajectory, jet width, centerline velocity, temperature difference and centerline dilution can be determined by solving equations 2.51-2.57 combined with 2.24 and 2.45-2.46 for given initial values for the jet parameters. The present model is compared to the previous model with the assumption of hydrostatic pressure distribution. The difference between the two models is indicated by the expression of db/ds. In the present model db/ds has extra terms containing I_5 and I_6. These terms represent the effects of density difference and curvature on the pressure. Letting $I_5 = 0$ and $I_6 = 0$ leads to a simple model combined with entrainment relationship Eqns. 2.47 and 2.48 and the T-ρ relationship.

Examination of these equations has shown that they are valid

either for buoyant jet or for a sinking (negative buoyant) jet. They reduce to the proper forms in case of a uniform ambient temperature environment $dT_a/ds = 0$, and for the case of a simple momentum jet (no buoyancy flux: $dT_a/ds = 0$ and $\Delta T_m = T_m - T_a = 0$).

2-3-6 Correction for the ZFE

The equations outlined above describing the gross behavior are valid only in the zone of established flow (fully turbulent region) where Gaussian profiles may be used. An adequate similarity solution for the zone of flow establishment is not available for a buoyant jet in a stratified ambient fluid. Albertson et al. (1950) have described the ZFE for a simple momentum jet. For the lack of more complete information of this region, their results are applied to define the initial conditions for the calculations for the ZEF. The initial values for jet trajectory (x,y), jet width and centerline temperature difference are therefore corrected to account for the ZFE. This zone was found to extend 6.2 (Singh suggested 4.5) source diameters for round jets and 5.2 source widths for slot jets from the actual source. The initial buoyancy of the jet is assumed to have no effects on the geometry in this zone. This assumption is good for the case with high Froude numbers (above about 10, Shirazi, 1972) but at lower Fr the

development length becomes less and the initial deflection due to buoyancy becomes apparant.

For round jets it can be seen that conservation of thermal energy ($2\int_0^\infty \pi r \Delta T u dr = \pi D_0^2 \Delta T_0 u_0/4$) and momentum ($2\pi\int_0^\infty ru^2 dr = \pi D_0^2 u_0^2/4$) between source and zone of established flow requires that the initial value of b be $D_0/\sqrt{2}$, where D_0 is the source diameter, and the initial value of ΔT_m ($= T - T_a$) be $(1+\lambda^2)/(2\lambda^2)$ times the value at the source, ΔT_0. For slot jets, in the same way, the initial half width b is adjusted to $\sqrt{(2/\pi)}W_0$, W_0 is the width at the source and the initial value of $\Delta T = T - T_a$ is corrected by multiplying it by the factor $\sqrt{(1+\lambda^2)}/\sqrt{(2\lambda^2)}$ to account for the effects of ZFE.

2-4 Results and Discussion

The set of first-order differential equations (Eqns. 2.55-2.61) describing the bulk behavior of the jet can be solved using a FORTRAN program. The numerical integrations were performed on a Cyber computer, adopting the Runge-Kutta method of integration . The integration of these equations by quadrature is a stepwise calculation along the trajectory. The local ambient temperature gradient, dT_a/dz, at the elevation corresponding to that point on the trajectory is specified so that the calculation of the jet parameters proceeds with continual adjustment of the ambient temperature gradient with changes in elevation, z. For the convenience of comparison, results shown and discussed in this section are limited to the case of linear stratification, dT_a/dz = constant. Numerical results obtained with the method and the system of ordinary differential equations are

compared with experimental data. Analysis and discussion of both the present approach and the conventional approach for the integral models are presented. The general characteristics of a slot jet are qualitatively identical with those of a round jet, although there are different equations describling each.

The centerline density and velocity decay, width growth and centerline dilution along the axis in round buoyant jet discharged vertically and horizontally in linearly stratified ambients are shown in Fig. 2-6. All other conditions are the same. The centerline dilution ratio is defined as the ratio of the centerline concentration of a conservative tracer substance at the given coordinates to that of the initial discharge. The initial value of this parameter is $(1+\lambda^2)/(2\lambda^2)$ because of the correction for the ZFE. It can be seen that u_m and $\Delta\rho_m$ of the vertical jet decay faster than that of the horizontal jet, especially beyond the neutral point ($\Delta\rho = 0$). The density difference changes sign much closer to the source when the fluid is discharged vertically. Physically, near the maximum height of rise, the vertical jet falls out of a jet pattern because of the horizontally spreading and mathematically, the equations derived with the similarity assumption and Gaussian profiles are no longer valid quantitatively.

Fig. 2-7 shows the the centerline dilution and trajectory of round jets discharged horizontally with various initial Froude numbers Fr_0. Fig. 2-8 shows comparisons between numerical calculations and experimental measurements of the centerline trajectory for several round buoyant jets discharged at various angles to stably stratified

ambients studied by Fan (1967). The quality of prediction is quite good for these flows. The calculations and measurements along jet axis are in essential agreement. The effects of ambient stratification and discharge angles on the jet trajectories are shown in Fig. 2-9 and Fig. 2-10 for slot jets.

Based on the integral conservation equations 2.33-2.37 describing the bulk characteristics of the jet flow, the volume flux, μ, the kinematic buoyancy flux, β, and the kinematic momentum flux, m, are defined as

$$\mu = \int_0^\infty 2\pi r u dr$$

$$\beta = -\int_0^\infty 2\pi r u g \Delta\rho/\rho_0 dr$$

$$m = \int_0^\infty 2\pi r u^2 dr$$

for round jets and

$$\mu = \int_0^\infty 2u dy$$

$$\beta = -\int_0^\infty 2u g \Delta\rho/\rho_0 dy$$

$$m = \int_0^\infty 2u^2 dy$$

for slot jets.

Approximate solutions for the maximum height of rise of a slot vertical jet and the centerline dilution at the terminal height were developed by a length scale analysis and experimental results by

Wright (1979). The fundamental argument is that the source volume flux is only important near the soure, the momentum flux next determines flow behavior, and finally the buoyancy effects becomes predominant. Based on dimensional reasoning, characteristic length scales associated with a description of this behavior are $l_Q = Q^2/M$, $l_M = M/B^{2/3}$ and $l_b' = B^{1/3}/\varepsilon^{1/2}$ for slot jets and $l_Q = Q/M^{1/2}$, $l_M = M^{3/4}/B^{1/2}$ and $l_b' = B^{1/4}/\varepsilon^{3/8}$ for round jets in which Q, M and B are the source volume, momentum and buoyancy flux respectively.

Neglecting the influence of initial volume the maximum height of rise, i.e. the top of the jet, z_t is related to M, B and ε. In particular, l_M/l_b' measures the relative important of the initial momentum, initial buoyancy, and the ambient density stratification. For buoyant jets that behave like plumes, $l_M/l_b' \ll 1$ and like momentum jets, $l_M/l_b' \gg 1$. The dilution in a jet at its maximum centerline rise, defined as $S_M = C_0/C_m$, can also be similarly correlated with length scales and fluxes.

The numerical calculations for z_t of the present integral model are compared with Wright's experimental data for slot jets as shown in Fig. 2-11 where $z_t = z_m + b$, z_m is the maximum centerline height of rise and b is the jet width. As Fig. 2-11 shows, the numerical and experimental results are in fairly good agreement but do not agree precisely. The assumption of similar velocity profiles of the theoretical model probably contributes to this deviation. The average jet momentum vanishes only when the centerline velocity goes to zero. It is assumed that a zero average momentum flux corresponds to the maximum rise of the numerical solution. In reality, Gaussian velocity

profiles are not valid near the maximum rise.

Fig. 2-12 and 2-13 show the comparison of numerical calculations and Lee's experimental results (1986) for z_t and S_M for slot jets discharged at a angle of 45°. The calculated results of z_t and S_M for round jets with various discharge angles are shown in Fig. 2-14. Fig. 2-15 and Fig. 2-16 show predictions of neutral points of jet centerlines z_n and the maximum height z_m plotted against Froude number Fr_0 for round jets discharged to a linearly stratified ambient. The results show that the increase in the Fr_0 does not necessarily contribute to the increase in the maximum height of the jet rise in cases of horizontal jets.

The above results show that the maximum rise z_t is reduced as the discharging angle is decreased with the same initial conditions for both slot and round jets, while z_t for the horizontal jet and the vertical jet varies with l_M/l_b' in the opposite directions in cases of round jets at $l_M/l_b' \gg 1$ and that the centerline dilution at the maximum rise is increased more slowly with l_M/l_b' for larger discharging angle θ_0.

The entrainment coefficient α and the local Richardson number Ri_1 as a function of dimensionless distance for a horizontal rond jet is shown in Fig. 2-17. Based on the analysis in section 2-3-4, α depends on the local Richardson number Ri_1. Since the jet is operating in a stably stratified environment, the buoyancy is continuously decreasing. Eventually buoyancy becomes negative, and when it does Ri_1 changes sign from negative to positive. In addition, the velocity is decreasing toward a very small value so that Ri_1 also increasing.

The entrainment may eventually change sign. It can be seen that the maximum entrainment occurs at the level below and near the neutral point and the transition from the positive entrainment to negative is at the level above the neutral point and near the maximum rise. The negative entrainment phenomenon is due to the fact that at the maximum height of rise jet fluid leaves the upflow region and enters into the downflow region and finally spreads out as analyzed in section 2-1 for basic jet behavior. The entrainment relationship (Eqns. 2.49-2.54) therefore allows a spreading velocity out of the jet near the maximum penetration. However, one can not expect the similarity analysis to hold quantitatively in this negative buoyancy regime, although the model gives a rather good prediction of the maximum level.

Fig. 2-18 shows the variation of maximum entrainment with initial Froude number Fr_0 and stratification number St. It can be seen that Fr_0 has more effects on α_m than St has.

The results of varying the value of the dispersion ratio λ over a range 0.9-1.4 for round jets are shown in Fig. 2-19. The values λ_s = 0.9 and λ_r = 1.16 are chosen in this study which are suggested by experiments and common used by investigators.

Based on the examination of each term of fluxes in the integral conservation equations in section 2-3-3 . The quantitative analysis of density difference and curvature effects on the jet motion through the presssure are presented here with the calculation results (see Fig. 2-20-2-21). The effect is negligible at the inertia-dominant region, i.e. near-source region and considerable at the buoyancy-

dominant region. At the positive and neutral buoyancy regions the ratios F_c/F_i and F_b/F_i are in the range of 10%-20%, but could reach to 40%-60% in the negative buoyancy region. However, due to the opposite signs, the effect of buoyancy and curvature is less than 5% at the first two regions and 25% near the jet top. It can be seen that the effect is large and increases rapidly near the height of maximum rise. The collapse phenomena may be related to this.

It is obvious that the simple model from the hydrostatic pressure assumption is appropriate for the positive and neutral buoyancy regions of the jet as it is applied to the lake mixing by buoyant jets which is the other portion of this study. Nevertheless, the dynamic pressure due to buoyancy and jet curvature should be considered in the study of jet properties (e.g. maximum penetration and dilution) at the negative buoyancy region near the maximum rise.

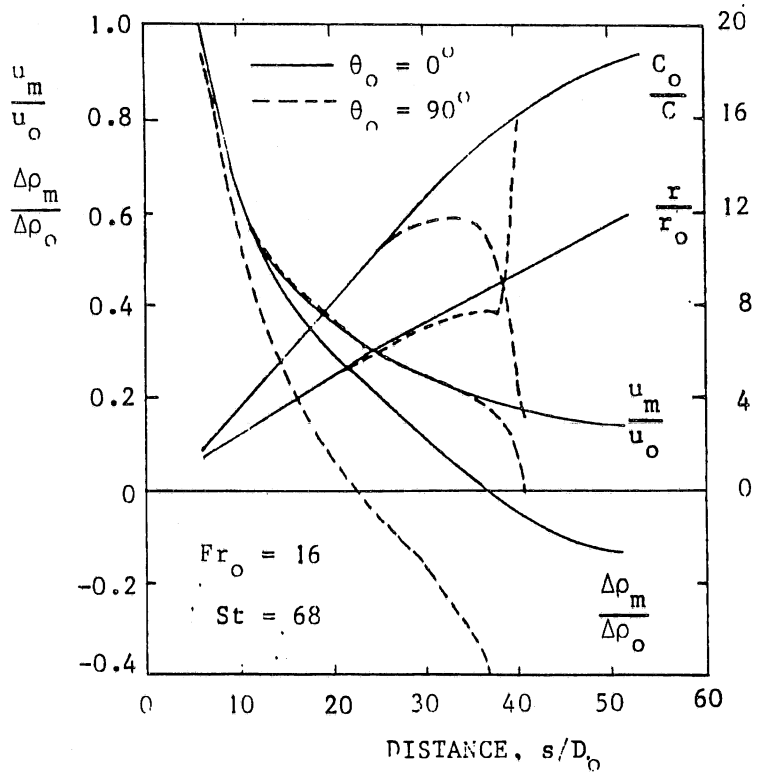

Fig. 2-6. General characteristics of the vertical horizontal jet from a round source.

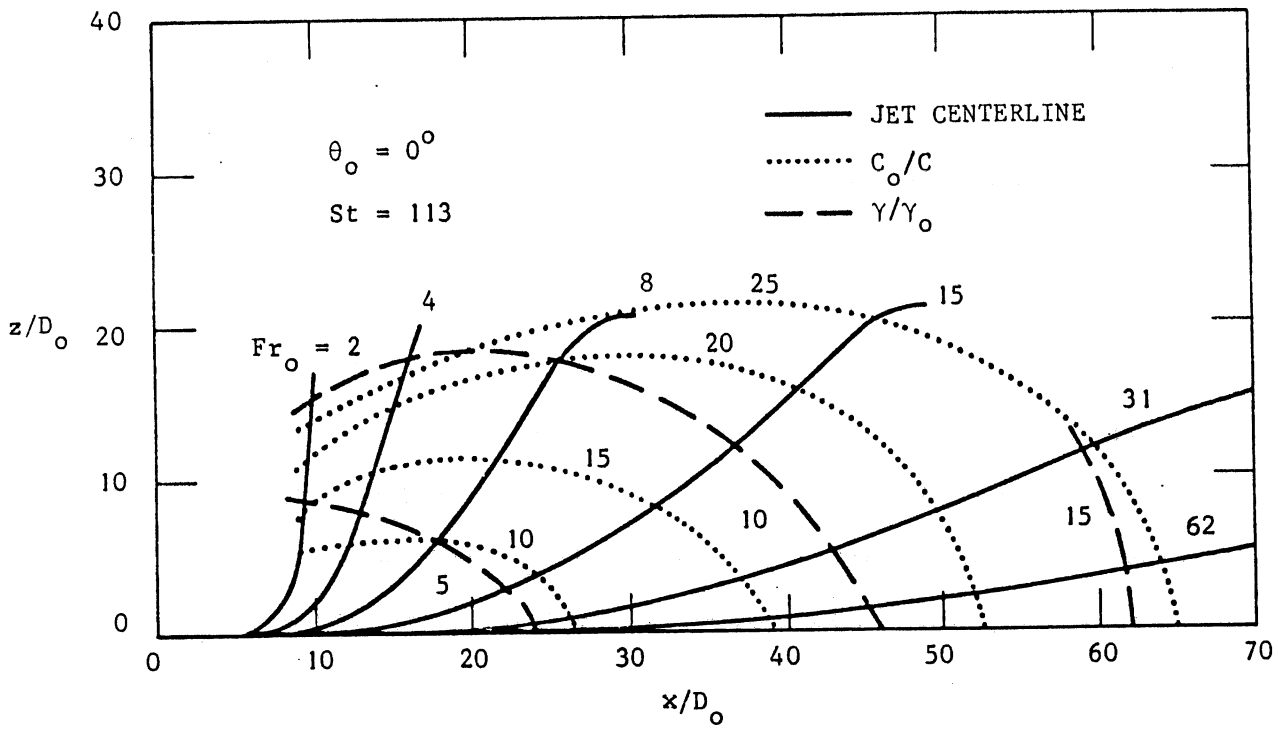

Fig. 2-7. Dilution and trajectory for round buoyant jets discharged horizontally to stratified fluids.

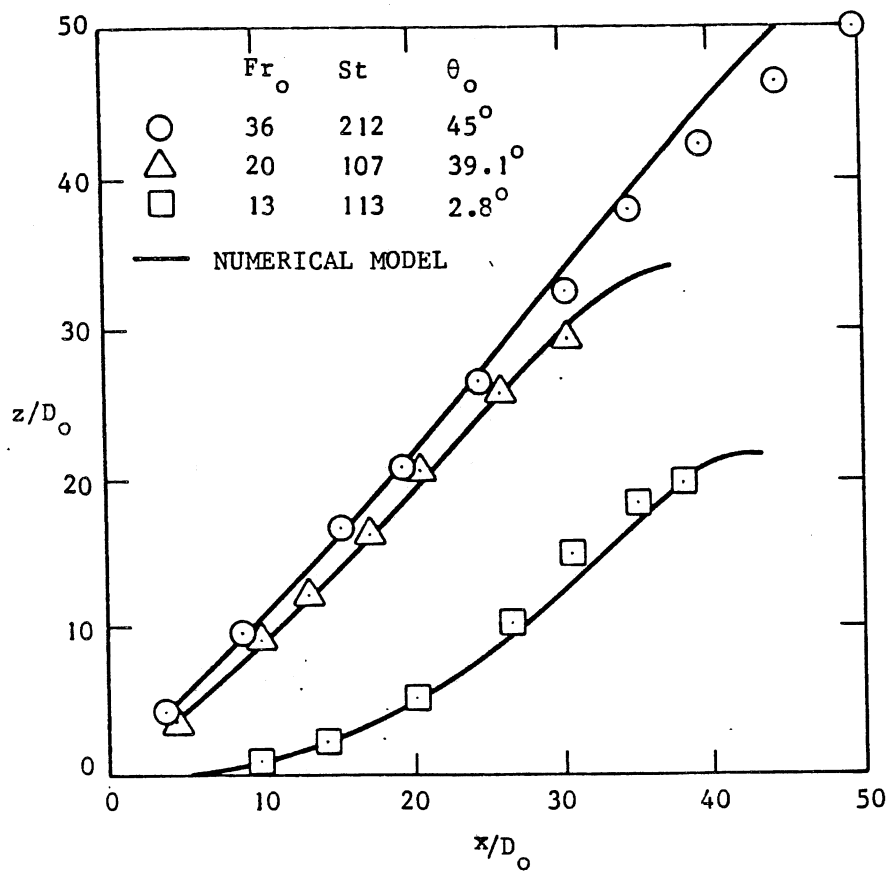

Fig. 2-8. Trajectory for round buoyant jets in stratified ambients.

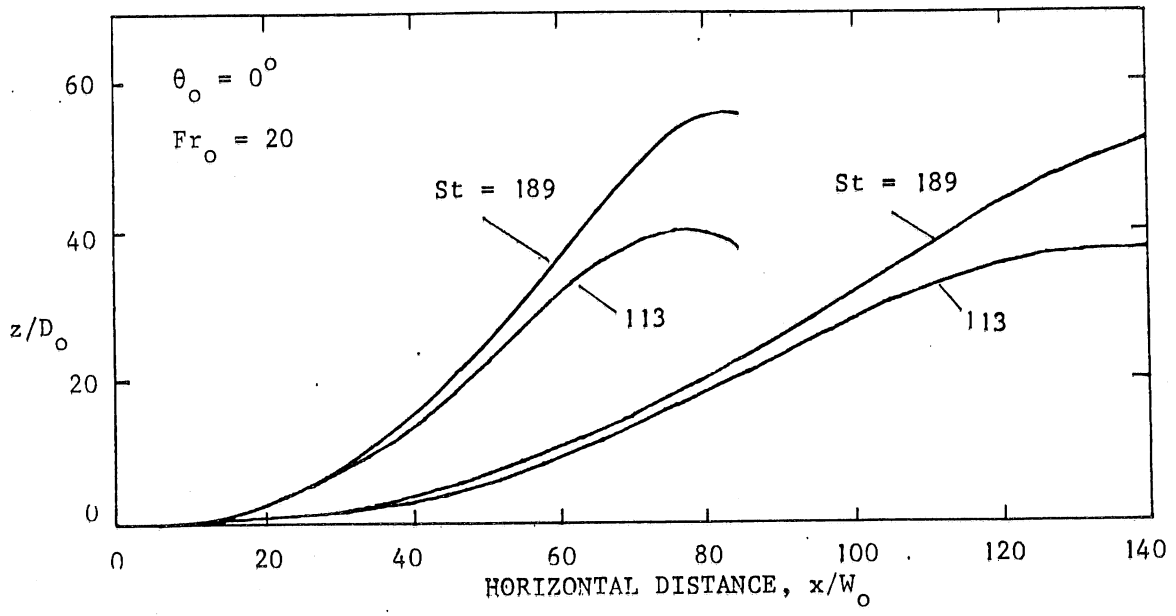

Fig. 2-9. Trajectory for slot jets with various St.

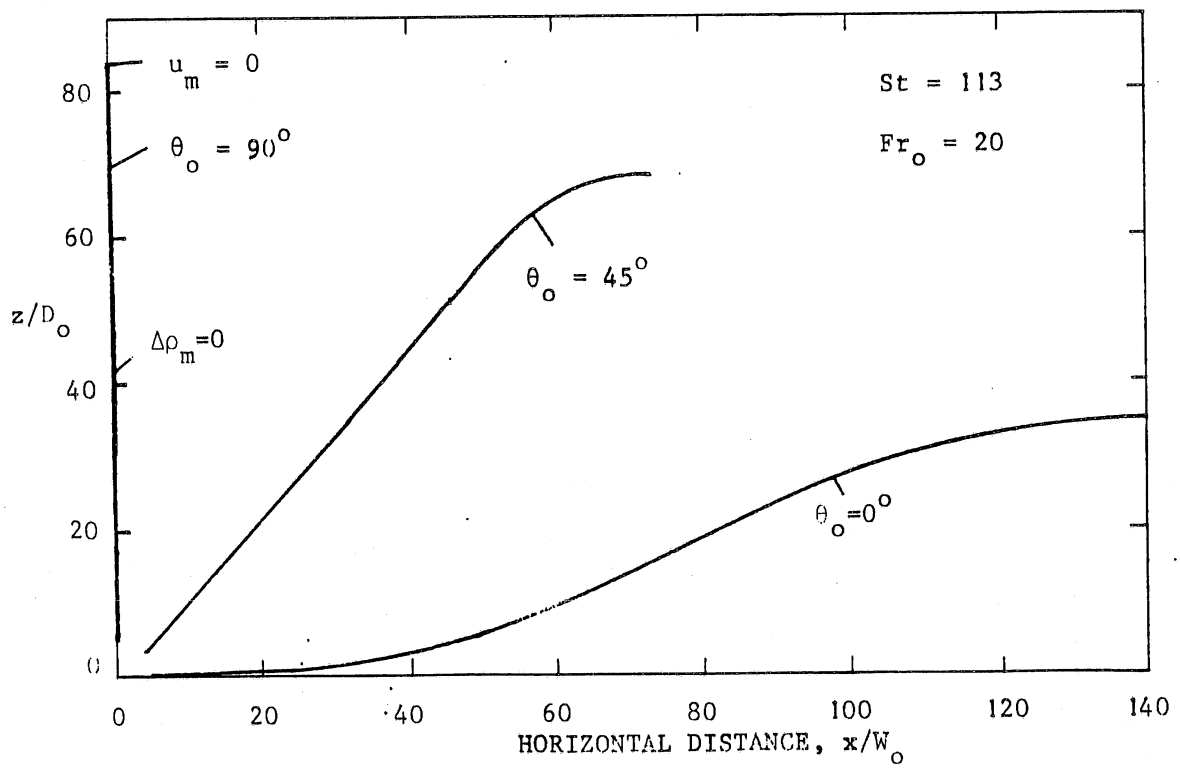

Fig. 2-10. Trajectory of slot jets discharged at various angles.

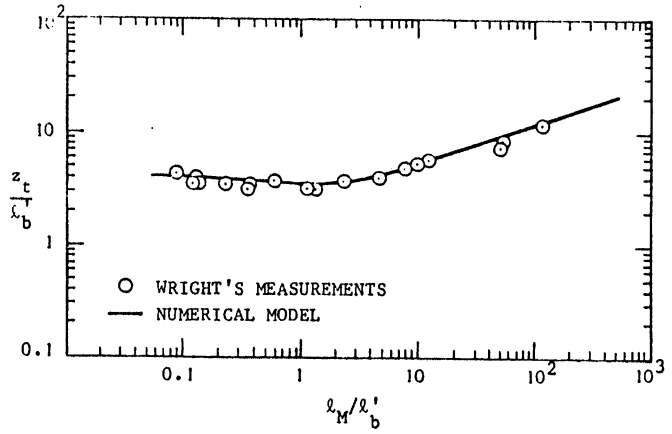

Fig. 2-11. Maximum height of rise for slot jets discharged vertically.

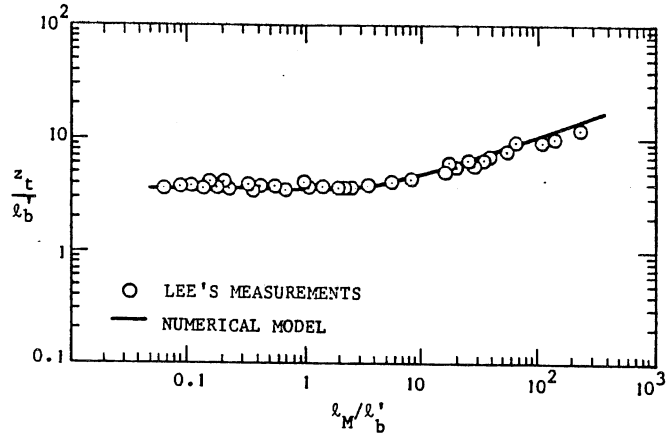

Fig. 2-12. Maximum height of rise z_t for slot jets with $\theta_o = 45^o$.

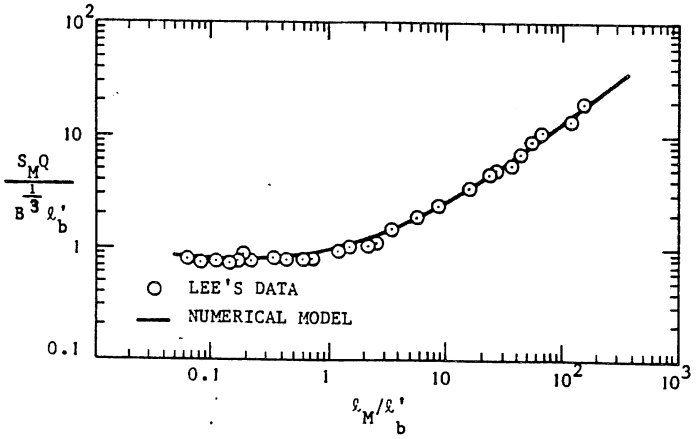

Fig. 2-13. Dilution in spreading layer for slot jets with $\theta_o = 45^o$.

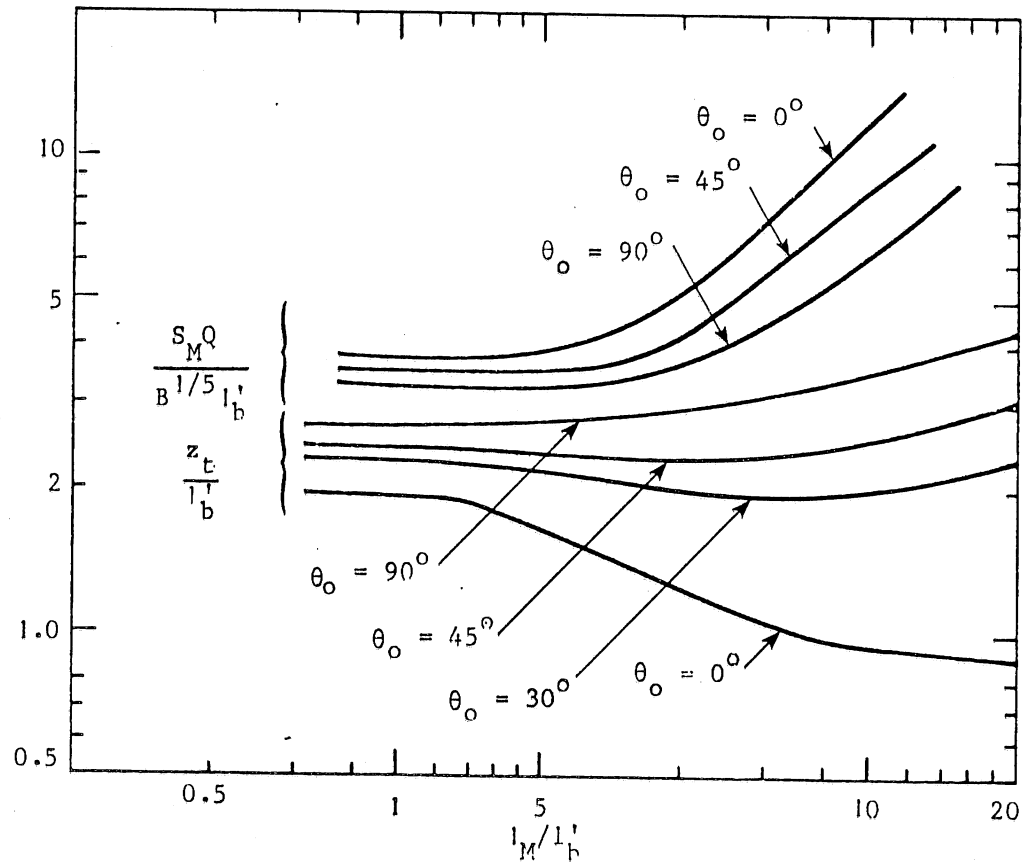

Fig. 2-14. Maximum height of rise z_t and dilution S_M for round jets.

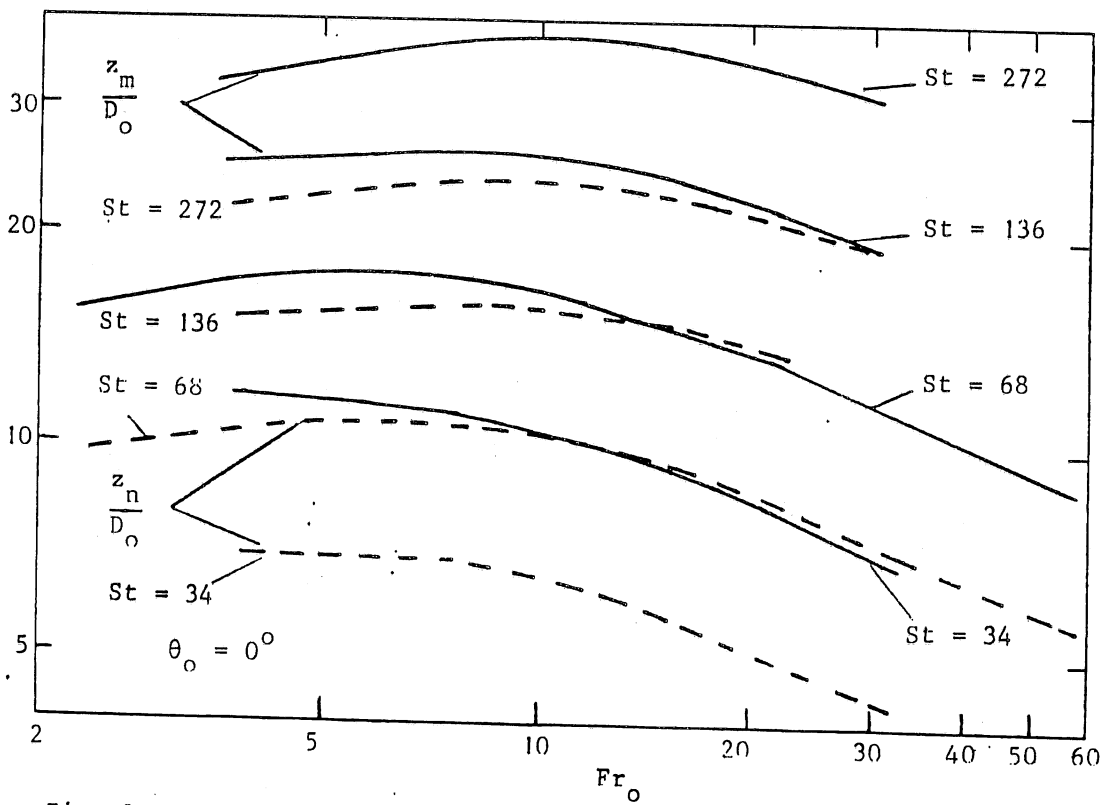

Fig. 2-15. Maximum height z_m and neutral height z_n for round jets.

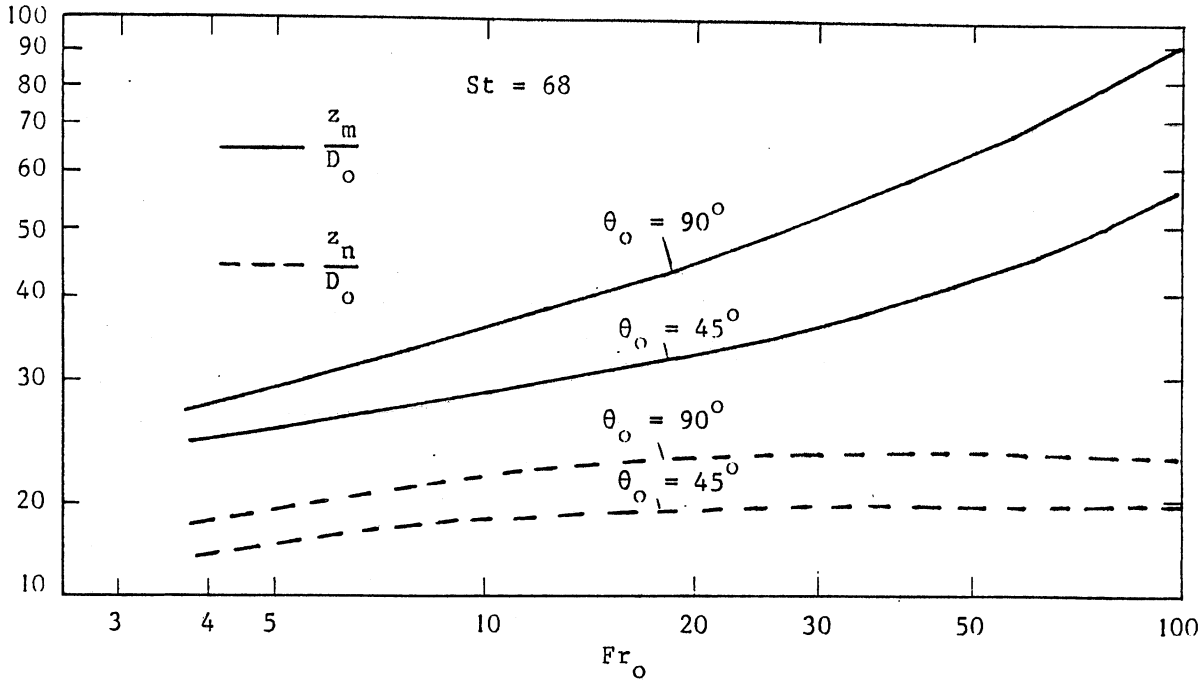

Fig. 2-16. Variation of z_m and z_n of round jets with Fr_o.

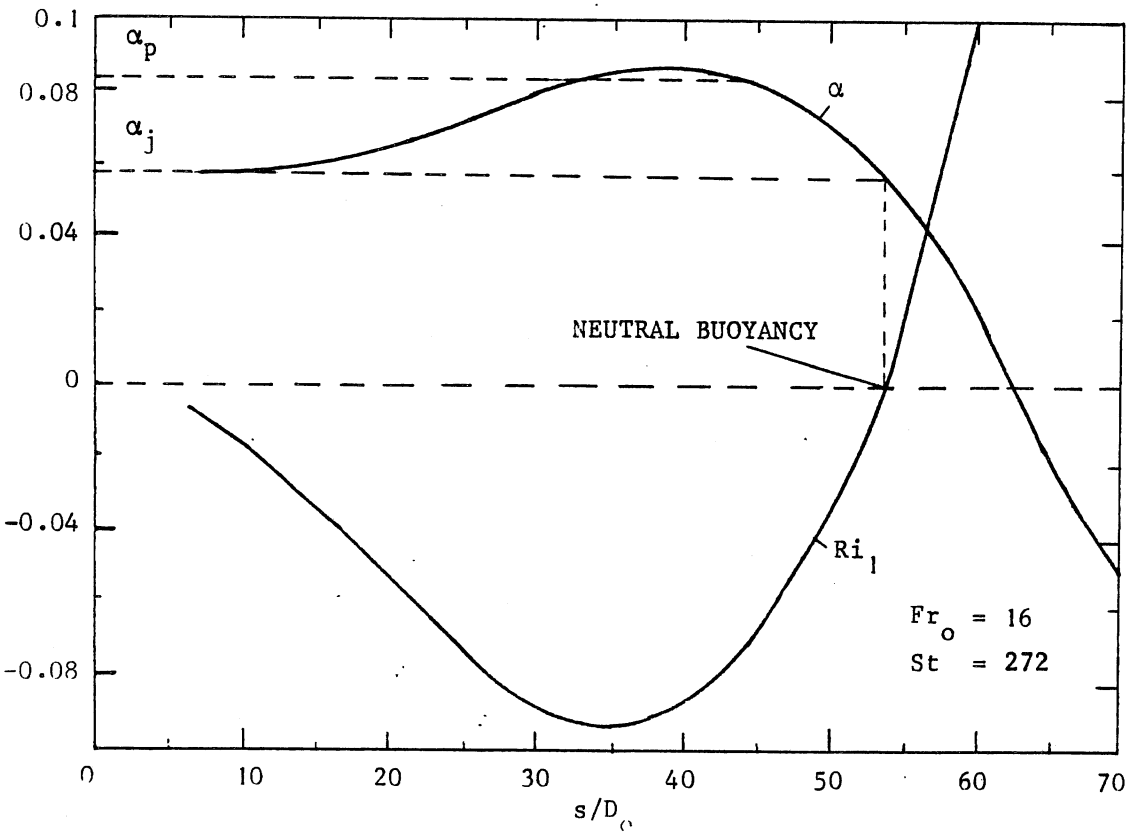

Fig. 2-17. Entrainment coefficient as a function of dimensionless distance from an axisymmetric source.

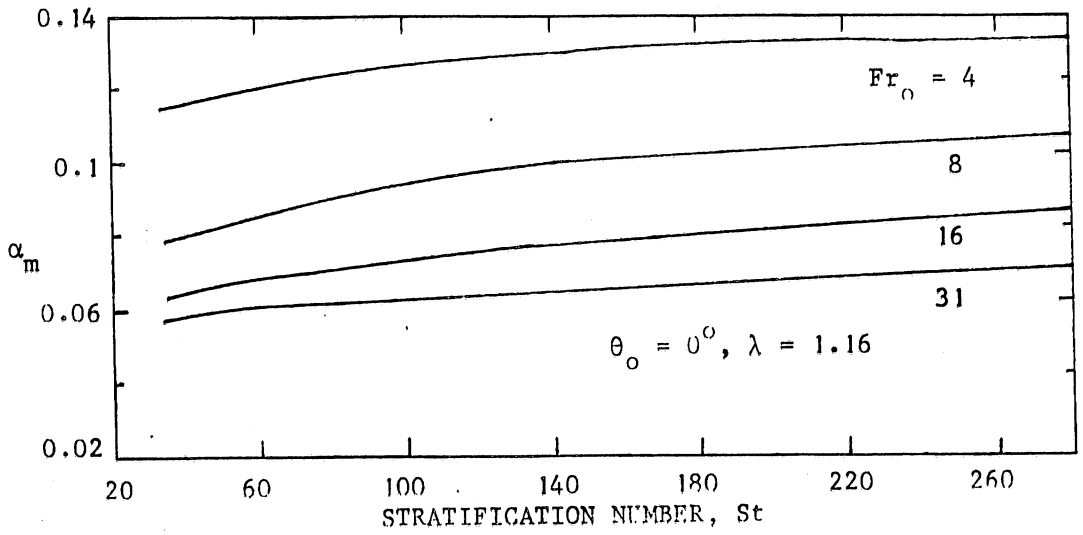

Fig. 2-18. Variation of maximum entrainment with Fr_o and St for horizontal round jets.

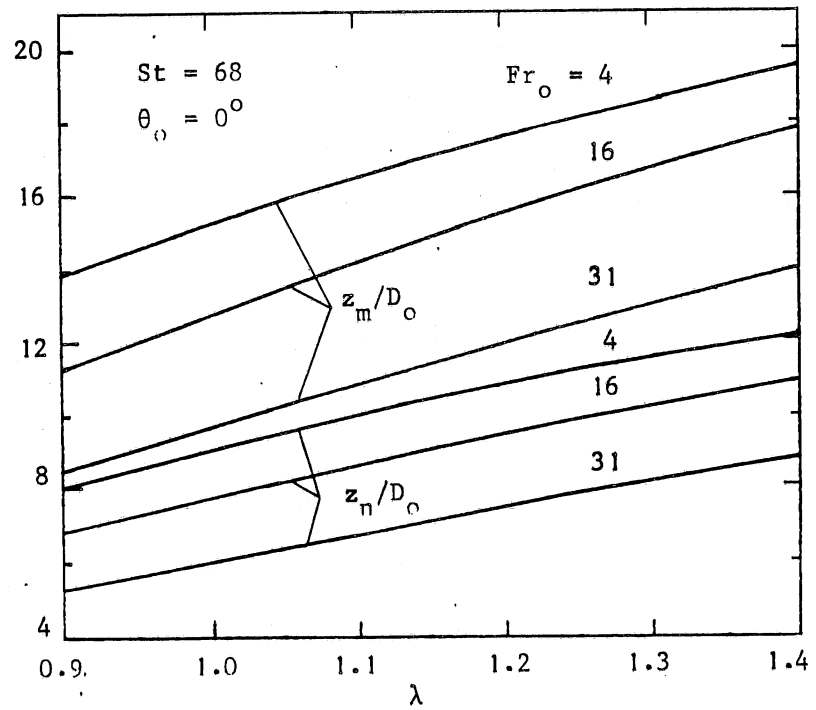

Fig. 2-19. Maximum height of rise of a horizontal jet from a round source as a function of the dispersion ratio for various Fr_o.

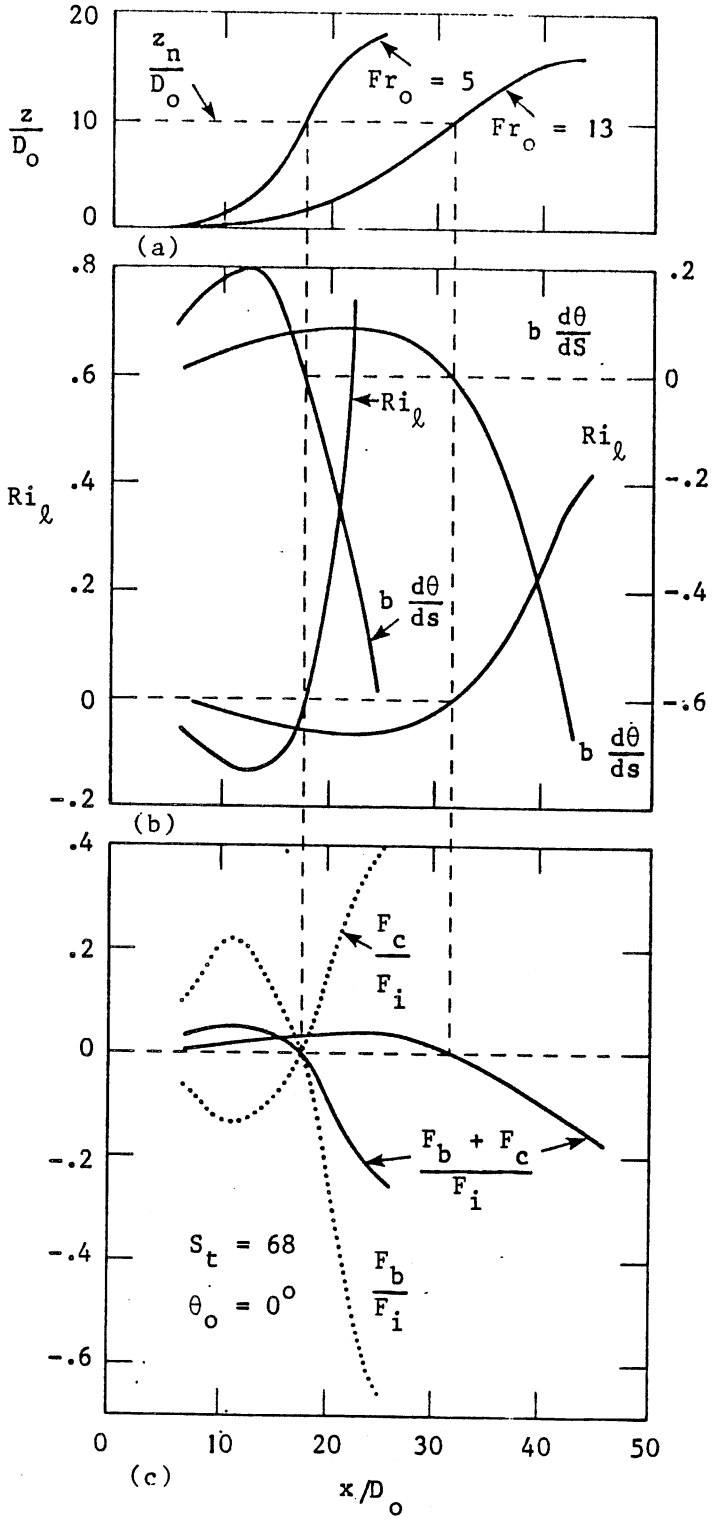

Fig. 2-20(a)(b). General characteristics of the round jet. (c) Variation of flux ratios.

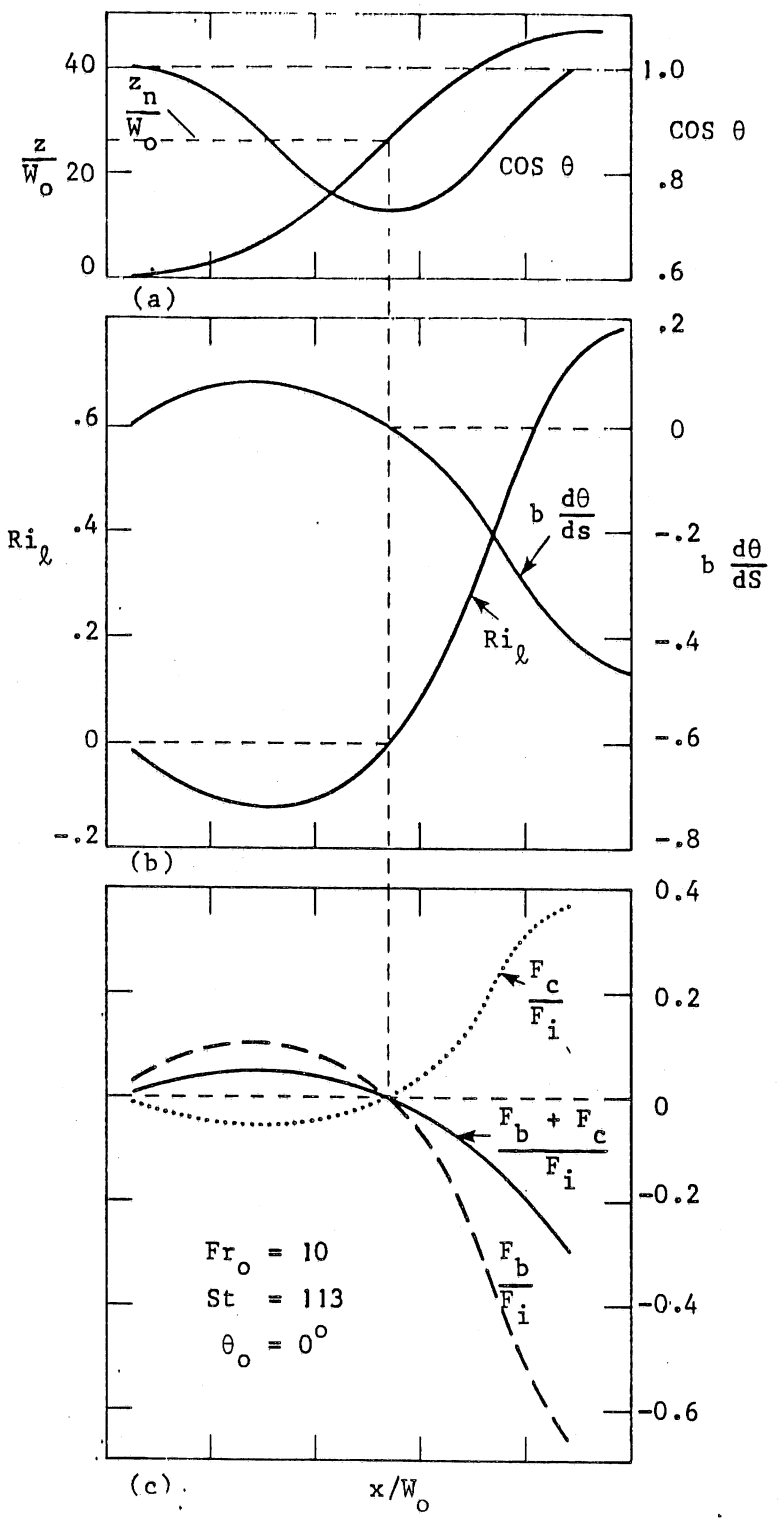

Fig. 2-21(a)(b). General characteristics of the slot jet. (c) Variation of flux ratios.

CHAPTER 3 Mixing of Temperature-Stratified Lakes and Reservoirs With Buoyant Jets

The quality of water in lakes and reservoirs is often related to the temperature structure. Thermal or density stratification often causes a general deterioration of the water quality. Mixing of temperature-stratified lakes or reservoirs using recirculating pumping systems can counteract the deterioration of water quality through jet mixing. In this chapter the physical aspects of the mixing processes are investigated, the development of a simulation model predicting the process of temperature destratification is presented, and the simulation results are given and compared with the existing field data. A comparison with laboratory experimental data is presented in the next chapter.

3-1 Mechanism of Mixing with Buoyant Jets

The pumping system considered in this study withdraws water from one elevation in a temperature-stratified lake or reservoir and discharges it to another elevation in the form of a buoyant jet as shown in Fig. 3-1. The pumping system is characterized by its properties of transport to and from the stratified ambient water. The buoyancy of the jet, positive or negative with respect to the surrounding fluid, causes it to move upward or downward. The fluid motion created by the pumping system is characterized by the buoyant jet generated at the discharge and the selective withdrawal layer in the stratified environment.

The behavior of a buoyant jet in a temperature-stratified environment has been analysed in section 2-1. The jet does not extend to the surface as contrasted with a buoyant jet in a uniform ambient. After reaching the maximum height of rise, the jet flow spreads horizontally and intrudes into the ambient fluid at its equilibrium level. Essentially, the buoyant jet entrains fluid from the ambient along its trajectory and delivers this fluid to a different elevation in the environment at a volume rate of flow several times the initial rate. In addition, the shear at the interface of the intruding layer and the ambient fluid at the equilibrium level will enhance the turbulent mixing in this region. Moreover, circulation patterns may be established by the entrainment of fluid and deliverance of fluid by the jet.

The withdrawal of fluid from the stratified lake or reservoir is restricted to a zone of limited thickness or height and temperature. This feature is different from the withdrawal from an environment of uniform temperature.

3-2 Governing Equations and a Simulation Model for Destratification

A simulation model is developed to predict in a gross way the changes in temperature stratification during the mixing process. It is a simple model of the pumping system and lake or reservoir, ignoring the complex fluid mechanical details which are considered having little effect on the overall response of the lake or reservoir to the mixing.

3-2-1 Governing Equations

For the simple simulation model several assumptions are made as follows:

1) The stratified lake or reservoir is considered to be a closed system. Mass is conserved and there is no energy exchange through the boundaries, except those of the pumping system. The temperature-depth profiles for a given pumping system are determined by the initial temperature profile. This assumption is valid if the mixing proceeds much more rapidly than changes in the heat budget. The present study isolates the effect of the pumping system from all external conditions (e.g. heat transfer through boundaries and wind effect).

2) The surfaces of constant temperature (or isothermal surfaces) of the stratified water are assumed to be horizontal planes. This means that the temperatures at a given elevation are the same throughout the lake or reservoir and that the only variation in temperature occurs vertically during the mixing process (one-dimensional problem), although the mechanics of the buoyant jet and withdrawal layer are treated in a three-dimensional manner. This assumption is correct for the lake or reservoir in a gross sense during mixing for the purpose of the simulation although it is obviously not true in the buoyant jet, return flow layers, or withdrawal layer.

3) The buoyant jet and withdrawal layers are assumed to be the only components of the mixing process that require modeling in the simulation. The natural mixing induced by the external factors (heat budget and wind), the turbulent mixing (eddy diffusivity) due to temperature gradients, and the contribution of horizontal motion of

the jet flow are considered to be small. It is assumed that the mixing due to the pumping system can be uncoupled from the other mixing process in the study of the response of the ambient water to the pumping system (creating the buoyant jet and selective withdrawal).

A stratified lake or reservoir is viewed in the one-dimensional sense as assumed above (see Fig. 3-2). The horizontal cross-sectional area, A, is a function of z, the vertical elevation. The relationship between A and z is assumed to be known. The response of the lake or reservoir to mixing is generated by the transfer of fluid between the region of buoyant jet and withdrawal layer and the region of stratified ambient. The pumping system removes fluid from the surrounding water body at various elevations and then injects it back into the ambient at other elevations.

The withdrawal layer and the buoyant jet remove or entrain fluid from the ambient as a whole. This fluid is transported by the enlarging buoyant jet until it is returned back into the ambient as a whole at its equilibrium level. The volume rate of flow per unit depth into or from the ambient water body at a given elevation is $q_e(z,t)$. It is positive for fluid transported into the ambient and negative for fluid extracted from the ambient.

Transport of fluid into and from the ambient at various elevations and the conservation of total mass require the fluid at some elevations to be moved up at a given time and at other elevations moved down. The effective transport velocity characterizing this vertical movements is $v(z,t)$.

Conservation of mass leads to the continuity equation

$$\frac{\partial(vA)}{\partial z} = q_e(z,t) \tag{3.1}$$

and conservation of heat requires that

$$A\frac{\partial T}{\partial t} + \frac{\partial(TvA)}{\partial z} = Tq_e \tag{3.2}$$

where T is the temperature of fluid in the lake or reservoir at the elevation z. T represents the temperature of the fluid transported into or from the ambient by the buoyant jet and withdrawal according to assumption 2).

Equation 3.2 is combined with Eqn. 3.1 and simplified as

$$\frac{\partial T}{\partial t} + v\frac{\partial T}{\partial z} = 0 \tag{3.3}$$

Eqn. 3.1 can be derived from the continuity equation for an incompressible stratified fluid by integrating over the horizontal area. Equation 3.3 follows from the heat conservation equation by neglecting vertical diffusion in the lake or reservoir and adopting the Boussinesque assumption (small density difference).

3-2-2 Analysis of the Governing Equations

The continuity equation relates the vertical transport velocity, v, to the transport from buoyant jet and withdrawal layer to the ambient, q_e, at a given time. The vertical distribution of q_e is required for the solution of the governing equations. The q_e due to the jet entrainment and selective withdrawal from the ambient is

negative and that due to flow return from jet into the ambient is positive.

Integrating of equation 3.1 gives

$$v(z) = \frac{1}{A(z)} \int_0^z q_e(\xi) d\xi \qquad (3.4)$$

It can be seen that the transport velocity v is positive above the equilibrium level and negative below.

The determination of q_e as a function of z at a given time requires the knowledge of the behavior of buoyant jet and withdrawal layer.

3-2-3 Application of Buoyant Jet Mechanics

Chapter 2 provides detailed information of the buoyant jet in a stratified ambient for the determination of the discharge or entrainment from the ambient into the rising round buoyant jet. The trajectory is calculated so that the entrainment q_e is known as a function of elevation z. The centerline velocity and width of the buoyant jet are known as a function of z to find q_e, the fluid entrainment from the ambient.

As previously discussed, the buoyant jet reaches a maximum height of rise at which the fluid in the jet is negatively buoyant with respect to the ambient fluid at that elevation. This is the elevation of zero vertical momentum and is predicted well by the model presented in Chapter 2, although the similarity assumptions break down. The fluid sinks back slightly to its eqilibrium level and spreads horizontally into the ambient. Although mixing occurs as the fluid reaches this level, the equilibrium level (or level of neutral

buoyancy) can be approximated by the elevation at which the center temperature (or density) in the rising jet is equal to the temperature (density) of the environment ($\Delta T_m = 0$).

The calculation of trajectory and the elevation at which $\Delta T_m = 0$ provides information for locating the elevation over which fluid is discharged back into the ambient.

The entrainment into the jet, $-q_e$, is the change in volume flux along distance. Combining Eqn. 2.38 and $E_r = \alpha_r u_m b$ (given in section 2-3-4) gives

$$\frac{d(\pi u_m b^2)}{ds} = 2\pi\alpha_r u_m b = -q_e \tag{3.5}$$

The integral $\int_0^z q_e(\xi)d\xi$ in eqn. 3.4 is the summation of all the jet entrainment up to the elevation z. This is simply the volume flux at z minus the initial fluid discharge, i.e.

$$\int_0^z q_e(\xi)d\xi = -\pi u_m(z)b^2(z) + Q_j \tag{3.6}$$

where Q_j is the jet discharge at the origin. Then

$$v(z) = -[\pi u_m(z)b^2(z) - Q_j]/A(z) \tag{3.7}$$

over the trajectory of the buoyant jet only.

3-2-4 Selective Withdrawal From Temperature-stratified Fluids

The thickness of the selective withdrawal layer and the distribution of velocity cross the layer (Fig. 3-3) are required to determine q_e for the simulation in this region. Brooks and Koh (1969) gave detailed information on the development of theoretical models for

selective withdrawal in stratified impoundments.

The flow is considered to be steady and 2-dimensional. From experiments performed by Debler and Yih (1958) the inviscid and nondiffusive withdrawal layer for a linearly stratified lake or reservoir can be expressed as

$$\delta/a = 2.7 \tag{3.8}$$

where $$a = (q^2/g\varepsilon)^{1/4} \tag{3.9}$$

$$\varepsilon = -\frac{1}{\rho_0}\frac{d\rho_a}{dz} \tag{3.10}$$

q is the discharge per unit width, and ε is constant. The solution indcates no growth in the thickness of the withdrawal layer with distance x from the source, but the inviscid and nondiffusive conditions under which it was found make it essentially a near-sink solution.

Since q is involved, equation 3.8 may be applicable only for a line sink. Spigel and Farrant (1984) proposed an expression for δ for a point sink:

$$\delta = 1.02(Q/N)^{1/3} \tag{3.11}$$

where $N = (\varepsilon g)^{1/2}$, Q is the total discharge.

Selective withdrawals associated with lakes or reservoirs are likely to be turbulent due to their large scale or large Reynolds numbers. Brooks and Koh presented the solution for turbulent, diffusive flow

$$\delta/a = 8.4(K_2 x/a)^{1/4} \tag{3.12}$$

for $2.7 < \delta/a < 13.7$,

$$\delta/a = 7.14(K_2 x/a)^{1/3} \tag{3.13}$$

for $\delta/a > 13.7$, where x is the distance from outlet. The coefficient K_2 is regarded as a universal constant with a value of 10^{-3}.

For a given density profile, δ is estimated by assuming a linear density gradient based on that at the elevation of the center line of the intake. A thickness near the intake is calculated using the solution to the inviscid and nondiffusive case given by Eqn. 3.11 for point sink and Eqn. 3.8 for line sink. The thickness of a turbulent withdrawal layer at the greatest distance, x, in the lake or reservoir from the sink is calculated by Eqn. 3.12 and 3.13. The two values for δ are assumed to bound the range of the growing layer. The mean of these two values is used to represent, in a gross way, the thickness of selective withdrawal.

The velocity distribution across a withdrawal layer of the thickness has been found following the similarity solution by Koh (1964). The distribution can be appropriated by means of the polynomial

$$u_* = 1 + 0.065z_* - 2.955z_*^2 + 1.89z_*^3 \qquad (3.14)$$

where $u_* = u/u_0$, $z_* = z/z_0$, u_0 is the centerline velocity and z_0 is the layer half thickness.

Considering

$$\int_0^{z_{wb}} q_e(\xi)d\xi = Q_j$$

where z_{wb} is the bottom of the withdrawal layer and using the nomalized velocity profile (Eqn. 3.14) for the withdrawal layer leads to the following expressions

$$v(z_*) = Q_j[1 - 0.96(1-z_*) - 0.03125(1-z_*^2) + 0.94575(1-z_*^3) - 0.4545(1-z_*^4)]/A(z) \quad (3.15)$$

for the lower half of the withdrawal layer,

$$v(z_*) = Q_j[-0.96(1-z_*) - 0.03125(1-z_*^2) + 0.94575(1-z_*^3) - 0.4545(1-z_*^4)]/A(z) \quad (3.16)$$

for the upper half of the withdrawal layer.

3-3 Numerical Solution

A numerical solution to equations 3-3 and 3-4 governing the simulation model, using the mechanics of buoyant jets and withdrawal provides the temperature profiles at any time during mixing for a given pumping system and initial profile.

A finite difference technique is employed for the numerical solution. An explicit scheme is used. The choice of the differencing scheme and the space-time grid is made after an examination of the truncation error incurred and the stability of a particular scheme. Minimizing the truncation error improves the approximation of the differential equation by the difference equation. A stable scheme guarantees that errors will not be amplified and that convergence to the solution is possible.

The vertical transport velocity, v, is a function of the temperature profile as well as elevation, z, and time, t. It must be calculated numerically in the buoyant jet region for a given temperature profile. Considering that the temperature profile must be known for v requires an explicit scheme for the finite difference form of equation 3.3.

With fluid entrainment from and fluid return into the ambient, and fluid transport downward and upward, the significant effects are considered to travel only from upstream to downstream. The conditions at a point are then affected largely by upstream conditions, and very little by the downstream ones. The transport of fluid can be called a "one-way process".

The finite difference equations approximating the differential equation 3.3 are

$$\frac{T_{i,j+1} - T_{i,j}}{k} + v_{i-1,j} \frac{T_{i,j} - T_{i-1,j}}{h} = 0 \qquad (3.17)$$

for $v > 0$

$$\frac{T_{i,j+1} - T_{i,j}}{k} + v_{i+1,j} \frac{T_{i+1,j} - T_{i,j}}{h} = 0 \qquad (3.18)$$

for $v < 0$, where k and h is the local time and space step or interval respectively. The explicit scheme is shown in Fig. 3-4.

Using a Taylor series expansion of t about the point (i,j) in the time and space variable yields the truncation error for this scheme (of order one)

$$ET = \frac{1}{2} v_{i-1,j} [(kv_{i-1,j}) - h] \frac{\partial^2 T}{\partial z^2} - \frac{k}{2} \left[\frac{\partial v}{\partial t} \frac{\partial T}{\partial z}\right] \qquad (3.19)$$

The first term of the truncation error is identically zero, if

$$h/k = v_{i-1,j} \qquad \text{for } v > 0 \qquad (3.20)$$

In the second term, the product $(\partial v/\partial t)(\partial T/\partial z)$ is usually small, although it is diffcult to bound as $\partial T/\partial z$ can be large and $\partial v/\partial t$ is

related to the temperature profile through the jet equations in a complicated way. Thus the time step, k, must be made sufficiently small, in addition to the relation given in Eqn. 3.20, for the truncation error to be minimized.

Similarly for region where $v < 0$, the truncation error is minimized by choosing

$$h/k = |v_{i+1,j}| \qquad \text{for } v < 0 \tag{3.21}$$

and k (i.e. Δt) sufficiently small.

Eqn 3.3 can be viewed as a kinematic wave equation. It has one set of characteristics in the time-space plane with slopes $dz/dt = v$ along which T = constant.

The Courant stability criterion for the kinematic wave equation is given by Newman's method, using Fourier series to express the solution, as

$$|v|k/h \leq 1 \tag{3.22}$$

Eqn 3.17 and 3.18 can be rewritten as

$$T_{i,j+1} = C1T_{i-1,j} + (1 - C1)T_{i,j} \qquad \text{for } v > 0 \tag{3.23}$$

$$T_{i,j+1} = C2T_{i+1,j} + (1 - C2)T_{i,j} \qquad \text{for } v < 0 \tag{3.24}$$

where C1 and C2 are Courant numbers,

$$C1 = v_{i-1,j}k/h \quad \text{and} \quad C2 = v_{i+1,j}k/h \qquad (0 \leq C1, C2 \leq 1) \tag{3.25}$$

Considering Eqn 3.20 and 3.21 from the truncation error analysis and the stability criterion Eqn 3.22 or 3.25 requires C1 = C2 = 1 i.e.

$$\frac{h}{k} = \frac{\Delta z}{\Delta t} = v_{i-1,j} \qquad \text{for } v > 0 \tag{3.26}$$

$$\frac{h}{k} = \frac{\Delta z}{\Delta t} = v_{i+1,j} \qquad \text{for } v < 0 \tag{3.27}$$

Therefore Eqn 3.23 and 3.24 become

$$T_{i,j+1} = T_{i-1,j} \qquad \text{for } v > 0 \qquad (3.28)$$

$$T_{i,j+1} = T_{i+1,j} \qquad \text{for } v < 0 \qquad (3.29)$$

Equations 3.26-3.29 essentially define the characteristics. Lines in the t-z plane which connnect points of constant T trace out these characteristics. Physically, at a given elevation and time, a parcel of fluid containing T would move upward (or downward if $v < 0$) a distance Δz in time interval Δt.

3-4 Computation and Results

The combination of the numerical calculation scheme and the knowledge of the buoyant jet and the withdrawal layer mechanics for the simulation of mixing by a pumping system is presented. The simulation procedure and computation technique is briefly described here. The typical results for linearly and non-linearly stratified ambients are presented. The simulation model verification with a set of existing field data is made.

The initial conditions of the lake or reservoir and information about jet and withdrawal are reqired to be specified for the simulation. The aera-depth relation, A(z), and the initial temperature profile are introduced at uniformly spaced intervals on the elevation axis, z. These intervals are small enough so that any temperature profile can be approximated. With this initial information, the jet trajectory and parameters are calculated using the simulation model for jets as described in Chapter 2 to the neutral level of the fluid in the jet. This level is assumed to be

the terminal level of the fluid although, physically, fluid with negative buoyancy overshoots this level before reaching approximately this position due to its momentum. The values of vertical transport velocity calculated along the jet trajectory at irregularly spaced elevations are interpolated into those at regularly spaced intervals.

The vertical transport velocity in the lake or reservoir due to the withdrawal layer is calculated at each of those regular intervals using Eqns. 3.15 and 3.16.

The integration of q_e from $z = 0$ to the neutrally buoyant level is the total volume flux entrained by the jet from the ambient water body Q_e plus the jet dischareg Q_j. This is the return flow from the jet to the ambient at the equilibrium level. Q_e is returned to the jet region ($0 \leq z \leq z_n$) to replenish the fluid entrained into the jet from the ambient and Q_j is moved to the withdrawal layer to replenish the fluid withdrawn by the pump from the ambient (see Fig. 3-5). Between the level of neutral buoyancy of the jet and the bottom of the withdrawal layer, there is no transport of fluid between the ambient and the jet or withdrawal layer. The integration of q_e from $z = 0$ to any elevation in this zone equals Q_j. The vertical transport velocity in this zone is then

$$v(z) = Q_j/A(z) \tag{3.30}$$

No fluid transport from the top of the withdrawal to the surface takes place. The integral of q_e from $z = 0$ to the top of the withdrawal layer equals zero, therefore v is zero above the top.

Finally, the temperature values at time t after one time step Δt are obtained at irregular intervals on the z-axis, they are found at

regular intervals by using an interpolation subroutine.

The time step Δt, elevation interval Δz and the jet centerline trajectory interval Δs are chosen small enough so that truncation errors are minimized. However, the choice should concern the computation cost. They are determined by the number of grids and the total time required to pump the volume of the lake or reservoir, the depth and the length of jet centerline respectively.

There is no energy exchange through the lake or reservoir boundaries (assumption 1). Therefore, a check of the heat balance for the system is made to estimate the error induced by the selection of steps and by interpolation. The heat balance in the lake or reservoir is represented by

$$\int_V (C_p\rho T - C_{p0}\rho_0 T_0)dV = 0 \tag{3.31}$$

Assuming $C_p\rho = C_{p0}\rho_0 \approx$ constant, then

$$\int_V (T - T_0)dV = 0 \tag{3.32}$$

The heat balance can be checked by comparing the temperature profile just calculated to the initial one and then a uniform correction is made for the temperature profile. Similarly, the mass balance also is checked.

Typical simulation results are shown in Fig. 3-6 and Fig. 3-7 for a prismatic shape lake or reservoir (A(z) = constant) with a linear stratification of initial temperature and Fig. 3-8 and Fig. 3-9 for non-linear cases. The dimensionless time t^* is equal to $t/(V/Q)$, where V/Q is the hydraulic resident time defined as the time required to pump the volume of the lake or reservoir V, which is included between the planes of the jet discharge and withdrawal layer. The

initial jet densimetric Froude number Fr_0 characterizes the buoyant jet in the initial temperature profile. The Froude number varies with time due to the changing temperature profile during mixing, therefore Fr also is a characterizing parameter for the mixing process.

Irwin, James and Symons (1966) reported field experiments of impoundment destratification by mechanical pumping in several lakes and reservoirs. The data taken during the mixing studies was related to water quality, though the time-histories of the temperature-depth profile are available for some experiments. In the field experiments of lake mixing, cold dense water was pumped from near the lake bottom to the surface where it could mix with warm water, lose considerable density, and sank to the level of its new density. Negatively buoyant jets were generated by this type of pumping system.

The behavior of the negative jets is exactly the same as that (with inverted sign of buoyancy) discussed in chapter 2. Only the sign of acceleratiion gravity, g, and the direction of the z-axis in the model for positive buoyant jets need to reverse for the simulation of negative jets. The mixing processes by negatively buoyant jets and the inverse are same for a linear initial stratification of temperature but different for nonlinear one. The type of jet buoyancy is chosen by considering the initial stratification so that fluid is withdrawn from the uniform region and discharged to the stratified region for higher efficiency of the mixing system.

Although the field experiments do not provide all boundary conditions and are not totally closed system as defined by the assumption, the simulation is applied to the mixing of Vesuvius Lake,

Ohio (Irwin et al, 1966). The comparison of the temperature profiles measured during the field experiment and the profiles predicted by the simulation model are shown in Fig. 3-10. The agreement is reasonably good and better for the 2.5-day profile than the 8.5-day. The fact that the field experiment is not closed to external influences probably accounts for the poorer agreement for 8.5-day profile.

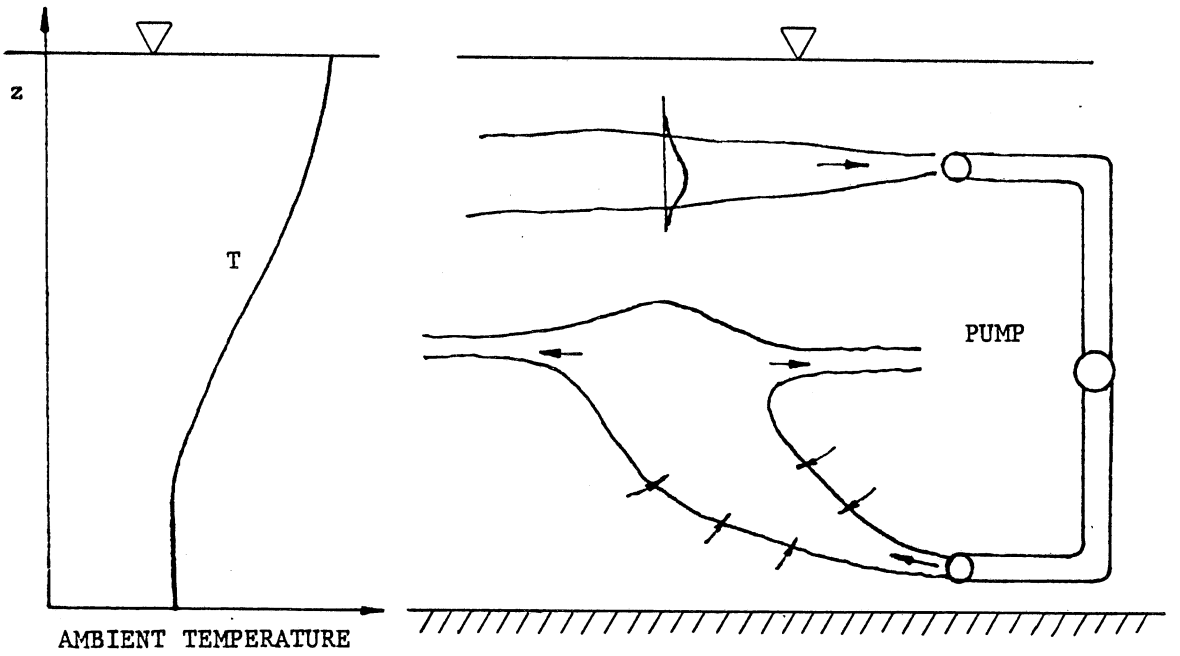

Fig. 3-1. Schematic diagram of a pumping system in a stratified impoundment.

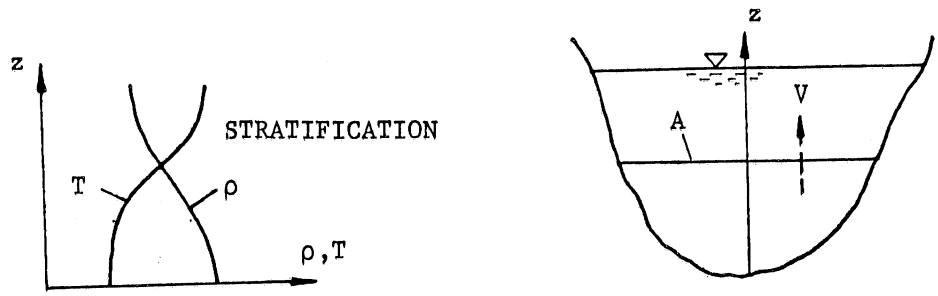

Fig. 3-2. Sketch of a lake.

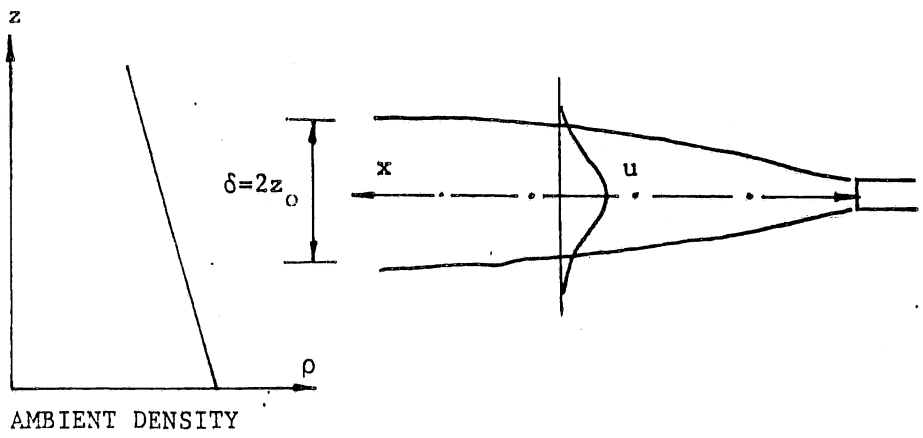

Fig. 3-3. Sketch for a withdrawal layer.

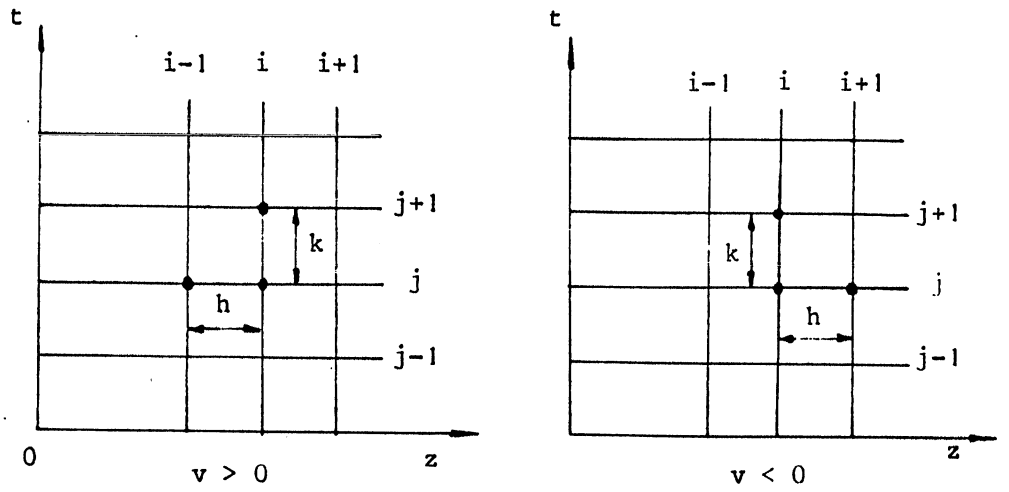

Fig. 3-4. Finite difference schemes.

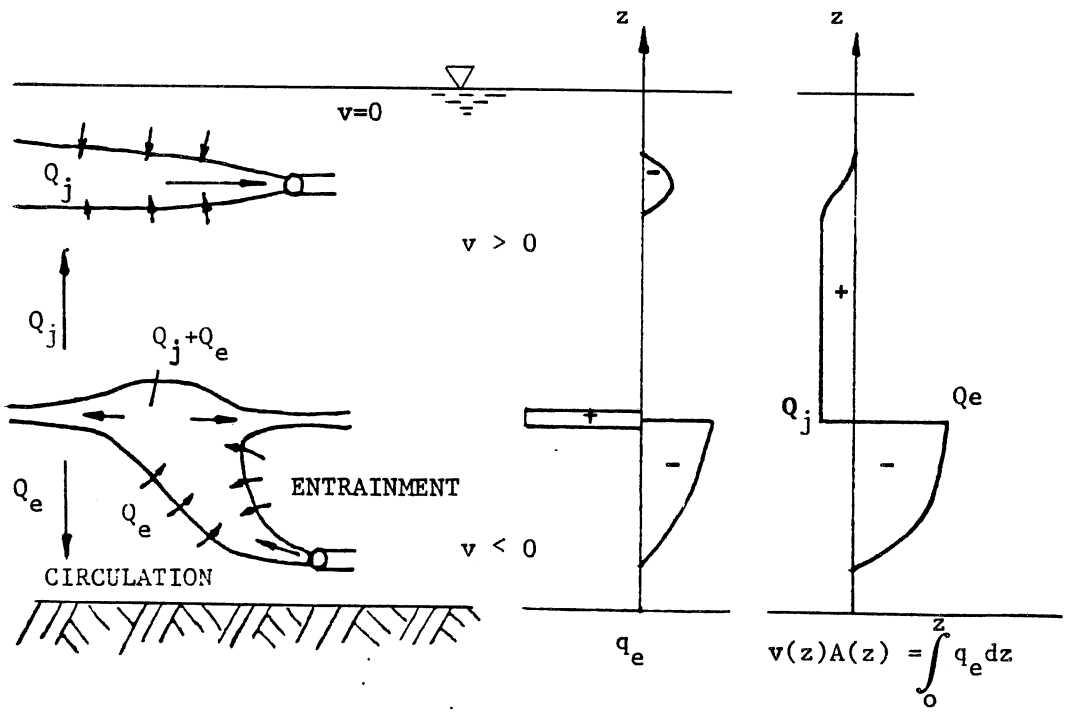

Fig. 3-5. Pumping system with vertical distributions of q_e and v.

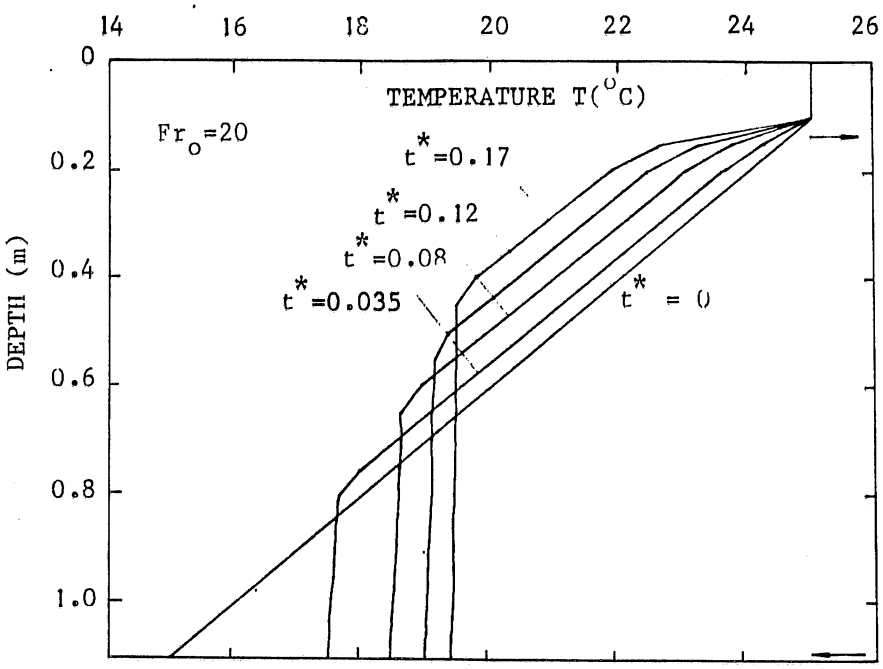

Fig. 3-6. Simulation result for Fr_o = 20.

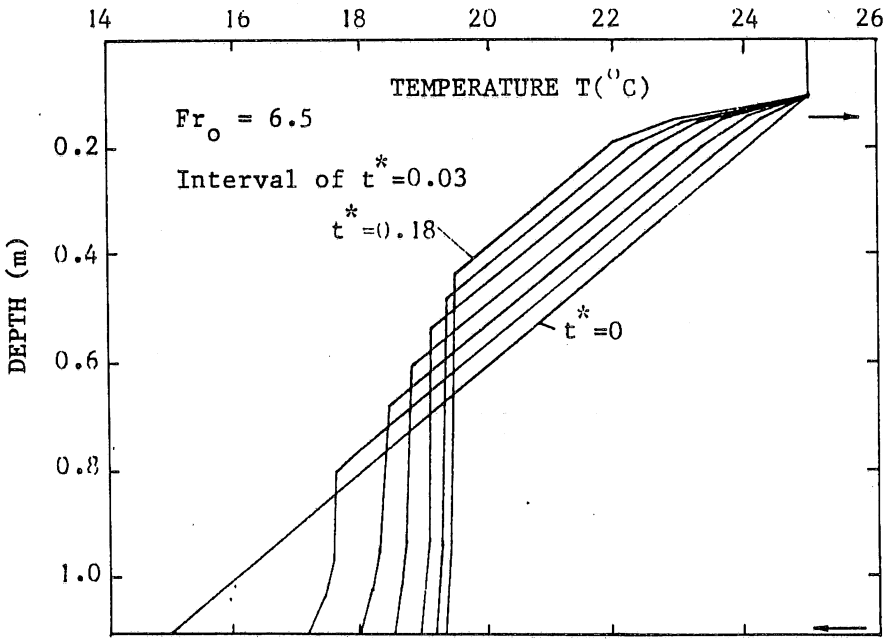

Fig. 3-7. Simulation result for Fr_o = 6.5.

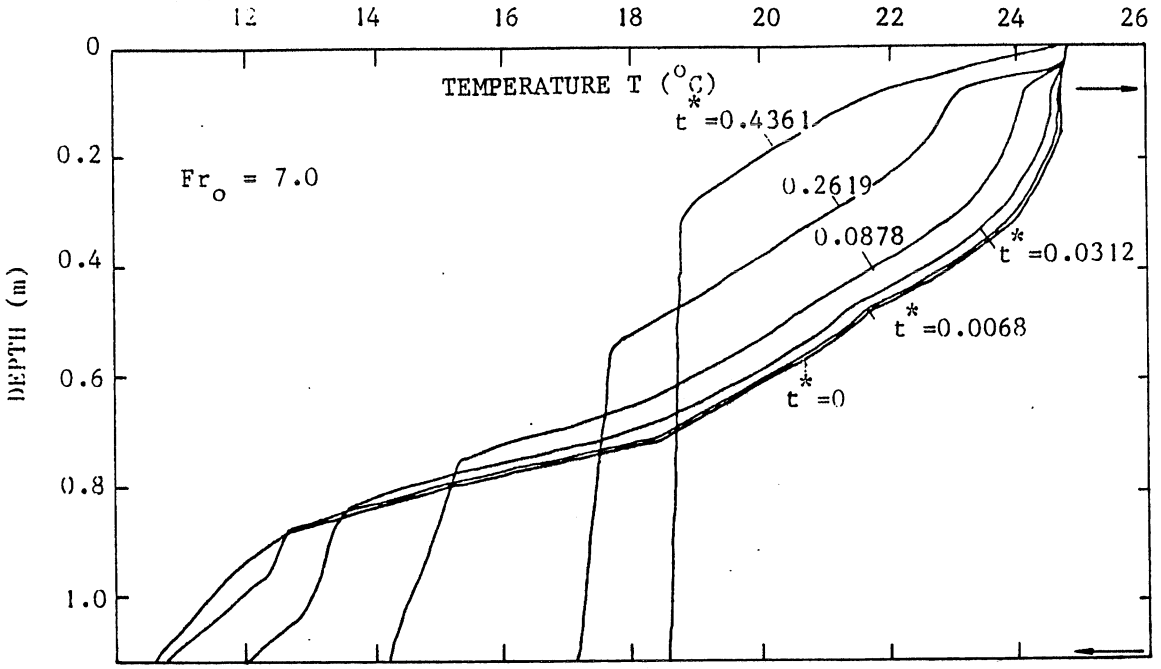

Fig. 3-8. Simulation result for Fr_o = 7.0.

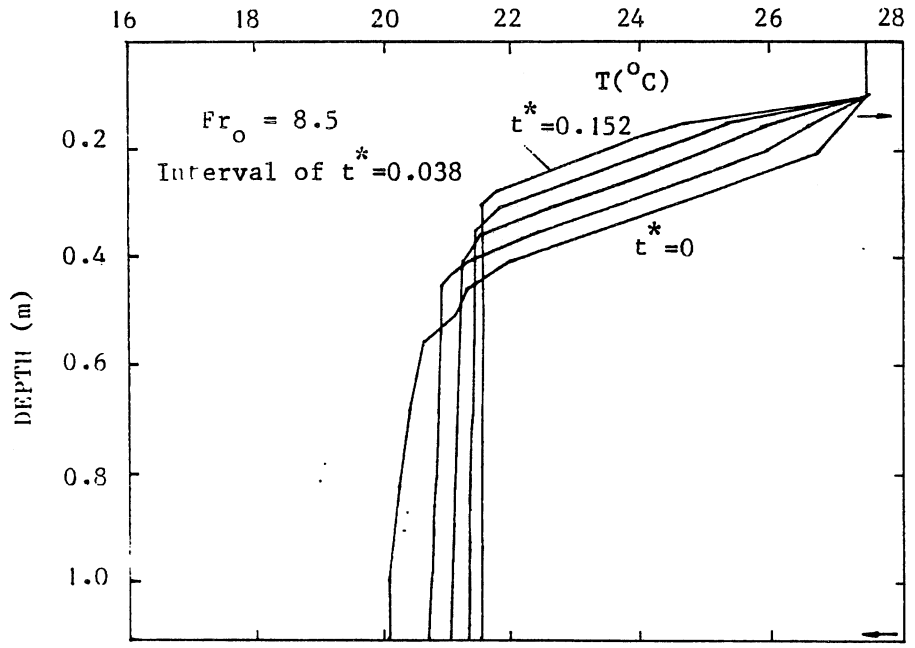

Fig. 3-9. Simulation result for Fr_o = 8.5.

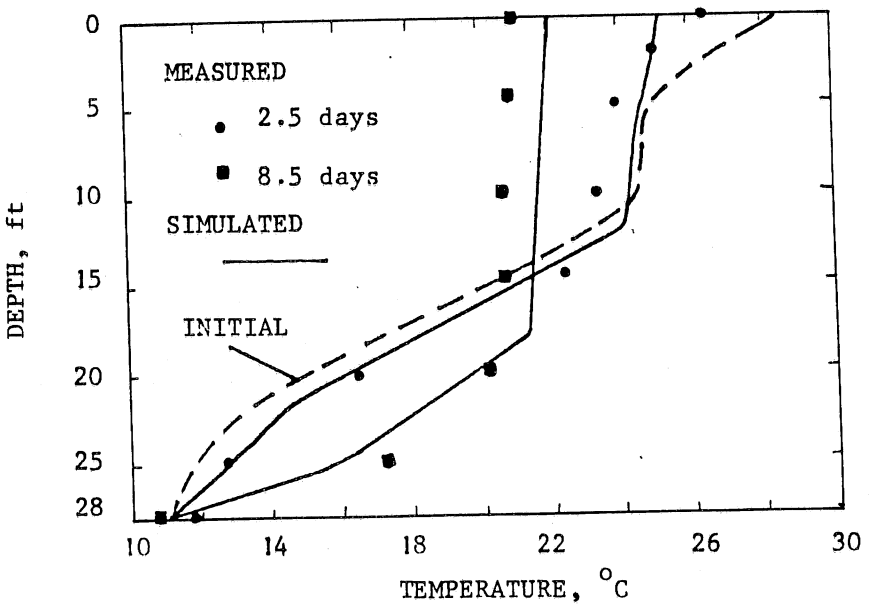

Fig. 3-10. Comparison of measured and simulated profiles for Vesuvius Lake, Ohio.

Chapter 4 Experiments on Mixing of Temperature-stratified Water With Buoyant Jets

4-1 Purpose

Temperature-stratified lakes and reservoirs can be mixed by pumping. The main physical features which need to be studied are mixing processes and jet behavior. The laboratory experiments served two main objectives: to verify the validity of the simulation model which predicts the bulk behavior of the mixing process with buoyant jets and to identify those phenomena associated with the mixing process which are not simulated by the model. A dye flow-visualization study was carried out to investigate the growth of mixing layers and the global behavior of the jet flow and its dependence on various parameters. The effects of the discharge Froude number Fr_0, which was adjusted by varying the flowrate and the temperature difference ΔT_0, were studied in the visualization.

4-2 Experimental Equipment

The main components of the experiment are shown in Fig. 4-1. The experiments were conducted in a glass-walled tank which was insulated. A water pump, hot and cold water sources, a rotameter, temperature probes (thermistors), a dye injection apparatus, copper tubes providing horizontal intake and discharge and a computer recording the temperature profiles are required for the experimental arrangement.

The nozzle was located near one wall to get significant distance to the other side of the tank. The sizes of the discharge tubes and

flowrate of the system for an experiment are determined by the desired range of Froude number Fr_0 and turbulence level (Re). The flowrates were restricted by the pump capacity and the tank size, therefore, tubes with various diameters were prepared for appropriate experimental arrangement. The position of the withdrawal intake and jet discharge tube in the tank were varied. Temperature probes were calibrated against a thermometer (temperature meter) placed in an equilibrium bath which had a constant temperature. Specific data regarding the location of the tubes, the hydraulic parameters, and initial temperature profiles for each experiment are given in Table 4-1. For the mixing system, the stratification number, S_t is equal to L/D_0.

4-3 **Experimental Procedure**

Temperature stratification was produced in the tank by using hot and cold water sources. Mixing was accomplished by using a laboratory pump connected to the intake and discharge tube in the tank. Temperature profiles were recorded at regular time intervals (5 minutes) during the mixing process by using an Apple computer connected to the temperature probes. The data were stored immediately on disk.

Temperature-stratified environments were created in the tank by filling with hot water and cold water to produce vertical temperature gradients. The shape of the temperature-depth profile was dependent on the manner in which the tank was filled. The water taken from the source was discharged into the bottom of the tank by using a radial spreader, that dissipates the water jet and minimizes the mixing

Table 4-1 Summary of the Experimental Runs

Exp. No.	Total depth d_t(m)	Distance between jet & intake L(m)	Jet disch. Qx10^5 (m^3/s)	Diffusor diameter D_0(m)	Initial diff. jet & intake ΔT_0(^{0}C)	Stra. No. St	Jet Froude No. Fr_0	Jet Reynolds No. Re	Charact. time T_c=V/Q (hr)
1	1.27	1.10	2.60	0.0095	10.7	116	29.1	3500	14.7
2	1.27	0.52	0.85	0.0095	14.5	55	8.4	1100	21.3
3	1.27	0.72	1.00	0.0095	9.8	76	11.5	1340	25.1
4	1.27	0.8	2.95	0.0254	18.3	32	2.0	1500	9.4
5	1.27	0.8	6.20	0.0254	17.2	32	4.2	3100	4.5
6	1.20	1.04	4.40	0.0191	14.1	55	7.0	2200	8.2
7	1.20	0.72	2.75	0.0191	6.3	48	6.4	1800	9.1
8	1.20	0.72	5.60	0.0191	9.8	48	10.0	3700	4.5

Notes:

(1) Aera of tank $A = 1.12 \times 1.12 = 1.254\ m^2$

(2) Volume $V = AxL$ m^3

during spreading. The filling started with the hot water and ended with the cold water. Floating insulate material were spreaded on the surface of the tank water to reduce heat exchange through the surface. The temperature at the water surface tends to move toward the equilibrium temperature if there is no insulate materials on the surface. After a suitable temperature profile was created, the water was then left undisturbed to allow turbulent mixing to die out and hydrostatic equilibrium to be reached before recording the intial temperature profile.

The equilibrium temperature T_e, the air temperature T_{air}, the initial temperature profile, and the location and size of the withdrawal tube and discharge nozzle were recorded before initiating circulation. Measurement were initiated at the beginning of pumping. The temperature probes were located near a corner of the tank approximately 25 cm from the wall and far away from the jet. The lateral gradients in temperature were assumed to be small due to the small size of the tank, and the temperature profiles recorded were considered representative of the whole tank.

The development of the mixing layer as well as the temperature profiles were recorded. Observations of jet trajectories and withdrawal layer were made using dye injection during experiments.

4-4 Results and Discussion

Results from several experiments on mixing by buoyant jets are presented in Fig.4-2 to Fig.4-9. The results are shown in the form of elevation-temperature profiles at various times during the mixing process. Temperature T was plotted against normalized elevation z^*,

which is equal to z/L, where z is the elevation above the centerline of the discharge tube and L is the distance between the discharge and withdrawal tubes. The dimensionless time is defined as $t^* = tQ/(LA)$, where Q/(LA) is the characteristic time for the system. The hydraulic data, location of the jet and withdrawal tubes and the charaterizing parameters for each experiment are listed in Table 4-1 and given with each figure.

The data points indicate the temperature profiles measured in the experiments. The temperature profiles predicted by the simulation model are indicated by solid lines accompanying each set of experimental data. The measured initial temperature profile and required information about the system is provided as input to the simulation. The temperature profiles at any time after pumping is initiated are produced by the simulation model. The experimental data for temperature profiles were taken at time intervals of 5 minutes. Only a few profiles at various times are presented in Figure 4-2 to 4-9.

The agreement between the experimental results and the temperature profiles predicted by the simulation model is good but some disagreement is shown spatially at both the water surface and the discharge region. Although differences also exist at the final stages of mixing, $t^* > 0.4$, the model does predict reasonably well the changes in the temperature structure of the tank during the mixing process for the experiments performed. The prediction, in a global way, is good and quite accurate in detail.

The discrepancies between the experimental results and those

predicted can be explained by some difficulties in experiments and the simplified nature of the simulation model.

The establishment of an initial temperature profile with horizontal isothermal surfaces throughout the tank was required as the proper initial condition for the simulation. This condition was not satisfied sometimes. However, for most experiments the essential features of the mixing process were not greatly affected by this slight alternation in initial condition.

Maintaining a closed system during the experiments is difficult. Energy exchange between the tank and the environment was designed to be zero for the simulation model. However, this was not completely accomplished in the experiments although insulation of the surface and walls of the tank was used to minimize the heat exchange. Fluxes of heat into or from the tank generated temperature gradients which induced motions independent of the mixing process and caused the heat in the tank not to be fully conserved. This could contribute to the disagreement between experimental and simulated profiles in the surface region, and at the final stages of mixing when changes due to the pumping system are small but the accumulative heat exchange with the environment is significant.

The buoyant jet mechanics used in the simulation is appropriate for a jet in a fluid of infinite extent, and the fact that the jets in the experiments were in a tank with a solid boundary was not considered in the simulation. The effect of the walls is significant when Fr_0 is very large since the jet axis becomes nearly horizontal and the jet impinges on the walls (see Fig. 4-10). It is obvious that

the larger the tank and the smaller the Froude number Fr_0, the less the effect of walls and the better the agreement between the prediction and measurements. Practically, low values of Fr_0 are recommended for efficient pumping in field applications as will be shown.

Horizontal planes of isothermal surfaces are assumed in the simulation technique. However, at a given time during mixing the isothermal surfaces are generally not horizontal planes. The horizontal variations of temperature along the tank at a given elevation and time are generally not considerable for a small tank as used in this study. A large tank is needed for taking data at several locations in the tank during mixing experiments to investigate the non-isothermal features of the impoundment.

The temperature profiles produced by the simulation extend only to the centerline of the discharge tube and do not reach the region below the jet centerline. The simulation model assumes that entrainment by the jet from the ambient occurs at elevations along the centerline trajectory of the jet. This assumption is good as the buoyant jet axis becomes vertical, but it is clear that while the jet axis is nearly horizontal some entrainment will occur below the jet centerline. Experiments show that horizontal jets do erode and mix the region below their origin as shown in Fig.4-11. From the dye flow-visualization, the visible upper and lower boundaries of the mixing layer are plotted against dimensionless time t^* in Fig. 4-12 which shows the growth of the mixing layer on top and bottom. The simulation model predicts no change in the temperature profile below

the jet origin. This is the cause for the disagreement of temperature profiles between experimental and simulated results in the discharge region. Therefore, the heat balance made for the tank from the discharge level to the surface does not agree with that made for simulated profiles. This could contribute to some of the disagreement between experimental and simulated profiles at final stages of mixing. However, this effect is not significant for small Fr_0 values (in the range from 2 to 10) for which the jet trajectory is strongly deflected to a vertical direction (see Fig. 4-10).

The elevation at which the centerline temperature of the jet equals the temperature of the fluid in the tank i.e. neutral buoyancy ($\Delta T_m = 0$) was chosen as the location of equilibrium level. Physically, the jet has vertical momentum at this elevation and continues above this elevation before coming back down to rest at the equilibrium level (see Fig. 2-1). The equilibrium level is difficult to predict as the similarity analysis breaks down here and the mixing that occurs is complicated. For the horizontal jets, an elevation somewhere between the point of neutral buoyancy ($\Delta T_m = 0$) and the maximum height of rise may be more representative of the equilibrium level.

The experimental results show that the changes in the temperature profiles in the withdrawal region are small relative to the effects of the buoyant jet in other parts of the profile. The simulation precedure models the withdrawal region in a simple and imperfect manner, but greater precision in simulating the withdrawal layer may have little or no effect on the simulated profiles as a whole.

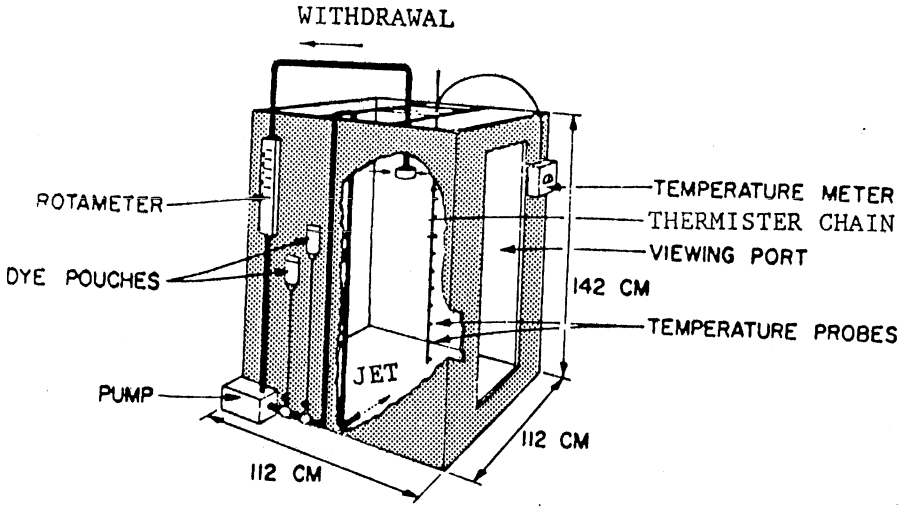

Fig. 4-1. Major equipment components.

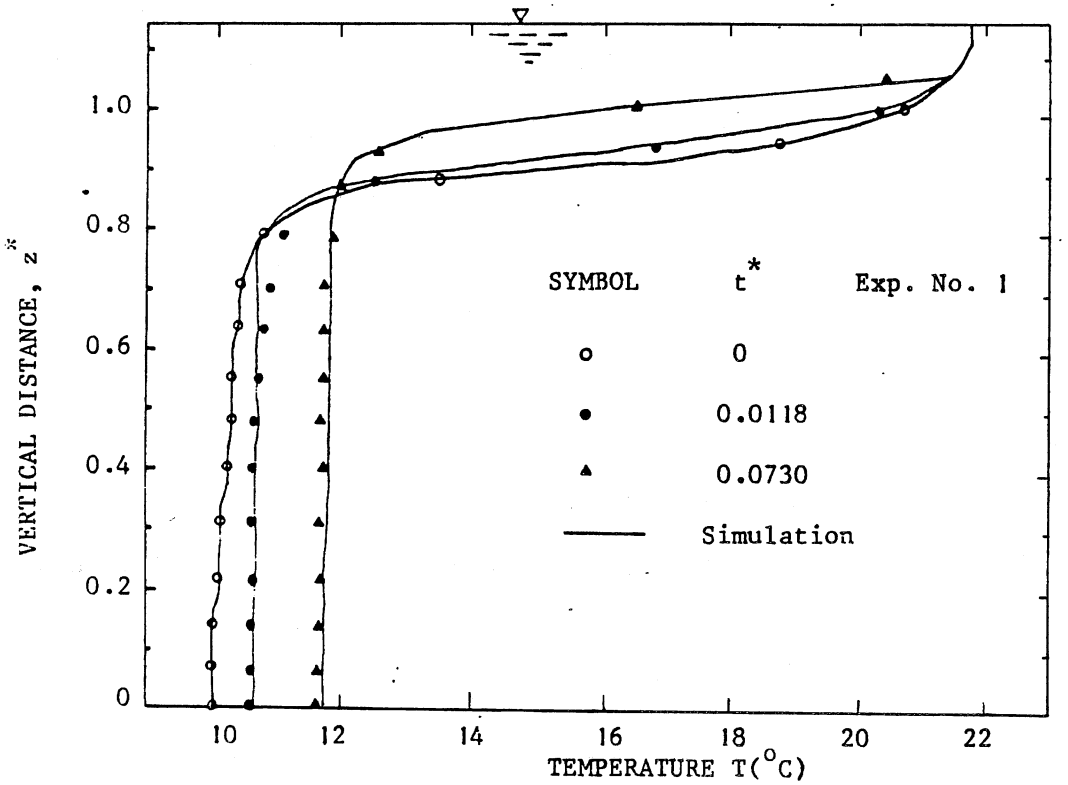

Fig. 4-2. Measured and simulated temperature profiles for experiment No. 1.

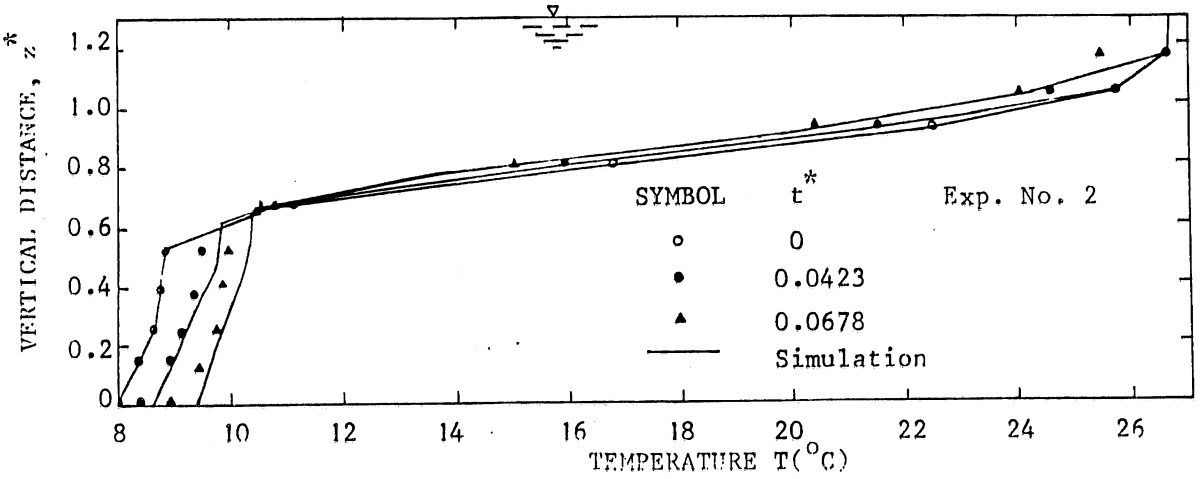

Fig. 4-3. Measured and simulated temperature profile for Experiment No. 2.

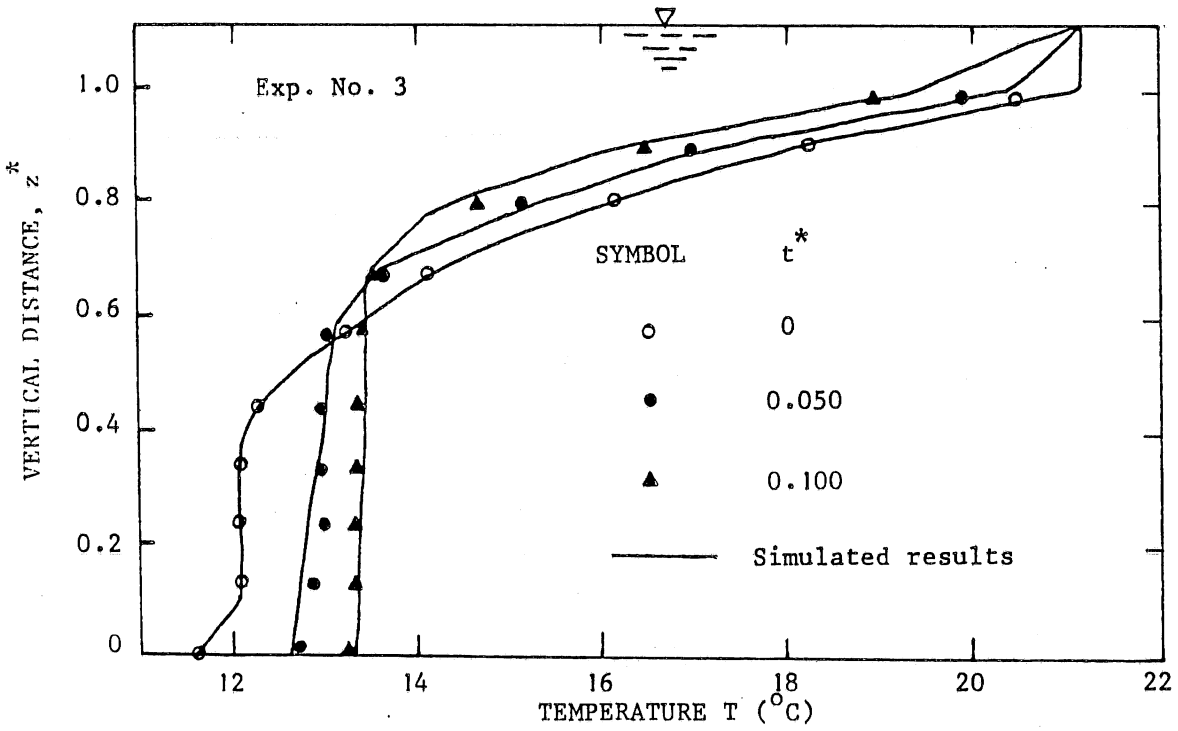

Fig. 4-4. Measured and simulated temperature profiles for Experiment No. 3.

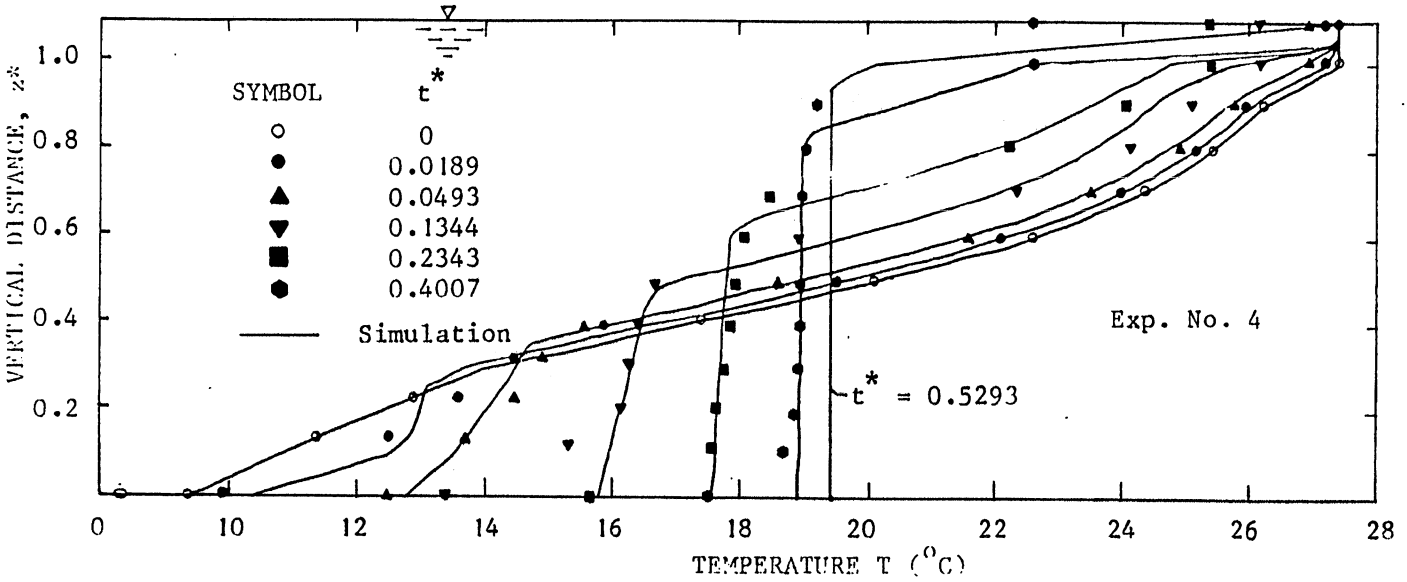

Fig. 4-5. Measured and simulated temperature profiles for Experiment No. 4.

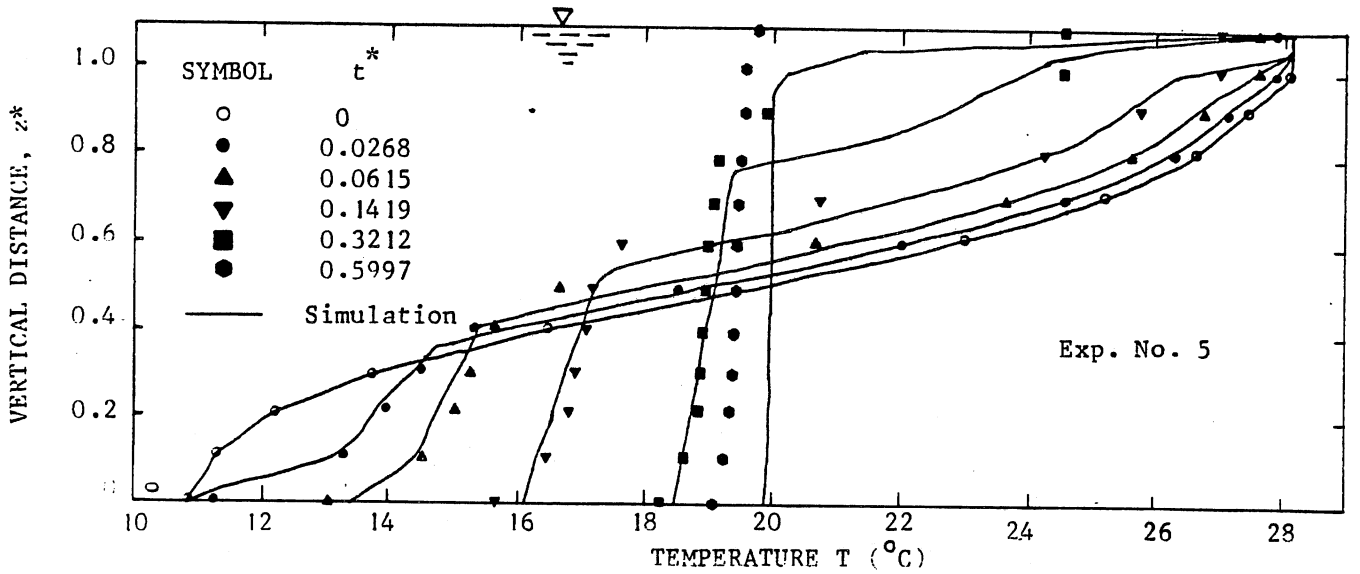

Fig. 4-6. Measured and simulated temperature profiles for Experiment No. 5.

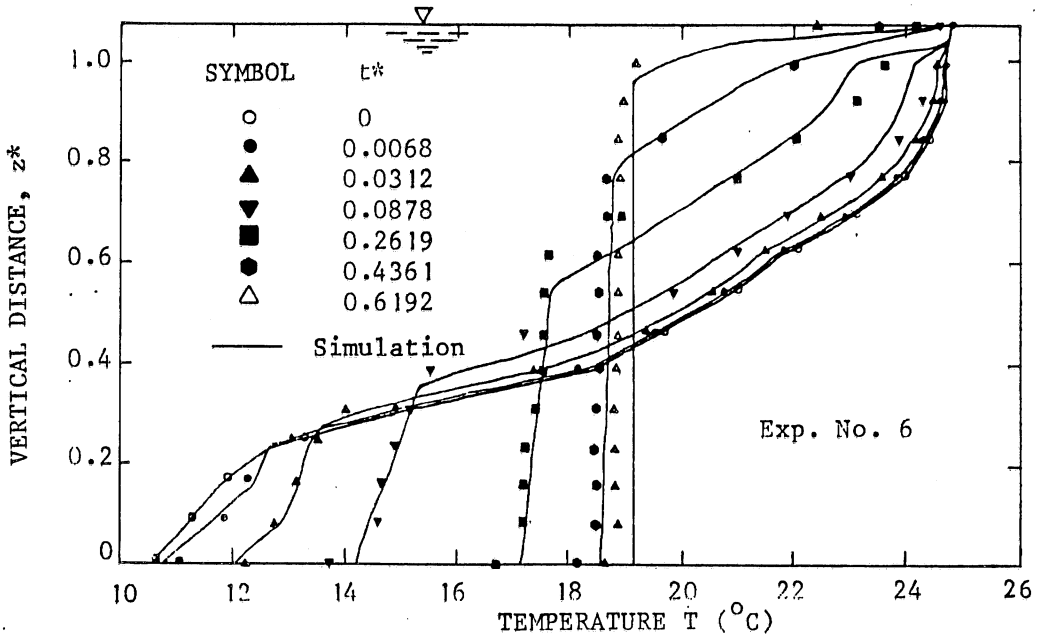

Fig. 4-7. Measured and simulated temperature profiles for Experiment No. 6.

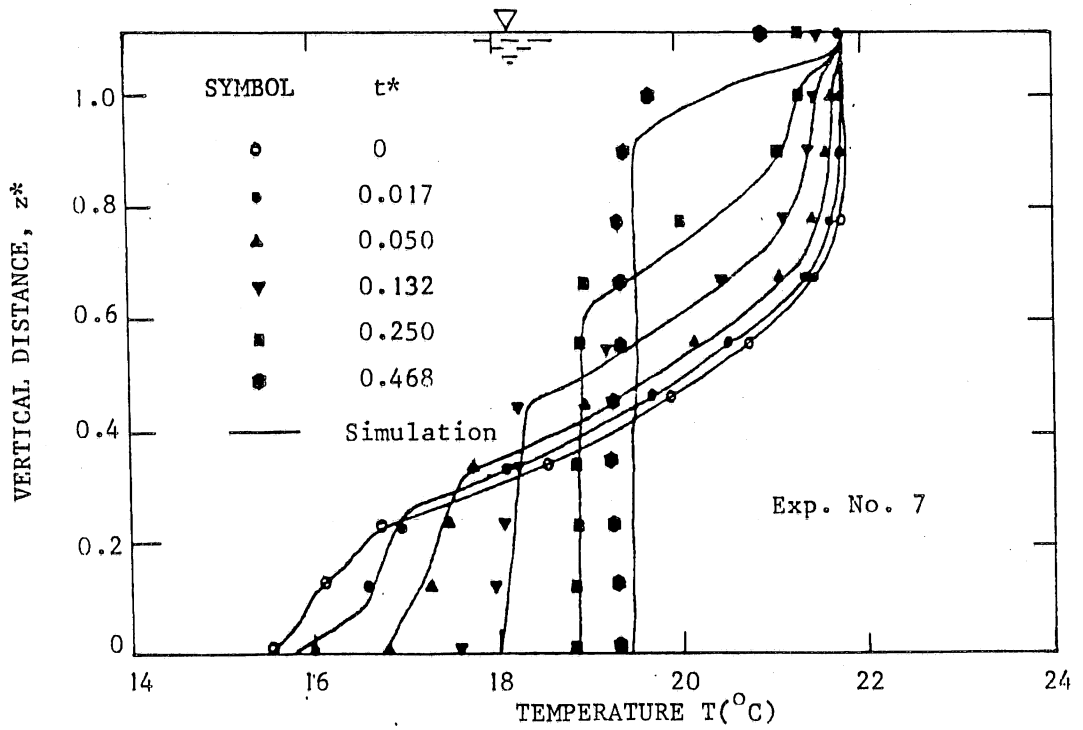

Fig. 4-8. Measured and simulated temperature profiles for Experiment No. 7.

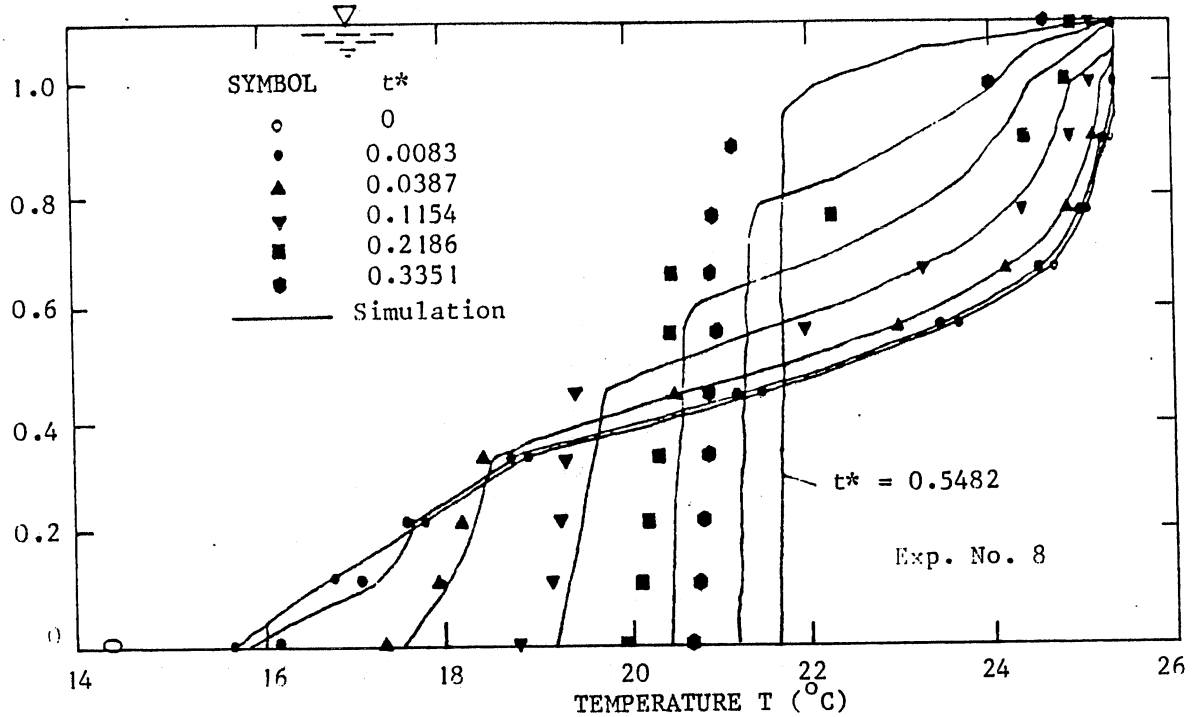

Fig. 4-9. Measured and simulated temperature profiles for Experiment No. 8.

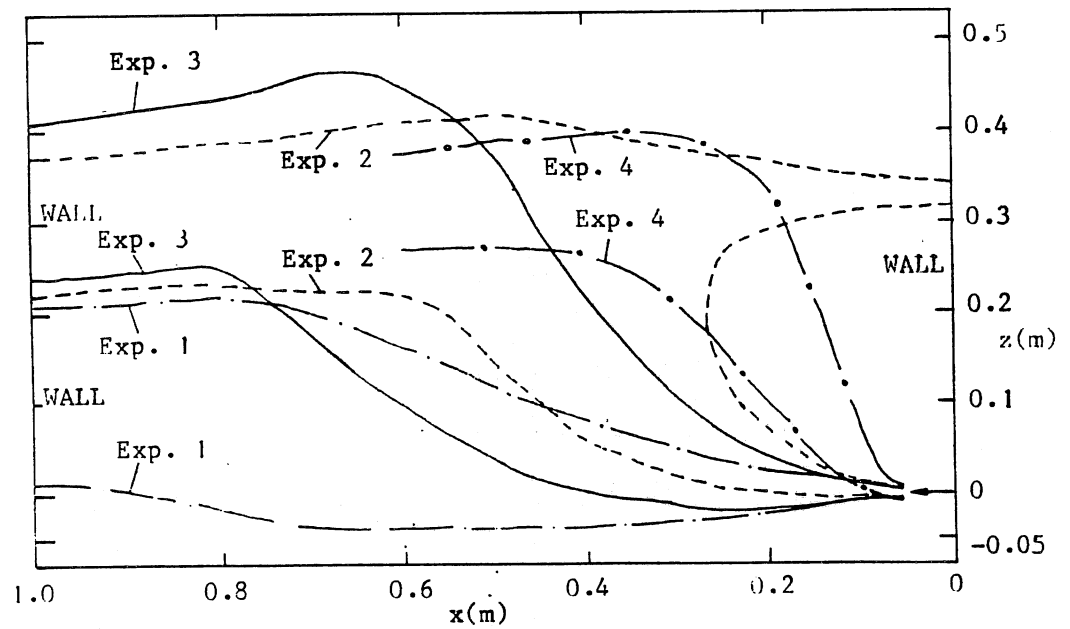

Fig. 4-10. Flow visualization: jet boundaries.

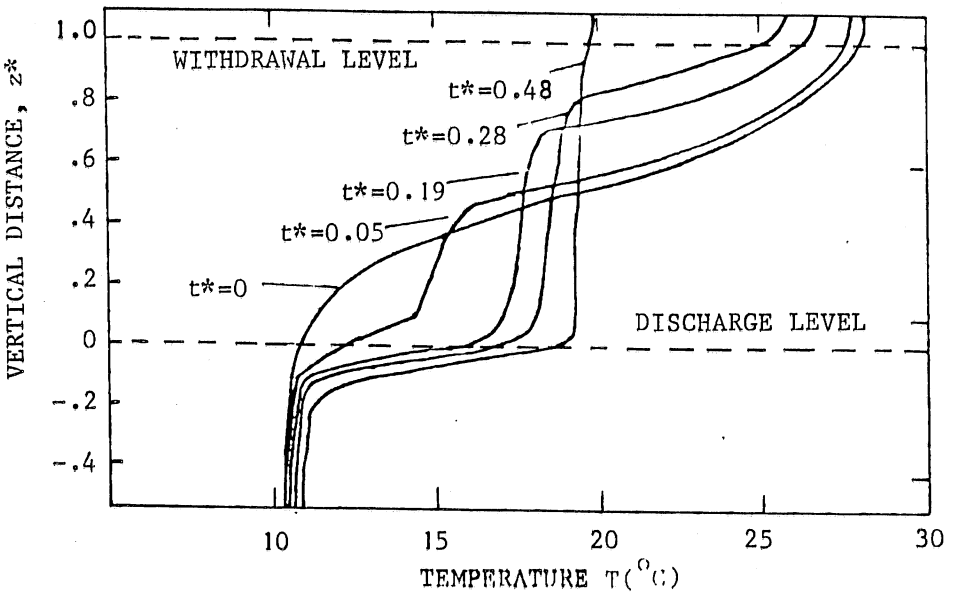

Fig. 4-11. Measured temperature profiles for Experiment No. 5.

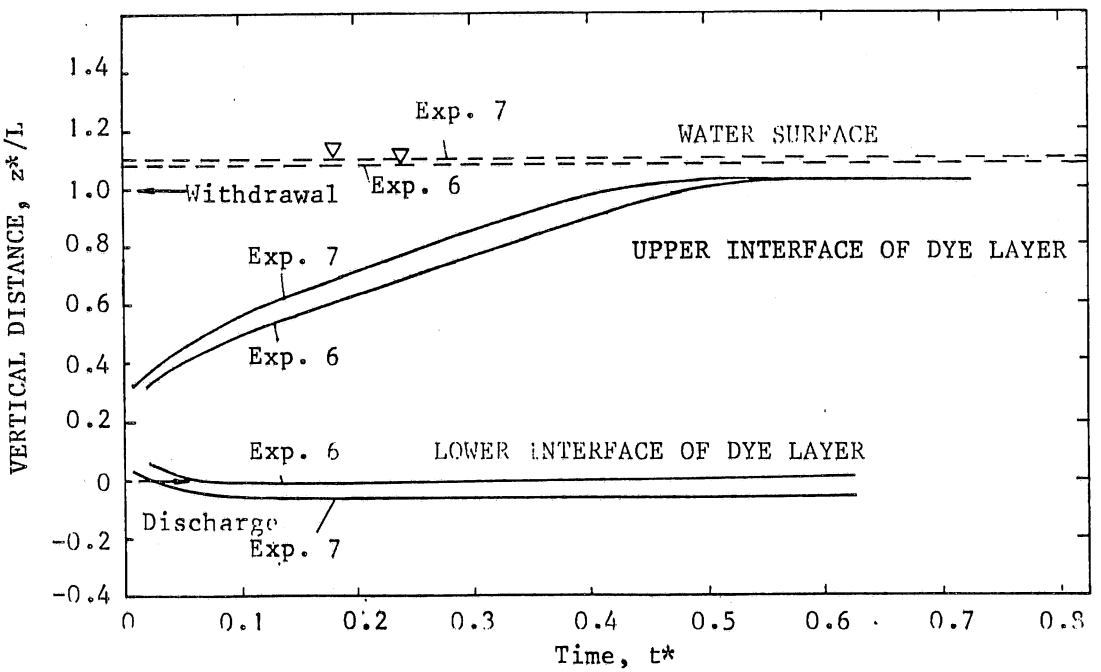

Fig. 4-12. Development of mixing layers.

Chapter 5 Summary of Generalized Simulations and Experiments

In this chapter results of the numerical and laboratory experiments for a constant area lake or impoundment are summarized. Numerical mixing experiments are generated for initially linear temperature profiles by use of the simulation model established in chapter 3. The results of these experiments are analyzed and condensed to provide some general conclusions about the mixing process and the application of the simulation model to lakes and reservoirs, and the design information for the selection of a destratification system.

Based on the results from the laboratory experiments presented in chapter 4, temperature profiles during the mixing process are characterized by parameters h_m, h_t and h_e, see Fig. 5-1 for definitions, and in dimensionless form, $h_m^* = h_m/L$, $h_t^* = h_t/L$, and $h_e^* = h_e/L$. These parameters describing the temperature profiles give the boundaries of the region influenced by the buoyant jet during the mixing process, i.e. the mixing layer. Fig. 5-2 to Fig. 5-6 show the growth of the mixing layer for the laboratory experiments. The dimensionless parameters h_m^*, h_t^* and h_e^* are plotted against time t^*.

The region below the discharge level which is eroded and mixed by the jet is indicated by parameter h_e^*. It can be seen that h_e^* and h_t^* change slightly with time t^* and keep almost constant for $t^* > 0.1$. This means that the development of the lower boundary of the mixing layer is small and becomes steady in a very short time after

initiating the pumping system. Therefore, the growth of the mixing layer during the mixing process may be reflected by the h_m^* vs. t^* curves. The mixing layers grow about linearly with time between the initial stages ($t^* \approx 0.1$) and the steady state ($h_m^* \approx 1.0$). In the initial stages the mixing layer grows rapidly. It grows more slowly when it approaches the withdrawal level ($z^* \approx 1.0$), and finally reaches steady-state. The tank was considered fully mixed once h_m^* was larger than about 0.98. This occurred at about $t^* = 0.45$ to 0.6 (see Fig. 5-2 to Fig. 5-6).

The laboratory experiments for mixing were carried out for various conditions as represented by the location of the discharge and withdrawal, the discharge hydraulic parameters, and the initial teperature profiles. The densimetric Froude number Fr_0, based on the initial linear temperature profile, and the stratification number St, characterize the initial buoyant jet and the stratification. These dimensionless parameters affect comprehensively the results, as shown in Fig. 5-2 to Fig 5-6.

Since there are not enough data from the laboratory experiments, it is difficult to analyse and illustrate effects on the results of changes in only one of the parameters while the others are held constant. However, the numerical experiments by using the simulation model can provide systematical investigation of the effects on the mixing of variations in the components of the pumping system and initial conditions. The simulation model provided with the linear stratification of the initial temperature profile makes it possible to analyze and summarize the effects of the factors on the mixing

process. The initial temperature-depth profile which is linear allows a generalization of the pumping system parameters and the response of the ambient water body. The time-history of mixing indicated by the temperature profiles during the mixing process is a function of the initial densimetric Froude number Fr_0, and the stratifiaction number St. Examples of results for the simulated mixing experiments are shown in Fig. 5-7 to Fig. 5-10.

The temperature profiles shown in Fig. 5-7 and Fig. 5-8 indicate that the pumping systems with large Froude number mix the lower regions of the tank (near the discharge) rapidly. The temperature profiles are nearly vertical in this region for $Fr_0 = 16.5$, while they have considerable gradients at the same time for $Fr_0 = 2.0$. These results are consistent with the behavior of buoyant jets in a linearly stratified environment. Jets with large Fr_0 entrain fluid rapidly at the beginning of their trajectories and reach a maximum height of rise at lower elevation than jets with small Fr_0. Fig 5-9 and Fig. 5-10 indicate that the tank is not as uniformly mixed near the discharge level for the low values of St, as it is for the high values of St.

For constant area tanks with linear initial temperature profile, the degree to which mixing has proceeded is measured by the parameter h_m^*, the ratio of the thickness of the mixing layer, h_m, at any particular time to the total distance between the discharge and withdrawal, L. Complete mixing is accomplished at $h_m^* \approx 1.0$. h_m^* is a gross measure of the mixing process as the temperature profiles are not uniquely reflected by this parameter. Plots of h_m^* as a function of t^* for the mixing simulation with various values of Fr_0 and St are

shown in Fig. 5-11 and Fig. 5-12. The effects of Fr_0 and St on the mixing process can be viewed in terms of the growth of h_m^* with time. The curves in Fig 5-11 show that larger Fr_0 results in more rapid growth of h_m^* when $t^* > 0.1$. However, the differences in h_m^* among the simulations are very small. By the time that the mixing is completed, the maximum difference in h_m^* among simulations is about 5%. Fig 5-12 shows that smaller St results in a faster increase in h_m^* throughout the mixing process. The difference in h_m^* for the range of St values from 15 to 150 is about 10%.

The results of several simulated conditions are summarized in Fig. 5-13 and Fig. 5-14. The time t^*, required to achieve a given fraction of mixing h_m^*, is plotted against Fr_0 and St. High values of Fr_0, or low values of St, in the range examined, give somewhat smaller times t^* for a given fraction of mixing. However, over the range of Fr_0 and St values presented, the times t^* for a given amount of mixing vary less than 10%. These results indicate that the time required for mixing is nearly independent of Fr_0 and only slight dependent on St.

The results of the generalized mixing experiments provide some guidance for the design of efficient mixing systems for lake and reservoir destratification. Although, these results must be applied recognizing the simplified form of the simulation technique.

The results from both simulations and laboratory experiments summarized in this chapter indicate that the time for 50% of complete mixing is about $t^* \approx 0.1$, for 80%, $t^* \approx 0.3$, for 90%, $t^* \approx 0.35$ and for 100%, $t^* = 0.45$ to 0.55. For mixing to be completed, the time in real units is very roughly $t = 0.5V/Q$. The choice of the mixing period

(t) and the volume (V) determines the required discharge Q for the mixing system.

When the flowrate Q is considered too large for one pump, the lake or impoundment can be divided into n regions, each with volume V/n and each provided with a pumping system.

For a given discharge Q, the densimetric Froude number Fr_0 for the system is determined by the choice of the discharge jet diameter. The effects of various Fr_0 on mixing have been discussed above. It was shown that the larger the Froude number, the greater the increse in the thickness of the mixing layer after a fixed time of pumping. However, Ditmars' calculations of efficiencies showed that high Froude number systems were less efficient than low Froude number ($Fr_0 < 3.0$) systems. Therefore the range Fr_0 = 2.0 to 4.0 is recommended for high efficiency of mixing systems. But if the lake or impoundment were too slowly mixed, an increased Fr_0 for a system of fixed discharge Q could decrease the mixing time at the expense of efficiency.

The last parameter for the mixing system is the stratification number St ($= L/D_0$) which depends on the choice of the distance between the discharge and withdrawal, L. Systems in which pumping is from top to bottom are usually adopted although the generalized results showed that at smaller stratification numbers, the growth of the mixing layers is somewhat larger.

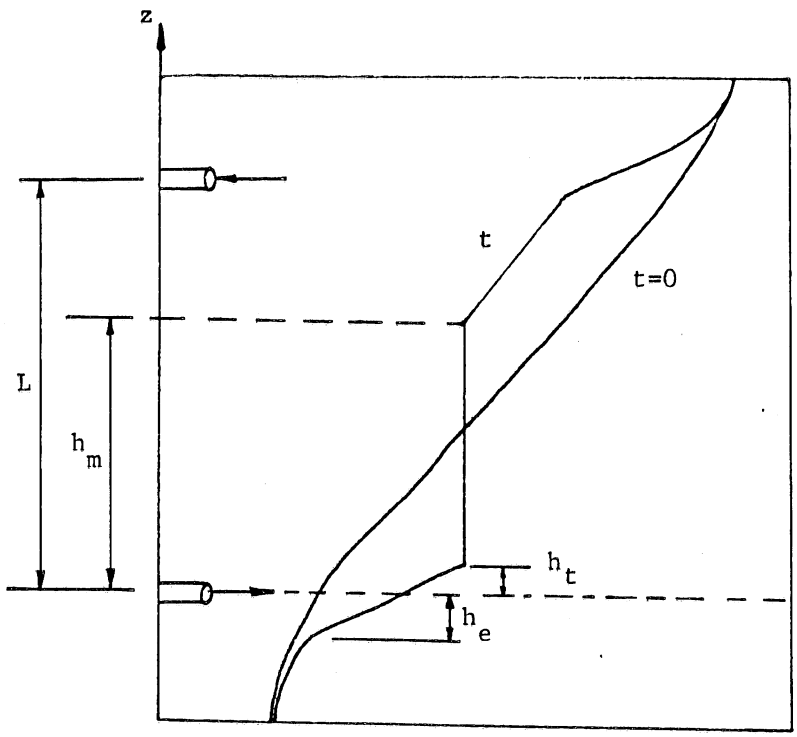

Fig. 5-1. Schematic diagram for definitions of h_m, h_t, and h_e in a temperature profile during mixing processes.

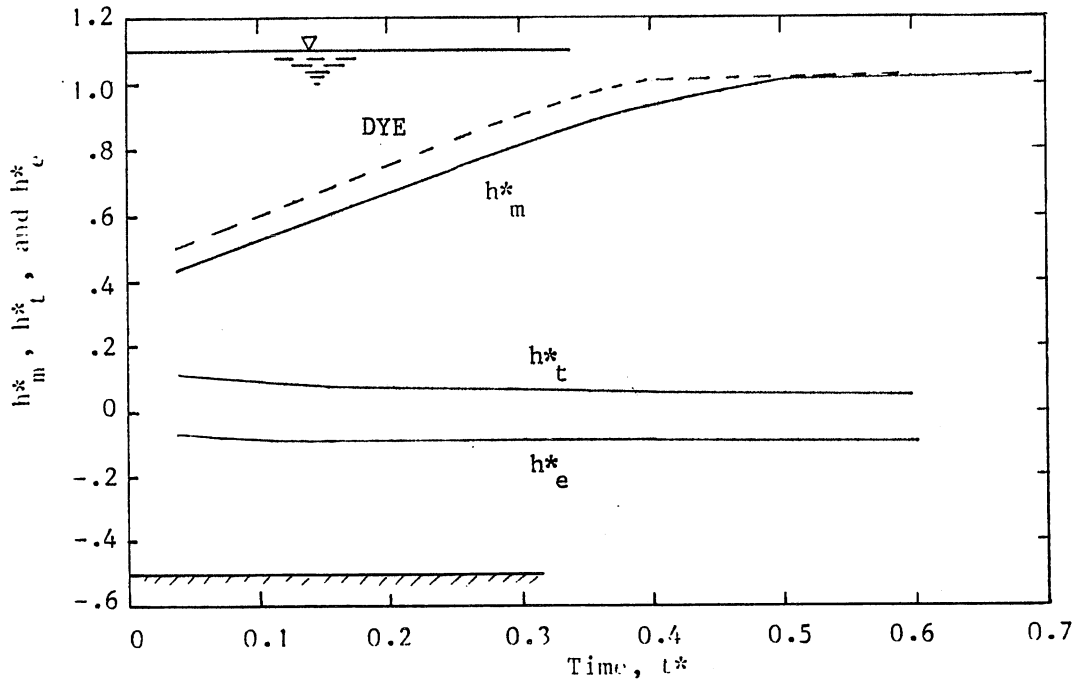

Fig. 5-2. Development of mixing layers for Experiment No. 4.

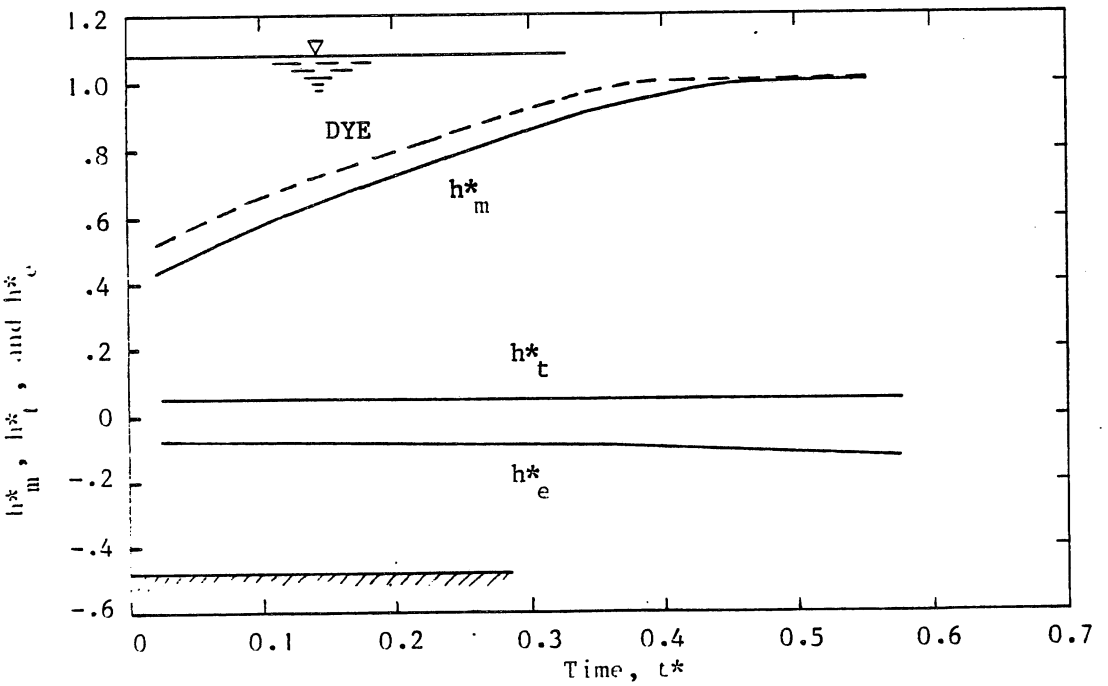

Fig. 5-3. Development of mixing layers for Experiment No. 5.

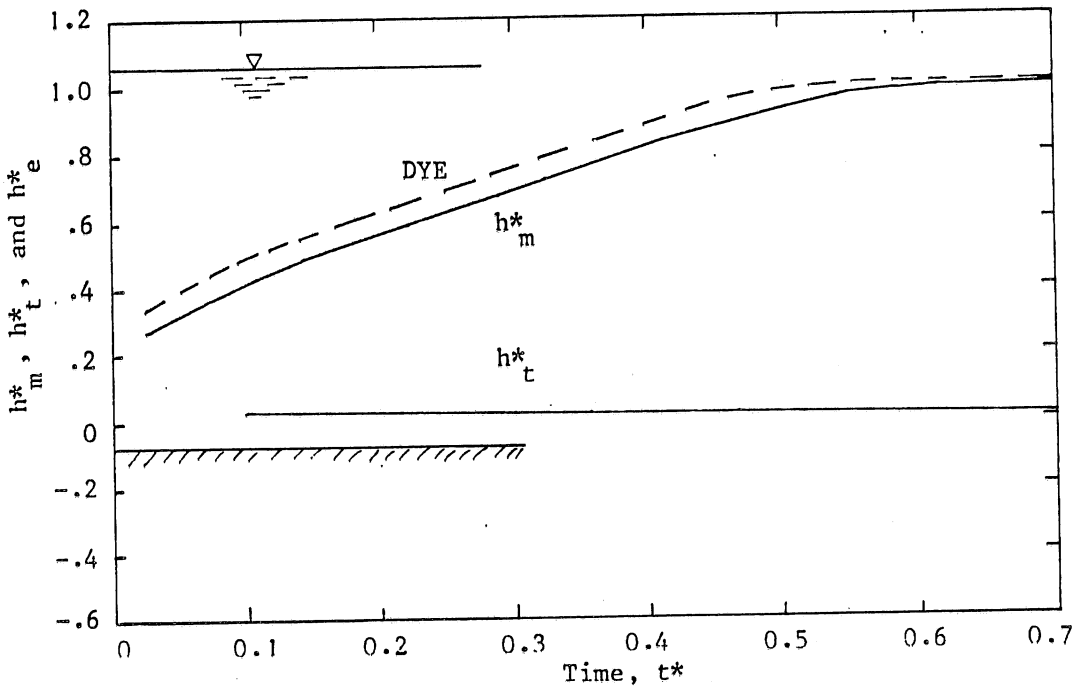

Fig. 5-4. Development of mixing layers for Experiment No. 6.

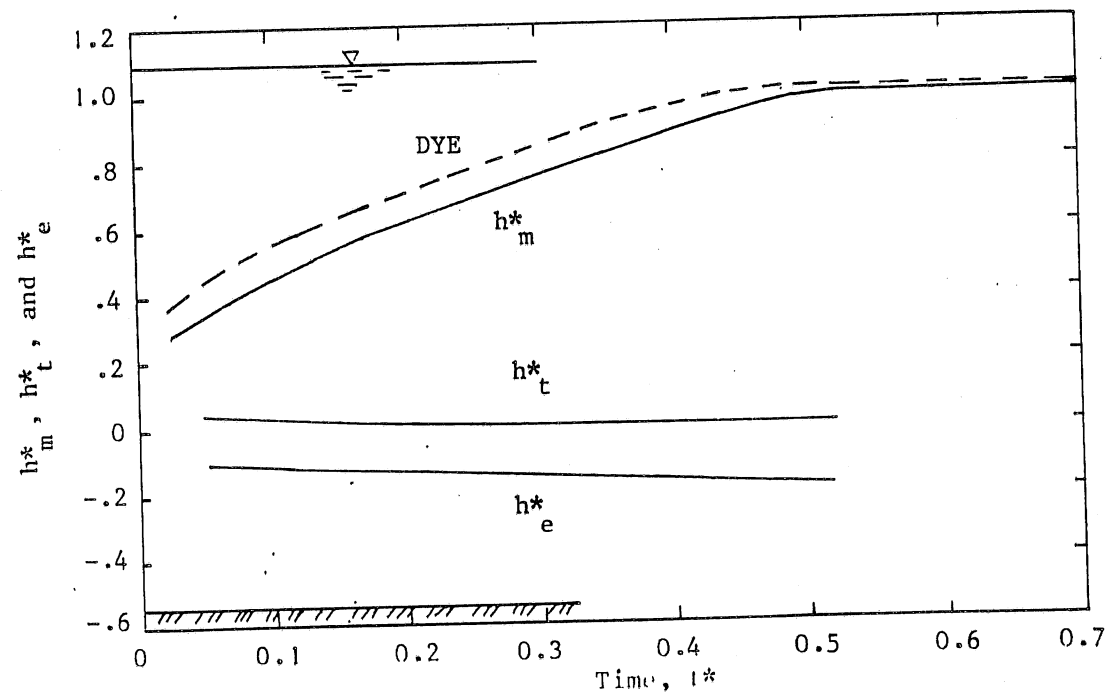

Fig. 5-5. Development of mixing layers for Experiment No. 7.

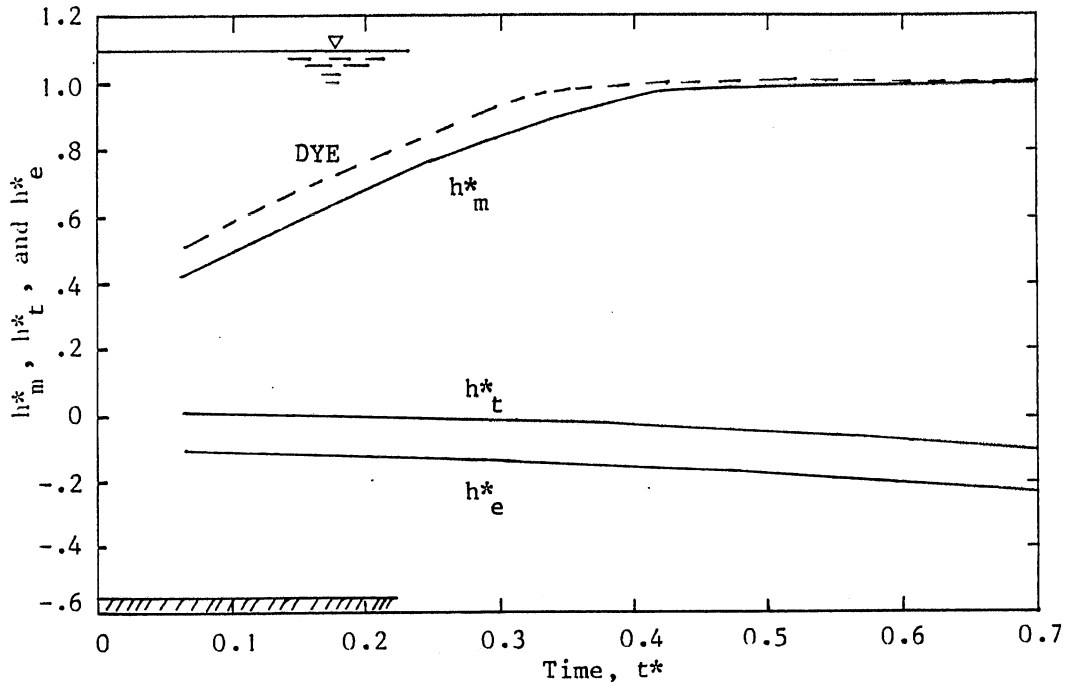

Fig. 5-6. Development of mixing layers for Experiment No. 8.

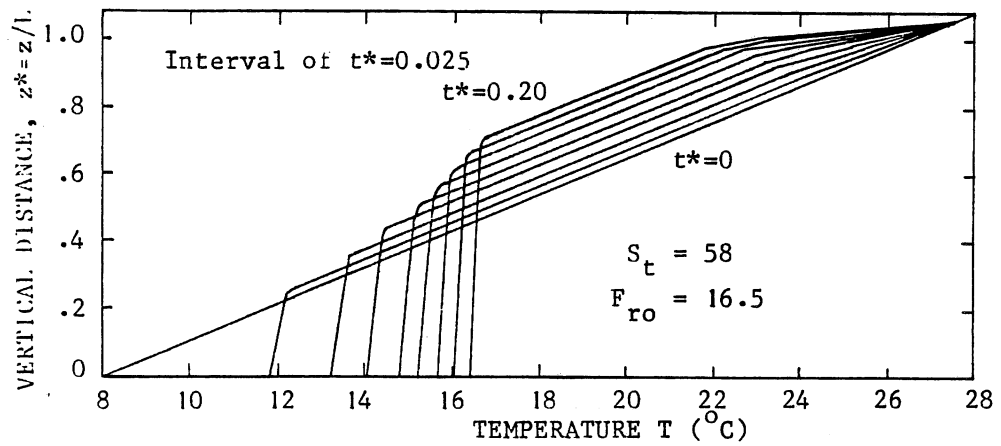

Fig. 5-7. Simulation result for F_{ro} = 16.5

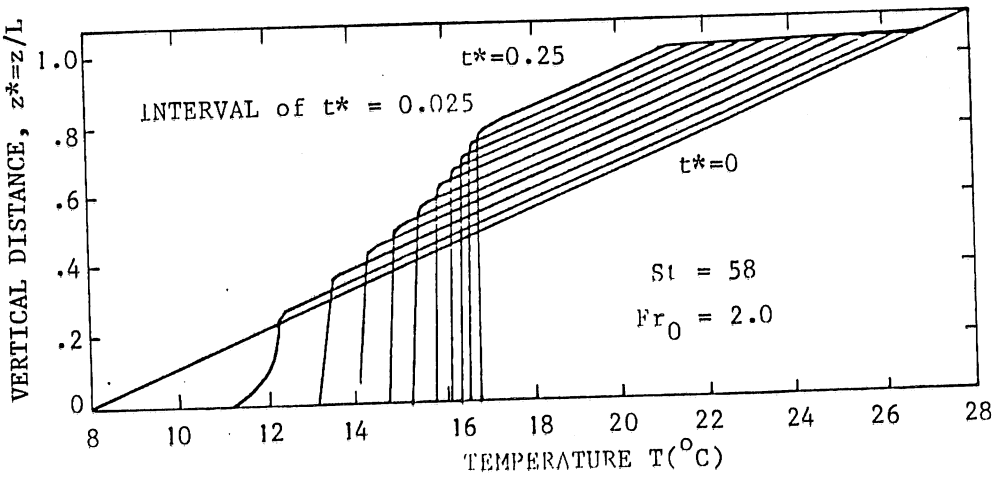

Fig. 5-8. Simulation result for Fr_0 = 2.0.

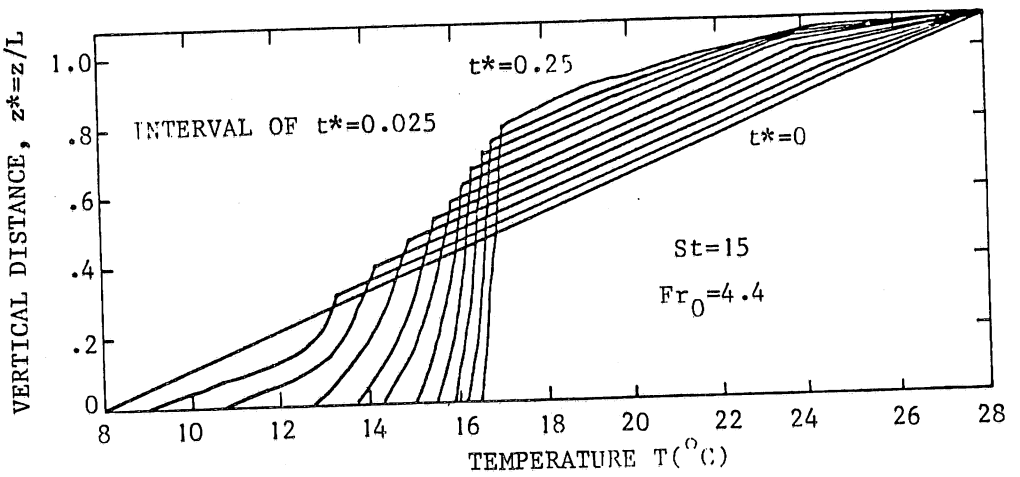

Fig. 5-9. Simulation result for Fr_0 = 4.4 and St = 15.

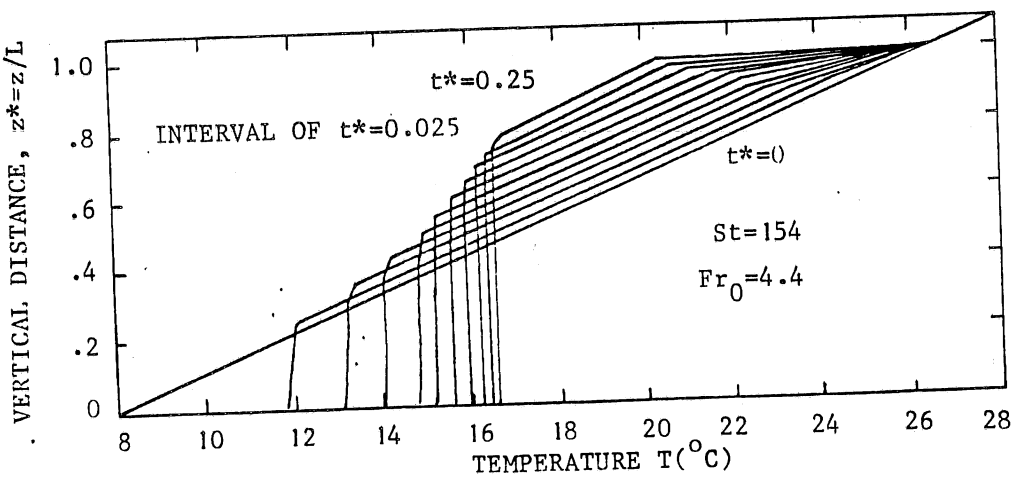

Fig. 5=10. Simulation result for Fr_0 = 4.4 and St = 154.

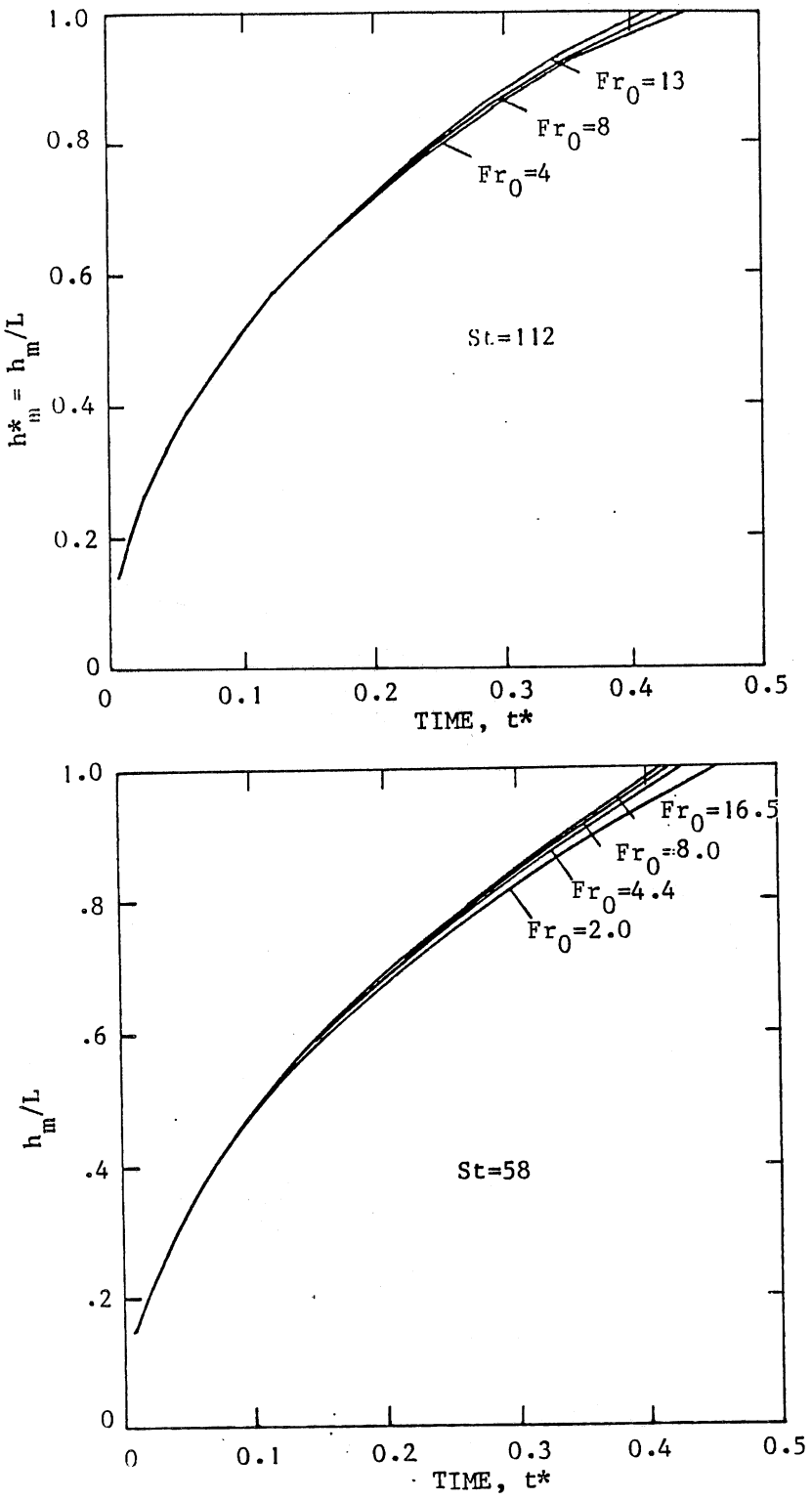

Fig. 5-11. Development of mixing layers as a function of Fr_0 and t*.

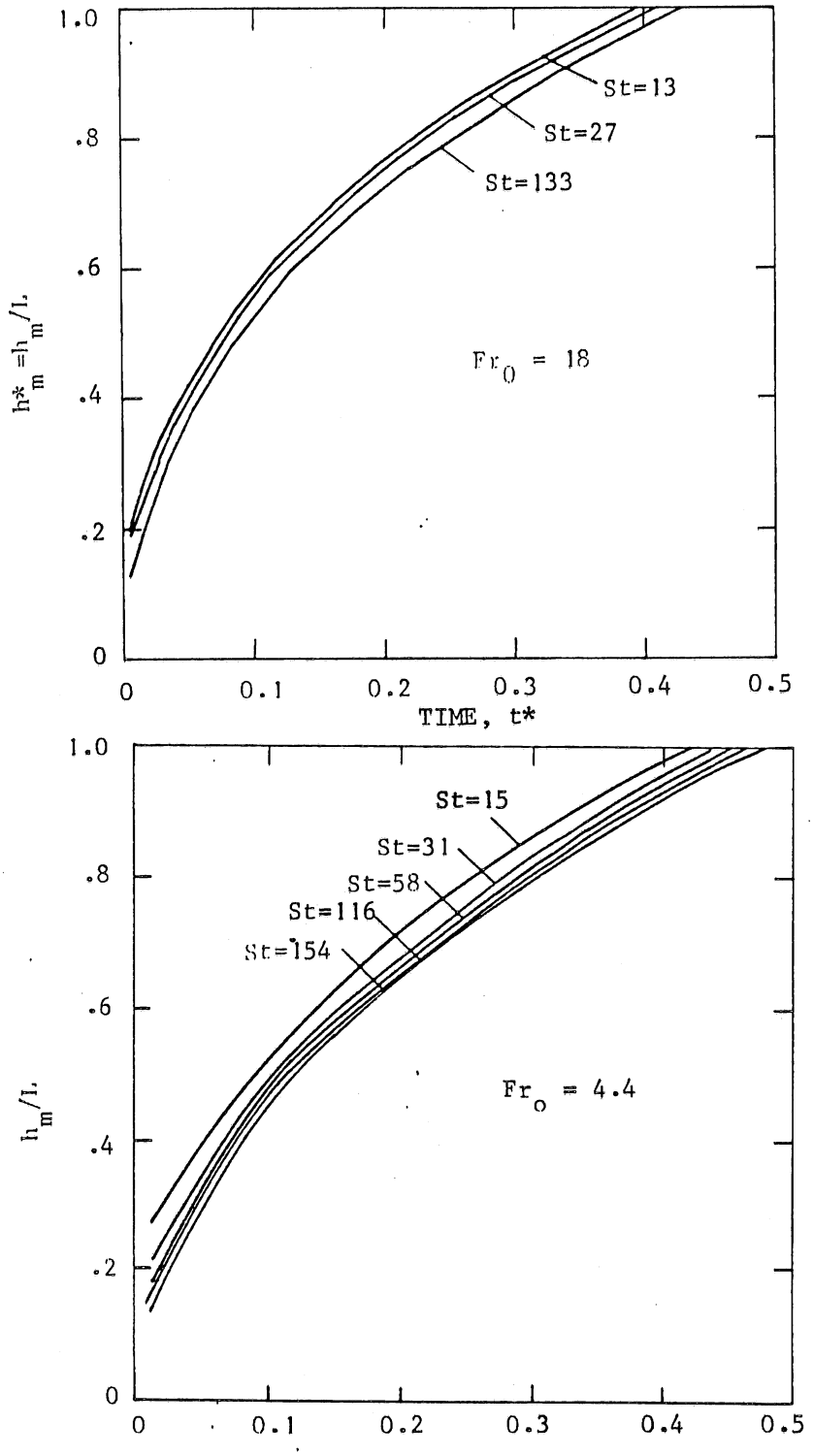

Fig. 5-12. Development of mixing layers as a function of St and t*.

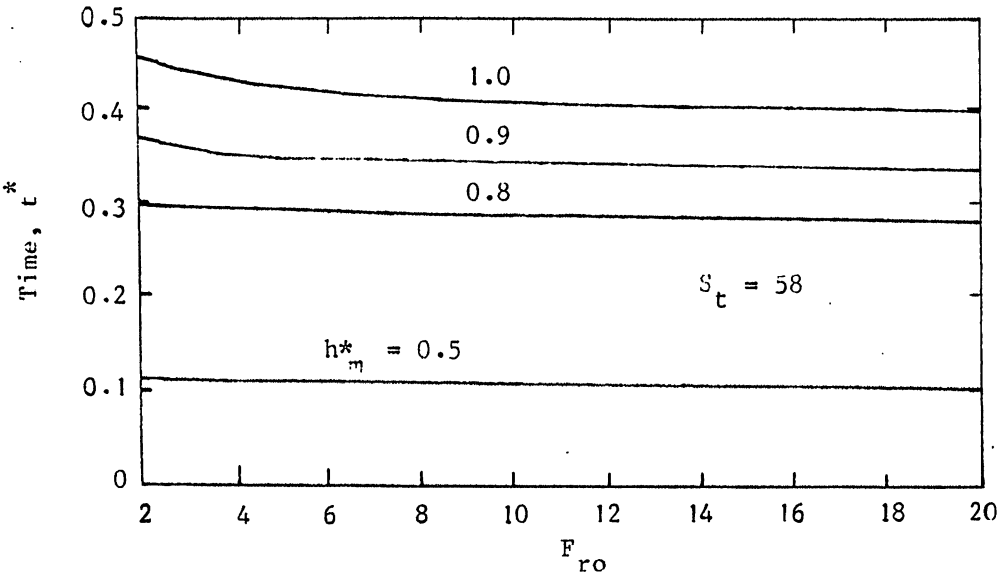

Fig. 5-13. Generalized simulation results: fraction of complete mixing as a function of F_{ro} and t^*.

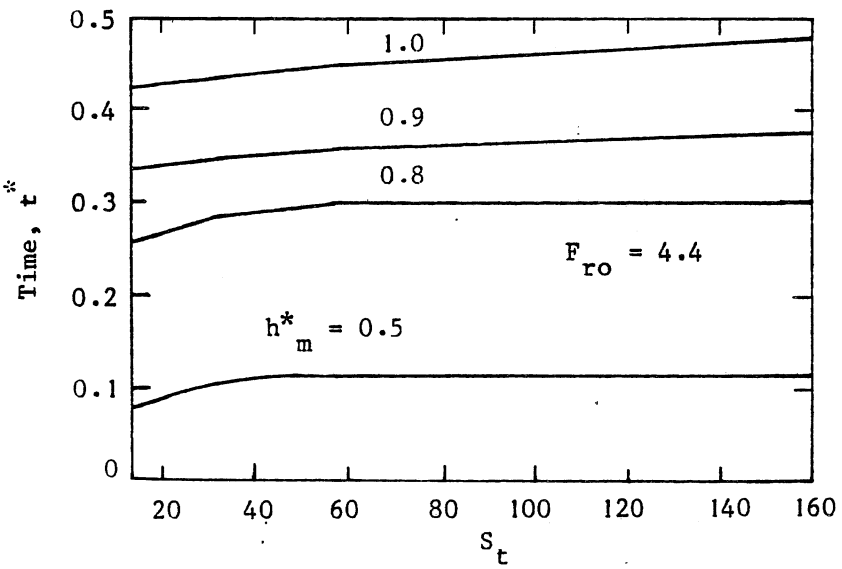

Fig. 5-14. Generalized simulation results: fraction of complete mixing as a function of S_t and t^*

Chapter 6 Conclusions

The integral model developed here is capable of predicting jet trajectories, jet width, centerline temperature or density and velocity decay, centerline dilution, point of neutral buoyancy and maximum height of rise for buoyant jets discharged at arbitrary angles to stratified or uniform ambients. The prediction has been found to be quite good.

The theoretical analysis for buoyant jets in stratified ambients uses the integral conservation equations with similarity hypothesis for velocity and temperature profiles to evaluate the integral appearing in these equations. The entrainment function is derived from the mechanical energy, tangential momentum and continuity equations.

The conservation equation of heat energy is used to replace the common used equation of buoyancy. A non-linear T-ρ relationship is introduced.

The y-direction (normal to the tangential direction) momentum equation which was ignored by previous investigators is retained as one of the governing equations to investigate the validity of the assumption of hydrostatic pressure. The effects of dynamic pressure to which buoyancy and curvature contribute are evaluated by the examination of flux terms. Results show that the effect on jet motion varies along the jet trajectory and that the contributions of buoyancy and curvature counteract each other. It is shown that the assumption of hydrostatic pressure is valid for the region between jet origin and

the neutral buoyancy level but not the negative buoyancy region near the maximum rise.

The effect of buoyant forces and centrifugal forces on the turbulence pattern is different at the upper side and lower side of a horizontal jet. Hence, the assumption of similarity of velocity and temperature profiles is not completely satisfied for small values of θ_0, provided that the value of Fr_0 is not so large that buoyant forces and centrifugal forces may be neglected entirely. It is recommended that further improvement of the integral method be based on more accurate expressions of velocity and temperature profiles which may be non-symmetric about the jet axis instead of the Gaussian distribution.

As an application of the buoyant jet mechanics, a simulation model for the prediction of changes in temperature structure of a lake or an impoundment due to mixing by a destratification device, a pumping system, has been developed. The response of the lake or reservoir to the pumping system is determined by the transport of fluid between the region of stratified ambient and the region of buoyant jet flow and withdrawal layer. Given the initial conditions and information about the lake or reservoir and pumping system, the model predicts the temperature profiles at successive time steps during the mixing process.

Experimental investigation in the laboratory on the mixing of a temperature-stratified tank by pumping shows that the simulation model predicts the process of temperature destratification during mixing well. The comparison of the temperature profiles measured during experiments performed in both laboratory and field with predictions

indicates good overall agreement. However, some discrepancies between measurements and simulation results in the details of the profiles are also shown by the comparison.

For the closed-systems, the model provides a good approximation to the response of the lake or reservoir to mixing. The simulation model can be applied to the mixing of lakes and reservoirs by pumping recognizing the assumptions underlying the simulation model. Dimensionless parameters h_m^*, h_e^* and h_t^* are introduced to describe temperature profiles during the mixing process. The growth of mixing layers is reflected by the $h_m^* \sim t^*$ relationships. The generalized results from numerical and laboratory experiments indicate that the time for complete mixing is about $t^* = 0.5$. The results also show that the time required for mixing is nearly independent of Fr_0 and slight dependent on St. Some information for the design of mixing system for lake and reservoir destratification are provided.

Natural mixing in lakes or reservoirs induced by the external conditions (heat exchange through boundaries and wind) and other factors often occur during mixing by pumping. If the time required for mixing by pumping system is very small relative to that required for natural changes, the simulation model can be applied directly, otherwise, the model should take account of the effects of a changing the heat budget and other external effects. It is recommended for future work that the simulation model should be coupled with the simulation of lake or reservoir stratification due to external energy (heat and wind) inputs. It is possible to alternate changes in the temperature profiles due to external effects with changes due to the

mixing by pumping because the solution to the model is a stepwise solution in time.

The simulation model predicts no change in the temperature profile below the jet origin while experimental data show that horizontal jets do entrain and mix the region below the jet origin to some depth. More experimental and analytical work is required to investigate the features of mixing in this region and to modify the model. Temperature profiles measured simultaneously at several locations in the tank during mixing and the study of features of the spreading layer and the equilibrium level could provide information necessary to improve the simulation model.

REFERENCES

Abraham, G., Entrainment principle and its restrictions to solve problems of jets, J. Hyd. Res., 31, 1-23, 1965.

Abraham, G., Jets and plumes issuing into stratified fluid, Proceedings, Inter. Symposium on Stratified Flows, Inter. Assoc. for Hyd. Res., Novosibirsk, 1972.

Andreopoulos, J., Praturi, A., and Rodi, W., Experiments on vertical plane buoyant jets in shallow water, J. Fluid Mech.(1986), Vol. 168, pp. 305-336.

Awar, H. O., Behavior of buoyant jet in calm fluid, J. Hyd. Div., ASCE, Vol. 95, No. HY4, 1289-1303, 1969.

Bender, M. D., and Stefan, H. G., Engineering analysis of lake aerators and design of a metalimnetic aerator, SAFHL, Project report No. 247, 1986.

Brooks, N. H., Synthesis of stratified flow phenomena for design of outfalls, Proceedings, Second Inter. Symposium on Stratified Flows, Norway, 24-27, June, 1980.

Brooks, N. H. and Koh, R. C. Y., Selective withdrawal from density -stratified reservoirs, J. Hyd. Div., ASCE, Vol. 95, No. HY4, July, 1969.

Chen, J.-C. Papanicolaou, and List, E. J., Discussion on "Two -dimensional jets in stratified fluid", J. Hyd. Div., ASCE, HY10, Oct., 1980.

Ditmars, J. D., Mixing of density-stratified impoundments with buoyant jets, W. M. Keck. Lab., Report No. KH-R-22, 1970

Fan, L., and Brooks, N. H., Discussion of "Horizontal jets in stagnant fluid of other density", by G. Abraham, J. Hyd. Div., ASCE, Vol. 92, No. HY2, March, 1966, 423-429.

Fisher, H. B., List, E. J., Koh, R. C. Y., Imberger, J., and Brooks, N. H.(1979), Mixing in Inland and Coastal waters, Academic Press

Fox, D. G., Forced plume in a stratified fluid, J. Geophys. Res., 75(33), 6818-6835, 1970.

Hart, W. E., Jet discharge into a fluid with a density gradient, J. Hyd. Div., ASCE, Vol. 87, No. HY6, Nov., 1961.

Hino, M., Forced plumes in a stable stratified fluid, Trans. of JSCE, No. 86, Oct., 1962, 29-37.

Hirst, E., Buoyant jets discharged into quiescent stratified ambients, J of Geophysical Research , 76 (1971), No. 30, Oct., pp. 7375-7384.

Irwin, W. H., Symons, J. M., and Robeck, G. G., Impoundment destraitification by mechanical pumping, J. Sanitary Eng. Div., ASCE, Vol. 92, No. SA6, Dec., 1966.

Koh, R. C. Y., and Brooks, N. H. (1975), Fluid mechanics of waste water disposal in the ocean, Ann. Rev. Fluid Mech. 7: 187-211.

Kotsovinos, N. E. and List, E. J (1977), Plane turbulent jets, Part 1, Integarl properties, J. Fluid Mech., 81: 25-44.

Lee, J. H. W., and Cheung, V. W. L., Inclined plane buoyant jet in stratified fluid, J. Hyd. Div., ASCE, Vol. 112, No. 7, July, 1986.

Liseth, P.(1976), Wastewater disposal by submerged manifolds, J. Hyd. Div., ASCE, Vol. 102, No. HY1: 1-13.

List, E. J. and Imberger, J.(1973), Turbulent entrainment in buoyant jets and plumes, J. Hyd.. Div., ASCE, Vol. 99, No. HY9: 1461-1474.

Pantokratoras, A., Calculation of a turbulent jet discharged downward, Proceedings, Inter. Symposium on Buoyant Flows, Athens-Greece, 1-5, Sept., 1986.

Rajaratnam, N., Turbulent Jets, Developments in Water Science, Elsevier, 1976.

Riley, M., and Stefan, H. G., Formulation of the Minnesota Lake water quality model I, SAFHL, Internal Memorandum. No. 111, May, 1985.

Rodi, W., Turbulent Buoyant Jets and Plumes, HMT, The Science and Applications of Heat and Mass Transfer, Reports, Reviews and Computer programs, Volume 6, Pergamon Press, 1982.

Rouse, H., Yih, C. S., and Humphreys, H. W., Gravitational convection from a boundary source, Tellus, 4, 1952, No. 3, Aug., pp. 201-210.

Schetz, J. A., Injection and Mixing in Turbulent Flow, Progress in Astronautics and Aeronautics, Volume 68, 1980.

Shirazi, M. A., and Davis, L. R., Workbook of thermal plume prediction, Volume I----submerged discharge, EPA-R2-72-005a, Aug., 1972.

Singh, R. A., A study of submerged and surface horizontal buoyant jets, PhD. dissertation, 1976.

Sini, J. F., and Dekeyser, I., Numerical prediction of 2-D turbulent forced plumes in stratified fluid, Proceedings, Third International Symposium on Stratified Flows, Pasadena, Feb., 1987.

Sotil, C. A., Computer progarm for slot buoyant jets into stratified

ambient environments, W. M. Keck Lab., Technical memorandum 71-2, June, 1971.

Spigel, R. H., Farrant, B., Selective withdrawal through a point sink and pycnocline formation in a linearly stratified flow, J. Hyd. Div., ASCE, Vol. 22, 1984, No. 1.

Tatom, F. B., Errors from using conservation of buoyancy concept in plume computations, J. Hyd. Div., ASCE, Vol. 111, No. 6, June, 1985, 1005-1009.

Wallace, R. B. and Wright, S. J., Spreading layer of two-dimensional buoyant jet, J. Hyd. Div., ASCE, Vol. 101, No. 6, June, 1984, 813 -828.

Wright, S. J., Wong, D. R., and Wallace, R. B., Buoyant discharge from outfall diffuser into stratified fluid, Proceedings, Second Inter. Symposium on Stratified Flows, Norway, 24-27, June, 1980.

Wright, S. J., and Wallace, R. B. (1979), Two-dimensional jets in stratified fluid, J. Hyd. Div., ASCE, Vol. 105, HY11: 1393-1406.

Yannopoulos, P. C., Momentum and energy equations in round turbulent buoyant jets, Proceedings, International Symposium on Buoyant Flows, Athens-Greece, 1-5, Sept., 1986.